UNIVERSITÉ DE BOURGOGNE
Laboratoire Interdisciplinaire Carnot de Bourgogne UMR CNRS 6303

NATIONAL ACADEMY OF SCIENCES OF ARMENIA
Institute for Physical Research

CONTROL OF PHOTOASSOCIATION OF ATOMIC BOSE-EINSTEIN CONDENSATES BY LASER FIELD CONFIGURATION

by
Mariam Gevorgyan

A Thesis in Physics

Submitted for the Degree of Doctor of Philosophy

Date of defense: October 11, 2016

The Jury:

Artur ISHKHANYAN	Professor Institute for Physical Research, NAS, Ashtarak, Armenia	*Supervisor*
Hans-Rudolf JAUSLIN	Professor ICB, Université de Bourgogne, Dijon, France	*Supervisor*
Vladimir KRAINOV	Professor Institute of Physics and Technology, Moscow, Russia	*Referee*
Viktor REDKOV	Professor B. I. Stepanov Institute of Physics of NAS, Belarus	*Referee*
Armen MELIKYAN	Professor Russian-Armenian (Slavonic) University, Yerevan, Armenia	*Examiner*
Atom MURADYAN	Professor Yerevan State University, Yerevan, Armenia	*Examiner*
Gayane GRIGORYAN	Professor Institute for Physical Research, NAS, Ashtarak, Armenia	*Examiner*
Claude LEROY	Professor ICB, Université de Bourgogne, Dijon, France	*Examiner*

LABORATOIRE INTERDISCIPLINAIRE CARNOT DE BOURGOGNE-UMR CNRS 6303
UNIVERSITÉ DE BOURGOGNE, 9 AVENUE A. SAVARY - 21078 DIJON - FRANCE

INSTITUTE FOR PHYSICAL RESEARCH, NATIONAL ACADEMY OF SCIENCES OF ARMENIA ASHTARAK-2, 0203 ARMENIA

Remerciements

J'aimerais exprimer ma sincère reconnaissance à mes Directeurs de thèse, les Professeurs Artur Ishkhanyan et Hans-Rudolf Jauslin pour les discussions utiles et leur permanente assistance pendant de mes travaux de doctorat. Merci au Prof. Stéphane Guérin qui a suggéré plusieurs idées fondamentales. Je voudrais aussi remercier le Prof. Gagik Demirkhanyan et Ashot Manukyan pour leur aide et soutien.

J'apprecie le soutien tous mes collègues de l'Institute for Physical Research de l'Académie Nationale des Sciences d'Arménie et du Laboratoire Interdisciplinaire Carnot de Bourgogne de l'Université de Bourgogne pour la résolution des questions administratives et leur attitude amicale, en spécialement les Profs. Aram Papoyan et Claude Leroy. J'aimerais aussi mentionner particulièrement Anahit Gogyan, Ara Tonoyan, Maud Louviot, Tatevik Hovhannisyan, Vincent Dorier, et David Dzsodjan. Un remerciement particulier à mes parents, Rafik Gevorgyan et Anahit Ghazaryan, pour leur soutien inébranlable.

Je remercie l'Ambassade de France en Arménie pour son aide financière, notamment la bourse No. 764489B en tant que Boursière du Gouvernement Français, ainsi que l'aide du State Committee of Science d'Arménie (Bourse SCS No. 14A-1c93 - 2014).

Acknowledgments

I would like to express sincere gratitude to my supervisors Profs. Artur Ishkhanyan and Hans-Rudolf Jauslin for their useful discussions and permanent assistance during my PhD work. And thanks to Prof. Stéphane Guérin, who proposed some of the basic ideas. I would also like to thank Prof. Gagik Demirkhanyan and Ashot Manukyan for their help and support.

And thanks go out to all the co-workers of the Institute for Physical Research of National Academy of Sciences of Armenia and the Laboratoire Interdisciplinaire Carnot de Bourgogne of University of Bourgogne for solving the administrative issues and kind attitude, especially to Profs. Aram Papoyan and Claude Leroy. I would also like to mention particularly Anahit Gogyan, Ara Tonoyan, Maud Louviot, Tatevik Hovhannisyan, Vincent Dorier, and David Dzsodjan. Special thanks to my parents, Rafik Gevorgyan and Anahit Ghazaryan, for their unwavering support.

I acknowledge the support of French Embassy in Armenia for Grant No. 764489B as Boursière du Gouvernement Français, as well as the support from the Armenian State Committee of Science (SCS Grant No. 14A-1c93 - 2014).

Research conducted in the scope of the International Associated Laboratory IRMAS.

Contents

Introduction

Relevance of the subject

The degenerate quantum gases (Bose-condensates and Fermi gases) are a hot topic of contemporary physics research potent to substantially contribute both to high technology and fundamental understanding of the nature. Our research is a part of the main stream effort in this direction.

The level-crossing models are in the heart of quantum optics from the very beginning of quantum physics. Because of the very limited number of exactly solvable models, each new one is expected to lead to numerous essential developments revealing the principal qualitative physical characteristics of many physical processes occurring in various domains.

The aim of the work

The goal of this work is to analyze the atom-molecule conversion dynamics in degenerate quantum gases to create a molecular Bose-Einstein condensate (BEC). A particular task is to control the photoassociation of atomic Bose-Einstein condensates by choosing the associating laser-field configuration.

The essence of Bose-Einstein condensation is a macroscopic occupation of a single quantum mechanical state. BEC is a state of matter, which occurs in a dilute bosonic gas (both atomic and molecular) cooled down to temperatures very close to absolute zero. Under such conditions, a large fraction of bosons occupy the lowest quantum state. For this reason, the quantum effects become visible on a macroscopic scale. These effects are known as macroscopic quantum phenomena.

Photoassociation is a process in which two colliding atoms interact with a laser field to

form an excited molecule. Thus, we deal with a chemical process.

The work concerns the control of the photoassociation process. The control can be achieved by different approaches, for instance, by change of density or applying a magnetic field. In our case the control is performed by choosing suitable field configurations.

The field configurations are described by the Rabi frequency and detuning. The Rabi frequency is the product of the transition dipole moment and the field amplitude. Detuning is the difference between transition and laser frequencies. The pair of the Rabi frequency and detuning is referred to as a field configuration. In this work the Rabi frequency and detuning are time-dependent functions.

The general idea is to search for the field configurations that will give the desired result. The desired result is formulated as the given time evolution of the population.

The problem is nonlinear, which means that the set of equations describing the photoassociation process are nonlinear. Hence, one needs new approaches, for which important steps are made in the work.

We start with the two-level model. The physical process we study is the following: we consider an initially pure-atomic condensate and would like to create a molecular state by applying laser radiation. We consider the atomic condensate as one state and the molecular state as the second. Such a process in the simplest approximation can be described by a nonlinear two-state model. To make the model more realistic we consider the third-order nonlinearities which describe the atom-atom, atom-molecule and molecule-molecule elastic interactions.

Further, to bring weakly coupled molecules to the stable ground molecular state, we use stimulated Raman adiabatic passage (STIRAP). A particular task here is to avoid the losses from the intermediate excited molecular state as much as possible. Also, we analyze robustness of linear and nonlinear STIRAP processes.

Finally, to advance in the approximate analytic description of the photoassociation by a previously proposed two-term ansatz that involves the solution of the associated linear problem, we consider the exact solutions of the linear two-state problem in terms of the bi-

confluent Heun functions. As a result, we introduce a new level-crossing model for which the solution of the linear two-state problem is written in terms of certain linear combinations of the Hermite functions.

The objectives of the thesis are

✓To develop an efficient and robust adiabatic passage technique based on the tracking of a desired solution for the transfer from an atomic to the molecular state.

✓ To explore if it is possible to achieve an efficient transfer in the presence of Kerr nonlinearities.

✓To discuss the stimulated Raman exact tracking method as a possible efficient transfer procedure. If possible, to include the irreversible losses from the second level.

✓ To identify the field configurations for which the linear quantum two-state problem is solvable in terms of the Heun functions.

✓To identify the level-crossing models solvable in terms of linear combinations of special functions simpler than the Heun functions.

Scientific novelty

We propose a technique of robust and efficient adiabatic passage from an atomic to a molecular state, based on the tracking of a desired time evolution of the populations.

We show that it is possible to achieve a good transfer in the presence of Kerr nonlinearities as well. This is achieved by a proper choice of the detuning that provides an efficient adiabatic tracking.

We present a stimulated Raman exact tracking in a quadratic-nonlinear quantum three-state system. We show that in the nonlinear case for an efficient transfer one needs to take the pump pulse stronger than the Stokes one, in contrast to the ordinary linear case. This transfer may also be robust.

We show that using stimulated Raman exact tracking technique it is possible to avoid the irreversible losses from the intermediate weakly bound molecular state, in the one- and two-photon resonance case.

We construct expansions of the solutions of the bi-confluent Heun equation in terms of

incomplete Beta functions as well as other simpler mathematical functions.

We develop a linear dissipative level-crossing model solvable in terms of the Hermite functions.

The practical value of the work

The results of the thesis can be used

✓for creation of *a priori* given superposition states of simple quantum systems

✓for achievement of prescribed population distribution

✓in physical situations where linear and nonlinear level-crossing models are applied (numerous possibilities)

✓in mathematics, chemistry, engineering, etc.

The derived results belong to the general tools of precision control of nonlinear dynamics of atomic systems. Hence, one may envisage numerous applications of the developed nonlinear models [1–12] in atom lithography, precision measurement, quantum information processing, nanotechnology, chemical dynamics, etc. As regards the linear models, the application domain here varies from quantum mechanics, nuclear physics to quantum gravity and cosmology.

Overview

In 1924-25, Satyendra Nath Bose and Albert Einstein predicted the phenomenon of Bose-Einstein condensation [13, 14]. Though predicted so long ago, only recently the "pure" Bose-Einstein condensation has been realized in practice. In 1995, the condensation was observed in a remarkable series of experiments on vapors of rubidium [15] and sodium [16], both in the atomic state, in which the atoms were confined within magnetic traps and cooled down to extremely low temperatures, on the order of fractions of microkelvin ($170nK$).

If compared with more commonly encountered states of matter, the Bose-Einstein condensates are seen to be extremely fragile. The slightest interaction with the external environment can be enough to warm them above the condensation threshold, thereby eliminating their interesting properties and forming a normal gas.

In the first experiments Rb atoms were used, since rubidium belongs to the alkali metal

group and is easy to vaporize, also has a convenient spectral absorption range, which makes it a frequently used choice for laser manipulation of atoms.

Ever since, the Bose-Einstein condensates and, generally, the physics of ultracold gases have developed into a very important field of research on the frontier between atomic- and condensed-matter physics, which allows to observe a whole series of unusual quantum phenomena (for reviews see, e.g., [17–19]).

For instance, numerous exciting experiments demonstrated the interference between condensates due to wave-particle duality [20], many probed the superfluidity in quantum gases, studied the creation of bright matter-wave solitons in condensates confined to one dimension, and the slowing-down of light pulses in a BEC to very low speeds using electromagnetically induced transparency [21], etc.

After the implementation of atomic BECs, the next step was to create a molecular BEC [22–24]. This is a very appealing task because the ultracold molecules, due to their complex internal structure, suggest a wider range of properties as compared to atoms. Such molecules have important applications such as ultraprecise molecular spectroscopy and low Doppler width studies of collision processes [25, 26], quantum gases with anisotropic dipolar interactions, precision tests of fundamental symmetries such as the search for a permanent electron's electric dipole moment (with certain polar molecules) [27, 28], study of rotational and vibrational energy transfer processes and coherent chemistry, where reactants and products are in coherent quantum superposition states [29], quantum computing [30, 32], and etc.

However, the complex internal structure precludes molecules from getting ultracold by merely slowing down their translational motion, because they store some energy in inner vibrational and rotational degrees of freedom. Laser cooling enables to freeze only the center of mass of a quantum object. In the case of atoms it is sufficient [33–35] but not with molecules.

A solution is to assemble molecules from ultracold *bosonic* atoms, a process which does not produce any vibrational and rotational excitation.

An interesting alternative is emerged by cooling *fermionic* atoms to extremely low temperatures. Since fermions are subject to the Pauli exclusion principle, in order to exhibit Bose-Einstein condensation, the fermions must "pair up" to form bosonic compound particles, e.g., Cooper pairs or molecules.

D. Jin created the first fermionic condensate composed of *Cooper pairs* [41]. The emergence of a *molecular* Bose-Einstein condensate from a Fermi gas has led to the direct observation of a molecular Bose-Einstein condensate created only by adjusting the interaction strength in an ultracold Fermi gas of atoms [40]. This process represents the predicted crossover from weak coupling Bardeen-Cooper-Schrieffer (BCS) pairing to a Bose-Einstein condensate of tightly bound pairs.

W. Ketterle and co-workers have used a $sodium-23$ BEC to help cool a gas of $lithium-6$ fermionic atoms to create a *degenerate Fermi-gas*. The fermionic atoms cannot fall into the single state available to bosonic atoms, but they can, if cooled low enough, occupy all the lowest energy quantum states, thereby forming a Fermi-sea.

A route (at least partial) to create a molecular BEC is cooling by evaporation. By using this technique, R. Grimm and co-workers have provided an indirect evidence for a long-lived condensate of lithium molecules [38]. They observed the formation of a condensate by evaporative cooling of a molecular gas close to equilibrium.

In other experiments, molecules were formed by sweeping an external magnetic field through a Feshbach resonance, adiabatically converting atoms to molecules. This atom-molecule coupling is a coherent two-body process [39].

The concept of the experiment [40] is also to start with a Fermi gas, which is evaporatively cooled to a high degree of quantum degeneracy, and adiabatically create molecules with a magnetic-field sweep across a Feshbach resonance. If the molecule creation conserves entropy and the initial atom gas is at sufficiently low temperature T compared to the Fermi temperature T_F, then the result should be a molecular sample with a significant condensate fraction.

In brief, the laser cooling and trapping of fermionic atoms followed by evaporative cooling

in a magnetic trap, owing to a Feshbach resonance, which occurs when the energy of a quasibound molecular state becomes equal to the energy of two free atoms [40], resulted in a molecular BEC. The BEC was detected through a bimodal momentum distribution, and effects of the strong inter-particle interaction were investigated. The molecular BEC appears on the repulsive side of the Feshbach resonance, which is related in a continuous way to BCS-type fermionic superfluidity on the attractive side of the resonance [40].

The group of R. Grimm reported on the Bose-Einstein condensation of more than $10^5 Li^2$ molecules in an optical trap starting from a spin mixture of fermionic lithium atoms. During forced evaporative cooling, the molecules are formed by three-body recombination near a Feshbach resonance and finally condense in a long-lived thermal equilibrium state. They measured the characteristic frequency of a collective excitation mode and demonstrated the magnetic field-dependent mean-field by a controllable condensate spilling [38]. The stability allows to use bosonic molecules composed of fermionic atoms in order to achieve molecular BEC.

Approaches

During the last years, various approaches have been used to create and manipulate molecules via cooling and trapping techniques [36, 37]. Among these, as far as the very molecule production from cold atoms is concerned, two main techniques are mostly used. These are the magnetic Feshbach resonance [25–29] and optical laser photoassociation [32, 42].

A Feshbach resonance is a scattering resonance, for which the total energy of two colliding atoms is equal to the energy of a bound molecular state, and an atom-molecule transitions can occur during a collision. Feshbach resonances are routinely used tools to govern the interaction strength between atoms in ultracold quantum gases [45].

This technique has also proved to be very efficient in controllably converting fermionic atoms into bosonic molecules [31]. For instance, using a magnetic field ramp across a Feshbach resonance is a clear evidence of diatomic molecule formation has been reported through direct, spectroscopic detection of these molecules. In another experiment, the crossing of a

Feshbach resonance was used to put the atomic condensates into an atom-molecule superposition state [31].

In the experiment [37], a mixture of atomic and molecular states of ^{85}Rb atoms has been created and probed by sudden changes in the magnetic field in the vicinity, but not across the Feshbach resonance. In this experiment, the variation of the magnetic field gave a rise to oscillations in the number of atoms that remain in the condensate. By measuring the oscillation frequency, for a large range of magnetic fields, it has first been proved that a quantum superposition of atoms and diatomic molecules has been created. Further, ultracold molecules have been formed in degenerate Fermi gases of Li atoms [54, 55] and, afterwards, a BEC has been created in the obtained ensemble of molecules [22–24].

An alternative for the Feshbach resonances is the photoassociation of atoms using optical laser fields. While Feshbach resonances have been efficient for the realization of molecular condensates, photoassociation has been widely used to study long range molecular interactions and to probe ultracold gases [53]. In addition, the photoassociation has also been used to produce ultracold molecules from atomic BECs [43, 44].

In the simplest case the photoassociation is described by a system of two coupled nonlinear first-order differential equations [48–52] obtained within the framework of the semiclassical mean-field Gross-Pitaevskii theory [37, 46, 47, 56]. This system can also be used for the description of bosonic molecule formation in degenerate Fermi gases. Interestingly, it has been noted in Ref. [57] that, within the mean-field approximation, association of diatomic molecules from degenerate Fermi gases is equivalent to dissociation of a molecular condensate into bosonic atoms, and vice versa, dissociation of a molecular condensate into degenerate Fermi atoms is equivalent to association of diatomic molecules starting from ultracold bosonic atoms.

Why we consider the photoassociation process? It is because we hope that with this process it will be possible to achieve an efficient transfer to the stable molecular state having an additional degree of freedom, which will be useful in various technological applications (quantum lithography, atom interferometry, quantum information processing, etc.).

To this end, it is important that in the framework of the basic quadratic-nonlinear quantum two-state approximation in the non-dissipative case the set of equations are mathematically the same for both photoassociation and Feshbach resonance. However, the physical meanings of the involved functions which define the field configurations are different. In the Feshbach resonance the amplitude modulation function is proportional to the square root of the magnetic-field width of the resonance, and the frequency modulation function is proportional to the external magnetic field. Importantly, the magnetic-field width of the resonance is always a fixed constant for a given Feshbach resonance.

In contrast, in the photoassociation process that we consider the field configuration is defined by two time-variable functions - the Rabi frequency and the frequency detuning of the applied optical laser field. In this case we have a large choice of field configurations due to the freedom in varying the Rabi frequency.

Thus, comparing the photoassociation process with the Feshbach resonance we note that in the case of photoassociation we have an additional degree of freedom. This is the Rabi frequency which can be varied independently. It is understood that this degree of freedom potentially may be useful for controlling the association process.

For instance, in the photoassociation process a major problem is caused by irreversible losses by several different physical mechanisms (spontaneous decay, correlated pairs, etc.). And the hope is that it will be possible to avoid the irreversible losses as well as other disadvantages by choosing a proper Rabi frequency.

And if we can avoid these disadvantages without an essential decrease in the freedom, we will get a tool which is more flexible compared with the Feshbach resonance.

Thus, in the present work we focus on the photoassociation which is currently considerably less explored. Discussing some theoretical aspects of this process, we specifically study the temporal dynamics of diatomic molecule formation by coherent photoassociation via one- or two-color schemes, (correspondingly, within two- or three-state models).

In both two- or three-state cases our mathematical analysis is based on a nonlinear system of coupled equations which was proposed in 1998-2000 simultaneously by two groups. Juha

Javanainen and coworkers proposed a simple scheme for molecule formation in an atomic BEC via photoassociation [48–51], and Peter Drummond et al. presented a quantum field theory describing coherent dynamics of coupled atomic and molecular BECs produced via photoassociation or Feshbach resonance [52].

The nonlinear *two-state* problem defined by the mentioned set of equations presents a theoretical basis for successful examination of a notable part of the available experimental data as discussed by many authors (see, e.g., Refs. [58] - [65]). However, for a deeper description of occurring physical processes, in many cases one needs a more elaborate approach involving at least *three states*. The necessity of such a generalisation is readily understood by noting that both Feshbach resonance and photoassociation lead to formation of molecules being in excited states, so that the formation of really ultracold molecules, i.e., those at deeply bound levels, remains an issue not described by the simple two-state model. The transition to the stable groud molecular state avoiding the irreversible losses from the weakly bound quasi-molecular state is one of the worthy topics of the research field that is possible to address only on the basis of at least three-state representations.

Approbation of the thesis statements

The statements of the thesis were presented and discussed at the seminars of the Institute for Physical Research, National Academy of Sciences of Armenia, at the Laboratoire Interdisciplinaire Carnot de Bourgogne, Université de Bourgogne, Dijon, France, as well as reported at the international conferences in Armenia, such as "IONS-2013" (Yerevan-Ashtarak, Armenia, 2013), "OPTICS-2012-2016" (Yerevan-Ashtarak, Armenia, 2012-2016), "Laser Physics-2013-2015" (Ashtarak, Armenia, 2013-2015) and "QuantArm-2014" (Yerevan-Tsaghkadzor, Armenia, 2014) [1–12].

The main results of the thesis have been published as 4 articles in peer reviewed journals and 8 abstracts in the conference book of abstracts represented in bibliography [1–12]. The thesis, which consists of introduction, four chapters and references, comprises 137 pages, contains 44 figures, 3 tables and 127 references.

In ***Chapter I*** we present the description of the nonlinear two-state system and discuss

the general properties of the transition from an atomic state to a molecular one. We propose a technique of robust adiabatic passage for a nonlinear quantum two-state system driven by a laser field, which provides an efficient transfer. By tracking the dynamics derived from a Hamiltonian formulation in the adiabatic limit we get the pulse characteristics. The dynamics is analyzed by determining the fixed points and separatrices.

It is shown that this nonlinear system does not have any solution that leads exactly to a complete population transfer in a finite time. For an infinite pulse area it can be reached only asymptotically.

The robustness of the derived technique with respect to the variations in the pulse area and detuning is anticipated to be a crucial property for practical implementations. The robustness for a particular implementation could necessitate optimizing the tracking specifically, as proposed for the linear case [66]. The achievement of an ultrahigh fidelity with an optimal exponential efficiency (see, for instance, [67]) is an open question.

In ***Chapter II*** the adiabatic tracking method is extended to models including Kerr nonlinearities. In the previous Chapter this tracking strategy was analyzed for a simplified model, which did not include elastic collisions between particles. In this Chapter the main point is to extend the analysis by including the Kerr nonlinearities. The developed tracking avoids the crossing of the fixed points and separatrix. This crossing is a main source of the molecular state's population decrease.

We note that in general the Kerr terms have some strong qualitative influence on the dynamics like the appearance of other hyperbolic points that can interfere with the desired tracking. Hence, one should obtain a particular suitable detuning that produces efficient tracking. Our main result is that it is still possible to have a good transfer and at the same time to avoid oscillations also in the presence of Kerr terms.

As it was already mentioned, for creation of a molecular BEC one needs to bring molecules to the ground state. Within the Rabi model, the particles stay in the weakly bound molecular state longer than in the atomic state. Hence, because of losses from that molecular state, the system will soon degrade. To avoid this, we need to bring the population to the ground

molecular state as fast as possible. There are various approaches for such a transfer. An advantageous one is the stimulated Raman adiabatic passage (STIRAP), which is a specific three-state field-matter interaction model.

Next, in ***Chapter III*** we consider the nonlinear STIRAP. The goal is to create a molecular Bose-Einstein condensate by coupling the initial pure-atomic state and the final molecular ground state by using a third, excited state of weakly bound molecules. We derive an efficient technique of stimulated Raman exact tracking for a nonlinear quantum system driven by external fields, which provides an efficient transfer from an atomic to a molecular Bose-Einstein condensate. The results show that for the transfer to be efficient, the technique features the need of a pump pulse to be stronger than the Stokes pulse, unlike the situation in the linear stimulated Raman adiabatic passage.

Since we have irreversible losses from the intermediate excited molecular state, we present a stimulated Raman exact tracking technique that takes into account this dissipation. We also show how to avoid the losses in the case of one- and two-photon resonances.

Further, we show the robustness for both linear and nonlinear STIRAP procedures.

In ***Chapter IV***, we note that the approximate solution of the nonlinear two-level problem for arbitrary field configuration is constructed by a two-term ansatz suggested earlier for the general case [68]. One term of this ansatz contains the main features of the nonlinear dynamics, and the second one is a correction obtained from a scaled linear model with changed parameters. Since the solution of the first term is known for all models, the problem is to study the second term. However, the exact solutions of the linear problem are very rare. Only 5 models are known, which are the Landau-Zener, Rosen-Zener, Demkov-Kunike, Nikitin and Crothers models.

To derive new exactly solvable linear models, we consider the cases when the linear two-level problem is reduced to the bi-confluent Heun equation. Discussing the solutions of this equation we construct an expansion of the bi-confluent Heun functions in terms of the incomplete Beta-functions and present an expansion in terms of the Hermite functions of non-integer order. We note that in general the latter functions are not polynomials.

We apply the constructed expansion to identify the field configurations for which the solution of the linear time-dependent two-state problem is written as a linear combination of a finite number of the Hermite functions.

Further, we identify the level-crossing bi-confluent Heun models for which the solution involves just two Hermite functions. We note that some of these models describe processes including losses from the upper level.

Finally, we present a particular exactly solvable level-crossing model for the quantum time-dependent linear two-state problem involving irreversible losses from the second level. The model is given by an exponentially varying Rabi frequency and a level-crossing detuning that starts from the exact resonance and exponentially diverges at the infinity. We derive the exact solution of the problem and discuss the dynamics of levels' populations of the system under different regimes of interaction.

Chapter 1

An efficient, robust adiabatic passage from an atomic to a molecular state

In the present Chapter we propose a technique of robust and efficient adiabatic passage for a nonlinear quantum two-state system driven by external optical fields to achieve the transfer from an atomic Bose-Einstein condensate to a molecular state. The pulse ingredients are obtained by tracking the dynamics derived from a Hamiltonian formulation, in the adiabatic limit. Its construction is based on a classical phase space representation, through the analysis of fixed points and separatrices

We prove the property that this nonlinear system does not have any solution leading exactly to a complete population transfer in a finite time. It can only be reached asymptotically for an infinite pulse area.

1.1 General model

Nonlinear quantum systems play an important role in contemporary physics, such as nonlinear optics and Bose-Einstein condensation (BEC). For instance, it has been established that the formation of molecules from ultracold atom gases by external fields are well described by a semiclassical mean-field Gross-Pitaevskii theory [69, 70]. More specifically, here we consider a model that includes third-order nonlinearities. The nonlinear collisions between

particles are important in the ultracold quantum degenerate atomic or molecular systems. A driven two-level model already features a very good approximation accounting for the one-color photoassociation and for magnetic Feshbach resonance [71–73]. This corresponds to the following set of nonlinear equations which include Kerr terms:

$$i\dot{a_1} = Ue^{-i\int^t \Delta(s)ds}\bar{a}_1 a_2 + (\Lambda_{11}|a_1|^2 + \Lambda_{12}|a_2|^2)a_1, \tag{1.1}$$

$$i\dot{a_2} = \frac{U}{2}e^{i\int^t \Delta(s)ds}a_1 a_1 + (\Lambda_{21}|a_1|^2 + \Lambda_{22}|a_2|^2)a_2, \tag{1.2}$$

where $a_1(t)$ and $\sqrt{2}a_2(t)$ are the atomic- and molecular-state probability amplitudes, respectively, satisfying the normalization condition $|a_1|^2 + 2|a_2|^2 = 1$, $U(t)$ is the (real) Rabi frequency associated to the external field, and the atom-atom, atom-molecule, and molecule-molecule elastic interactions are described by the terms proportional to the scattering lengths Λ_{11}, $\Lambda_{12} = \Lambda_{21}$, and Λ_{22}, respectively. In the photoassociation theory, the Rabi frequency is proportional to the amplitude of the photoassociating laser field, $\Delta(t)$ is the detuning: difference between the frequency of the atom-molecule transition and the chirped driving laser frequency [24].

In this Chapter, we first show the important result of nonexistence of a solution leading exactly to the complete population transfer in a finite time. The complete transfer occurs only for an infinite pulse area. By using the notation $\Omega(t) = \sqrt{2}U(t)$ and applying the transformation

$$a_1 = c_1 e^{-i\int \Delta(s)ds/3}, \qquad a_2 = c_2 e^{i\int \Delta(s)ds/3},$$

we can recast Eqs. (1.1) and (1.2) in the following form

$$i\dot{c_1} = \frac{\Omega(t)}{\sqrt{2}}\bar{c}_1 c_2 + \left[-\frac{\Delta(t)}{3} + \Lambda_{11}|c_1|^2 + \frac{\Lambda_{12}}{2}|c_2|^2\right]c_1, \tag{1.3}$$

$$i\dot{c_2} = \frac{\Omega(t)}{2\sqrt{2}}c_1 c_1 + \left[\frac{\Delta(t)}{3} + \Lambda_{21}|c_1|^2 + \frac{\Lambda_{22}}{2}|c_2|^2\right]c_2, \tag{1.4}$$

with the normalization condition $|c_1|^2 + 2|c_2|^2 = 1$. We define $P = 2|c_2|^2$ and $|c_1|^2 = 1 - P$.

The function c_1 is interpreted as the atomic state probability amplitude and the function $\sqrt{2}c_2$ as the molecular state probability amplitude. Hence, we refer to $|c_1|^2$ as the atomic state probability and to $P = 2|c_2|^2$, as the molecular state probability. We will consider a condensate being initially in all-atomic state: $|c_1(-\infty)| = 1$, $|c_2(-\infty)| = 0$.

1.1.1 Analysis of the model without Kerr nonlinearities

1.1.1.1 Hamiltonian formulation

An adiabatic treatment of a nonlinear model, which will allow the extension of the standard adiabatic passage in linear models, can be accomplished by a classical Hamiltonian formulation of the problem. For (1.3) and (1.4) we can write the equations of motion as

$$i\frac{\partial c_1}{\partial t} = \frac{\partial H}{\partial \bar{c_1}},$$

$$i\frac{\partial c_2}{\partial t} = \frac{\partial H}{\partial \bar{c_2}}$$

with a Hamiltonian, given by

$$H = -\frac{\Delta}{3}|c_1|^2 + \frac{\Delta}{3}|c_2|^2 + \frac{\Omega}{2\sqrt{2}}(c_1^2\bar{c_2} + \bar{c_1}^2 c_2) \tag{1.5}$$

The complex variables c_j can be written in terms of standard real canonical coordinates p_j, q_j as

$$c_j = \frac{(q_j + ip_j)}{\sqrt{2}}$$

Another pair of variables I_j and φ_j, defined from $c_j = \sqrt{I_j}e^{-i\varphi_j}$ are canonically conjugate:

$$\{I_j, I_k\} = 0; \qquad \{\varphi_j, \varphi_k\} = 0;$$

$$\{I_j, \varphi_k\} = \delta_{jk}$$

A new pair of angle variables (γ, α) can be determined from the original angles (φ_1, φ_2) by the following canonical transformation of coordinates (J, γ, I, α) :

$$\gamma = \varphi_1,$$

$$\alpha = -2\varphi_1 + \varphi_2,$$

$$J = I_1 + 2I_2,$$

$$I = I_2,$$

since they satisfy Poisson bracket relations $\{J, \gamma\} = 1$, $\{I, \alpha\} = 1$ and the other brackets are zero.

The solution of (1.3) and (1.4) can be thus parametrized in the most general way as:

$$c_1 = \sqrt{J - 2I}e^{-i\gamma},$$

$$c_2 = \sqrt{I}e^{-i(\alpha+\gamma)}e^{-i\gamma},$$

where γ is the global phase of the wave function, $\alpha + \gamma$ is its internal relative phase. $P = 2I$ corresponds to the probability of the molecular state.

With the mentioned variables the Hamiltonian reads:

$$H = -\frac{\Delta}{3}J + \Delta I + \frac{\Omega}{\sqrt{2}}(J - 2I)\sqrt{I}\cos\alpha \tag{1.6}$$

The corresponding equations of motion, using $J = 1$, are

$$\dot{J} = -\frac{\partial H}{\partial \gamma} = 0, \tag{1.7}$$

$$\dot{I} = -\frac{\partial H}{\partial \alpha} = \frac{\Omega}{\sqrt{2}}(1 - 2I)\sqrt{I}\sin\alpha, \tag{1.8}$$

$$\dot{\alpha} = \frac{\partial H}{\partial I} = \Delta + \frac{\Omega}{2\sqrt{2}}\frac{1 - 6I}{\sqrt{I}}\cos\alpha, \tag{1.9}$$

$$\dot{\gamma} = \frac{\partial H}{\partial J} = -\frac{\Delta}{3} + \frac{\Omega}{\sqrt{2}}\sqrt{I}\cos\alpha = 0. \tag{1.10}$$

We see that the Hamiltonian is independent of γ. This allows one to define a reduced phase space of only two dimensions (I, α), and γ is determined from Eq. (1.10).

We notice, that the angle α is not well defined for $I = 0$, nor for $I = 1/2$. This is similar to the linear two-state problem formulated on the Bloch sphere, on which the angle at the poles is not well defined.

1.1.2 Necessity of infinite pulse area for the complete transition to a molecular state

The main goal of the present Chapter is to analyze the dynamics of coherent molecule formation for different external field configurations. We start from Eq. (1.8)

$$\dot{I} = \frac{\Omega}{\sqrt{2}}(1-2I)\sqrt{I}\sin\alpha.$$

Integrating (1.8) we obtain

$$\int_0^I \frac{dI'}{(1-2I')\sqrt{I'}} = \int_{t_0}^t \frac{\Omega(s)}{\sqrt{2}}\sin\alpha(s)ds.$$

By using the notations $y = \sqrt{I'}$, $I' = y^2$ we get:

$$\int_0^{\sqrt{I}} \frac{2ydy}{(1-2y^2)y} = \frac{1}{\sqrt{2}}\int_{t_0}^t \Omega(s)\sin\alpha(s)ds.$$

Doing some simplifications we can write

$$\int_0^{\sqrt{I}} \frac{dy}{1-2y^2} = \frac{1}{2\sqrt{2}}\int_{t_0}^t \Omega(s)\sin\alpha(s)ds$$

After integration we have

$$\tanh^{-2} P(t) = \frac{1}{2} \int_{t_0}^{t} \Omega(s) \sin\alpha(s) ds$$

Thus, we get the following equation for $P(t)$

$$P(t) \equiv 2I(t) = \tanh^2 \left[\int_{t_i}^{t} \frac{\Omega(s)}{2} \sin\alpha(s) ds \right]. \tag{1.11}$$

It shows directly the remarkable result that the targeted molecular state $P(t) = 1$ can be reached only asymptotically, i.e. for $\int_{t_i}^{t_f} \Omega(s) \sin\alpha(s) ds \to \infty$, which is possible only for an infinite pulse area, and with $0 < \alpha(t) < \pi$ for large times [1].

A crossing model [74] leads also to a complete transfer in the limit of infinite pulse area (adiabatic limit), like in the corresponding linear problem. However, unlike the corresponding linear problem, near the end of the process, the transfer becomes oscillatory due to the crossing of a separatrix which strongly reduces the expected efficiency [75–77]: a much larger pulse area is needed to reach the same efficiency as in the corresponding linear model.

We can notice that an infinite area is not a sufficient condition since $\sin(\alpha)$ can be positive or negative. In absence of third-order nonlinearities, and for $\Delta = 0$, which corresponds to the Rabi model, a solution is given by $\alpha = \pi/2$. One can notice, that Eq. (1.11) shows that the Rabi model is the most efficient one in terms of accuracy for a given pulse area. In the linear case the π-pulse area corresponds to the smallest pulse area leading to a complete transfer [78].

1.2 Adiabatic tracking

1.2.1 Adiabatic theorem

We start with explanation of quantum adiabatic process, which we can define as: gradually changing conditions allow the system to adapt its configuration, hence the probability density is modified by the process. If the system starts in an eigenstate of the initial Hamil-

tonian, it will end in the corresponding eigenstate of the final Hamiltonian. Thus, it will follow the corresponding instantaneous eigenstate of the slowly varying Hamiltonian [79].

The classical adiabatic theorem states that the instantaneous action variables are adiabatic invariants. If the initial condition is an instantaneous elliptic fixed point, then in the adiabatic limit, the solution follows the corresponding instantaneous fixed point, provided that it does not cross other fixed points.

The classical adiabatic theorem for a system with one degree of freedom is generally presented [80–82] as the statement that the action variable is an adiabatic invariant, i.e. it stays constant in the asymptotic limit when the parameters of the system are slowly varying.

The relation between the classical and the quantum adiabatic theorem can be explained by considering the example of a two-level system, i.e. four dimensional phase space. After a change of coordinates, as we did in the nonlinear case, we can determine a reduced phase space of two dimensions. The eigenvectors from the four dimensional phase space correspond to fixed points in the two dimensional reduced phase space.

The adiabatic theorem that we apply in this work, in the adiabatic limit $T \to \infty$, is a particular case of this general adiabatic theorem [83], for which the initial condition is a stable fixed point and the value of the corresponding action variable is equal to zero. The statement that the value of the action variable stays constant implies in this case that the adiabatic evolution follows the instantaneous stable fixed points. The adiabatic evolution breaks down when there is a bifurcation, in which the followed stable elliptic fixed point crosses an unstable hyperbolic fixed point and becomes itself hyperbolic.

1.2.2 Adiabatic passage for nonlinear systems and adiabatic tracking

The idea of adiabatic tracking is that first we choose a pulse shape $\Omega(\frac{t}{T})$ and a molecular population evolution $P_{track}(t) = f(\frac{t}{T})$ that one wishes to follow, then we find $\Delta_{track}(\frac{t}{T})$ such that the exact solution $P(t)$ of the equation defined by $\Omega(\frac{t}{T})$ and $\Delta_{track}(\frac{t}{T})$, in the adiabatic limit $T \to \infty$ approache is $P(t) \to P_{track}(t)$.

In order to achieve this goal, by the first step we have to determine $\Delta_{track}(\frac{t}{T})$ such, that the conditions for the adiabatic theorem (stated in the next section) are satisfied, i.e. the instantaneous fixed point must have no crossing of a separatrix (nor other fixed points), and should satisfy $P(t) = P_{track}(t)$.

For Eqs. (1.8)-(1.10), (see for instance [1]) adiabatic passage can be defined as follows: For a sufficiently slow evolution of the parameters Ω and Δ, featured by the quantity $1/T$ (where T is characteristic duration), i.e. satisfying $1/T << \omega_d$ with ω_d a typical frequency of the dynamics, the solution follows the instantaneous fixed points of the reduced phase space, given by $\dot{I} = 0$ and $\dot{\alpha} = 0$ at the considered instantaneous values Ω and Δ. The obstacles to the adiabatic following come

1. from regions surrounding the instantaneous separatrices involving arbitrary small frequencies for the dynamics,

2. from the crossing of fixed points.

The conditions of validity of the adiabatic theorem are thus met if the adiabatically followed fixed point does not cross any separatrix nor other fixed points, in the same manner as crossing of eigenvalues has to be avoided in linear models.

The second step is to verify if the dynamics defined by this $\Omega(t)$, $\Delta_{track}(t)$ satisfies the conditions of validity of the adiabatic theorem. We should choose $I_{track}(t)$ and $\Delta_{track}(t)$, such that the conditions for the validity of the adiabatic theorem are satisfied, no crossing of separatrices, nor of other fixed points. Thus, the main point is to verify whether there is a crossing of the tracked fixed point (which starts out as a stable elliptic fixed point) and other fixed points of hyperbolic type.

Below, we determine the fixed points and the separatrices, and show that any adiabatic solution $I_{track}(t)$, which satisfies the appropriate initial and final conditions $I(t_i) = 0$ and $I(t_f) = 1/2$, can be obtained by a choice of $\Omega(t)$ and $\Delta_{track}(t)$ satisfying the conditions of the adiabatic theorem. This is referred as an *adiabatic tracking*.

1.2.3 Determination of fixed points

In this section we start with fixed points

$$0 = \dot{I} = \frac{\Omega}{\sqrt{2}}(1-2I)\sqrt{I}\sin\alpha, \tag{1.12}$$

$$0 = \dot{\alpha} = \Delta + \frac{\Omega}{2\sqrt{2}}\frac{1-6I}{\sqrt{I}}\cos\alpha. \tag{1.13}$$

For $I = 0,\ 1/2$ the angle α is not defined. $I = 1/2$ is a hyperbolic (unstable) fixed point. For $I \neq 0$ (1.13) can be written as

$$2\sqrt{2}\sqrt{I}\Delta + (\Omega - 6\Omega I)\cos\alpha = 0 \tag{1.14}$$

For given values Ω and Δ, the fixed points corresponding to $\dot{\alpha} = 0$, $\dot{I} = 0$ are determined by the relation

$$\Delta = -\frac{\Omega}{2\sqrt{2}}\frac{1-6I}{\sqrt{I}}e^{i\alpha}; \qquad \alpha = 0, \pi \tag{1.15}$$

Thus, for a given $P_{track}(t)$ and $\Omega(t)$, adiabatic limit $lim_{1/T\to 0}P(t) - P_{track}(t) = 0$, i.e. for $\Delta(t)$ from (1.15) the solution $P(t)$ will track $P_{track}(t)$ in the adiabatic limit, if there is no intersection with a separatrix.

Since $P = 2I$, we can present Eq. (1.15) also as:

$$\Delta = -\frac{\Omega}{2}\frac{1-3P}{\sqrt{P}}e^{i\alpha} \tag{1.16}$$

where $P(t)$ is the probability of a molecular state.

From Eq. (1.14) we can find I as a function of detuning $\Delta(t)$ and the coupling $\Omega(t)$. For the fixed point (I_0, $\alpha = 0$) we can write

$$\Delta\sqrt{I_0}2\sqrt{2} + \Omega - 6\Omega I_0 = 0. \tag{1.17}$$

For $\alpha = 0$ we will get

$$I_0 = \frac{1}{18}(2\mu^2 + 3 + 2\mu\sqrt{\mu^2+3}), \qquad \mu = \frac{\Delta}{\Omega} \tag{1.18}$$

and similarly for $\alpha = \pi$:

$$I_\pi = \frac{1}{18}(2\mu^2 + 3 - 2\mu\sqrt{\mu^2+3}). \tag{1.19}$$

1.2.4 Global coordinates of the reduced phase space

From the previous section we know that α is not defined in the points $I = 0, 1/2$. However, we need $I = 0$, because it is an initial condition and, according to the adiabatic theorem, if the initial condition is a fixed point, the solution follows this fixed point.

Since α is not defined in the points when $I = 0, 1/2$, we need global coordinates, which are well defined everywhere. Such coordinates are [84]:

$$\Pi_0 \equiv J = |c_1|^2 + 2|c_2|^2, \tag{1.20}$$

$$\Pi_1 = |c_1|^2 - 2|c_2|^2, \tag{1.21}$$

$$\Pi_2 = 2(c_1^2\bar{c_2} + \bar{c_1}^2 c_2), \tag{1.22}$$

$$\Pi_3 = -2i(c_1^2\bar{c_2} - \bar{c_1}^2 c_2). \tag{1.23}$$

Instead of Π_1 we will use

$$P = \frac{1 - \Pi_1}{2}.$$

For $J = 1$ the three coordinates satisfy the relation

$$\Pi_2^2 + \Pi_3^2 = 8(1-P)^2 P.$$

This equation defines the nonlinear generalized Bloch sphere [84], which is the reduced

phase space of the model. The coordinates of the fixed points ($\alpha_0 = 0$, P_0) are

$$P_0 = \frac{1}{18}(2\mu^2 + 3 + 2\mu\sqrt{\mu^2+3}),$$

$$\Pi_{2,0} = \frac{4}{\sqrt{2}}(1-P_0)\sqrt{P_0},$$

$$\Pi_{3,0} = 0. \tag{1.24}$$

We choose these coordinates, because they are defined everywhere. At the points, where α is well defined, the relation with these global coordinates is

$$P = 2|c_2|^2,$$

$$\Pi_2 = 2(c_1^2\bar{c_2} + \bar{c_1}^2 c_2) = \frac{4}{\sqrt{2}}(1-P)\sqrt{P}\cos\alpha,$$

$$\Pi_3 = -2i(c_1^2\bar{c_2} - \bar{c_1}^2 c_2) = \frac{4}{\sqrt{2}}(1-P)\sqrt{P}\sin\alpha,$$

with the constraint $\Pi_2^2 + \Pi_3^2 = 8(1-P)^2 P$.

1.2.5 Separatrix

For the Hamiltonian (1.25)

$$H = -\frac{\Delta}{3} + \Delta I + \frac{\Omega}{\sqrt{2}}(1-2I)\sqrt{I}\cos\alpha \tag{1.25}$$

separatrices are curves I_s, α_s in the reduced phase space of energy H_s passing through the hyperbolic fixed point, i.e. $I = 1/2$. From Eq. (1.25), if we put $I = 1/2$, we obtain

$$H_s = \frac{\Delta}{6},$$

and thus the equation for the separatrix is

$$\frac{\Delta}{6} = -\frac{\Delta}{3} + \Delta I_s + \frac{\Omega}{\sqrt{2}}(1-2I_s)\sqrt{I_s}\cos\alpha_s,$$

which leads to $(1-P_s)(\Delta - \Omega\sqrt{P_s}\cos\alpha_s) = 0$. We can thus write the equation for the separatrix as:

$$\cos\alpha_s = \mu\frac{1}{\sqrt{P_s}}, \qquad \mu \equiv \frac{\Delta}{\Omega}. \tag{1.26}$$

From this equation we can conclude that since $|\cos\alpha_s| \leq 1$, $\frac{\mu^2}{P_s} \leq 1$, we can write $P_s \geq \mu^2$.

Both, the separatrix and the hyperbolic fixed point exist only when $|\mu| \leq 1$ with $\mu^2 \leq P_s \leq 1$.

For $\mu > 0$, the coordinates of the separatrix on the nonlinear Bloch sphere can be parameterized by:

$$P_s \in [\mu^2, 1],$$

$$\Pi_{2,s} = \frac{4}{\sqrt{2}}(1-P_s)\mu,$$

$$\Pi_{3,s} = \pm\frac{4}{\sqrt{2}}(1-P_s)\sqrt{P_s-\mu^2}.$$

1.2.6 Conditions for non-crossing of separatrix

According to the Eq. (1.24) the fixed points lie on the plane $\Pi_{3,0} = 0$. Therefore, we have to determine the intersection of the separatrix with this plane to determine under which conditions there is a crossing.

The separatrix intersects the plane Π_3 at two points: $P = 1$ and at a second point whose coordinate P we denote by Q_s. This point has the coordinates

$$P = Q_s = \mu^2, \tag{1.27}$$

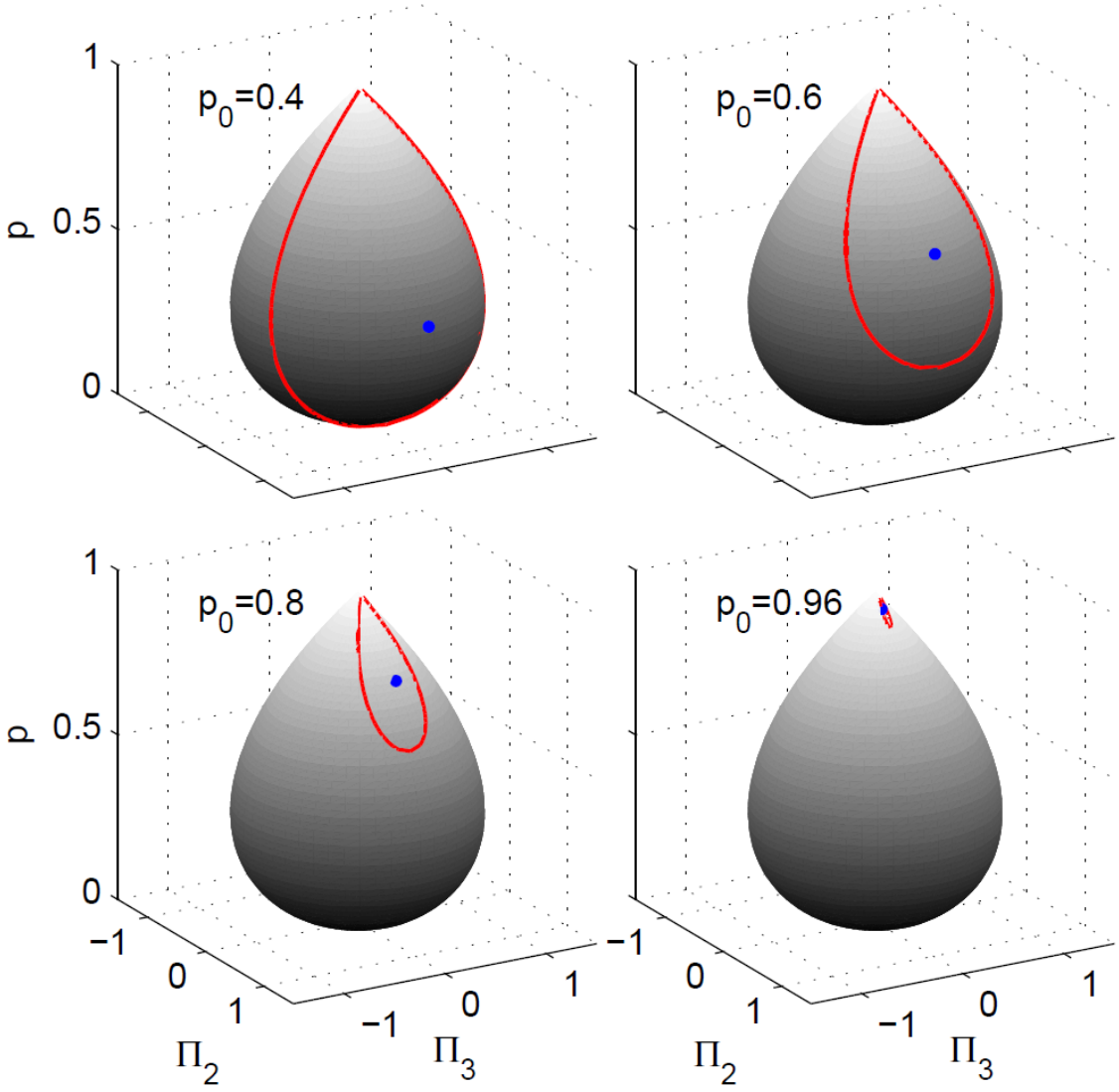

Figure 1.1: Representation of the fixed point (1.15) with $\alpha = 0$ for $P = P_0 = 0.4, 0.6, 0.8, 0.96$ and the corresponding separatrix curve (1.26), (1.29) on the nonlinear generalized Bloch sphere.

$$\Pi_{2,s} = \frac{4}{\sqrt{2}}(1-\mu^2)\mu,$$

$$\Pi_{3,s} = 0,$$

and for the fixed point we have the equation

$$\mu^2 = \frac{(3P_0 - 1)^2}{4P_0}. \tag{1.28}$$

Thus, the condition for a crossing of the fixed point and the separatrix is

$$Q_s = \mu^2 = \frac{(3P_0 - 1)^2}{4P_0}. \tag{1.29}$$

If we put $Q_s = P_0$ in the Eq. (1.29), solutions will be $P_0 = 1$ and $P_0 = 1/5$, but the latter is excluded since it gives $\mu < 0$.

For $\mu < 0$, $\Pi_{2,s}$ is negative, which excludes the intersection of the fixed point with the separatrix. Thus we get $Q_s \leq P_0$, where the equality arises only for $P = 1$. Thereby, there is no crossing between the fixed point I_0 and the separatrix except for $\mu = 1$.

1.2.7 Implications of the choice of $\Delta(t)$, $\Omega(t)$

We want to choose $\Omega(t)$ and $\Delta(t)$ such that

1. $(\alpha_0,\ I_0)$ is the fixed point followed by the adiabatic dynamics, with initial condition $I = 0$. From Eq. (1.12) for the fixed point this condition is satisfied if $\Omega(t_i) = 0$ and $\Delta(t_i) < 0$, where t_i is the initial time.

2. $\lim_{t\to\infty} I_0(t) = 1$. This is satisfied if $\mu(t) \to 1$, when $t \to \infty$.

3. There are no crossings of the fixed point and the separatrix at any finite time. This is satisfied if $|\mu(t)| < 1$ for all times t.

If we choose $\mu(t) = \frac{\Delta}{\Omega}$ such, that $\mu(t) < 1$ for all finite t and $\mu(t) \to 1$ for $t \to \infty$ there will be no crossing of the fixed point with the separatrix.

Remark: When the fixed point disappears by collision with the hyperbolic point, the adiabatic approximation is not valid anymore, and this leads to strong oscillations. If the approach $\frac{\Omega(t)}{\Delta(t)} \to 1$ at the final time $t \to \infty$ is sufficiently slow, one can expect that there will be no non-adiabatic effects due to the separatrix. There will just be the usual non-adiabatic corrections due to the finite rate of variation of the parameters.

1.2.8 Properties of adiabatic tracking

The principle of adiabatic tracking is that first we choose $\Omega(\frac{t}{T})$ and $P_{track}(t) = f(\frac{t}{T})$. Then we find $\Delta_{track}(\frac{t}{T})$ such, that the solution $P(t)$ of the equation defined by $\Omega(\frac{t}{T})$, $\Delta_{track}(\frac{t}{T})$ in the adiabatic limit $T \to \infty$, $P(t) \to P_{track}(t)$.

In order to reach this aim we should choose $\Delta(\frac{t}{T})$ such, that the conditions for the adiabatic theorem are satisfied, i.e. the instantaneous fixed point must have no crossing of separatrix (nor other fixed points).

A possible choice consists in choosing $P(t)$ such that the transfer tracks the solution given by the linear case, in the adiabatic limit. This is achieved if one takes $\Omega(t)$ and the probability $P(t)$ from the corresponding linear model and determine the nonlinear $\Delta(t)$ from Eq. (1.15). This allows one to define the corresponding nonlinear tracking models from a given linear crossing model, whose dynamics is expected follow closely the corresponding $P(t)$ dynamics in the adiabatic limit.

We want to determine $\Delta(t)$ for a chosen equation $P_{track}(t) = P_L(t)$ from a linear model and $\Omega(t)$ such that

1. the adiabatic approximation has no crossing of separatrix in finite times,

2. the adiabatic approximation reaches $P = 1$ for $t \to \infty$,

3. the adiabatic approximation is on a fixed point of the instantaneous Hamiltonian at each t.

Remark: In the linear case adiabatic tracking is always possible. The only thing that has to be avoided is the crossing of eigenvalues at finite times.

For linear two level systems with trace $H = 0$ the two eigenvalues cross only if $H(t_i) = 0$ (if $\Omega(t_0) = 0$, $\Delta(t_i) = 0$).

Most of the usual models have a crossing of the separatrix, at finite times. For instance, the Demkov-Kunike model.

1.3 The Rabi model for linear and nonlinear cases

In the present section, we present the Rabi model for the linear and the nonlinear cases and describe their main characteristics. This model has the feature, that both the linear

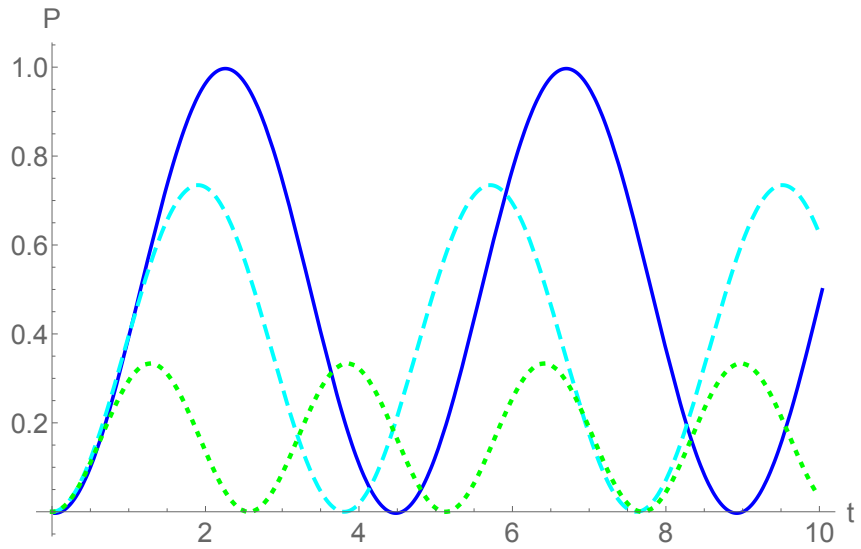

Figure 1.2: The linear Rabi model, resonance case, $\Omega_0 = 1$. The solid, dashed and dashed-point lines correspond to $\delta_t = 0, 0.85, 2$.

[85, 86] and nonlinear set of equations for two-level system are exactly solvable. The Rabi model [87] is the simplest possible model, for which the Rabi frequency and detuning are constant:

$$\Omega(t) = \Omega_0, \qquad \delta_t(t) = \delta_0. \tag{1.30}$$

where $\Omega(t)$ is the Rabi frequency and $\delta_t(t)$ is the detuning. The solution of the problem is written as:

$$(P')^2 = P[\Omega_0^2(1-2P)^2 - \delta_0^2 P]. \tag{1.31}$$

One can see, that in the case of the linear Rabi problem the probability to occupy a certain state is an oscillatory periodic function of time for any Ω_0 and δ_0 (Fig. 1.2). Whereas, in the nonlinear resonance case, where $\delta_0 = 0$ for certain initial conditions this probability increases monotonically (Fig. 1.3). The details of the nonlinear Rabi problem solution is presented in Ref. [87].

In absence of third-order nonlinearities, the Rabi model leads to a complete transfer

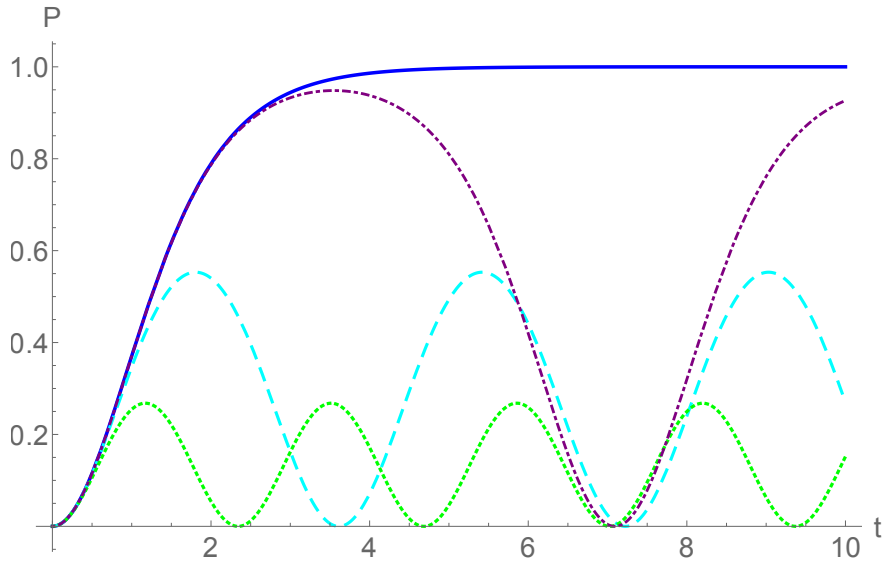

Figure 1.3: The nonlinear Rabi model, $\Omega_0 = 1$. The solid, dashed and dashed-point lines correspond to $\Delta_0 = 0, 0.075, 0.85, 2$.

($|a_2(t_f)|^2 = 1/2$ with t_f the final time) only asymptotically, in the limit of an infinite pulse area. The transfer is monotonic in time only for the exact resonance $\Delta = 0$.

Both, in the linear and nonlinear Rabi model there exist big oscillations of time, there are not oscillations only in the nonlinear resonance case (see Fig. 1.3), however, the process in the later case is not robust.

1.4 Adiabatic tracking. Example of linear Demkov-Kunike model

The adiabatic dynamics can be designed by the tracking of a desired function $P(t)$. A possible choice, in the adiabatic limit, consists in choosing $P(t)$ such, that the transfer tracks the solution given by the linear case. This is achieved if one takes the probability $P(t)$ and $\Omega(t)$ from the corresponding linear model and determines the nonlinear $\Delta(t)$ from Eq. (2.20). This allows to define the corresponding nonlinear tracking models from a given linear crossing model [88–90].

This procedure is numerically shown in Fig. 1.4 for a specific example. We consider a

Demkov-Kunike model for the corresponding linear model which has a symmetric detuning:

$$\Omega(t) = \Omega_0 \mathrm{sech}(t/T), \qquad \Delta_{lin}(t) = B \tanh(t/T) \tag{1.32}$$

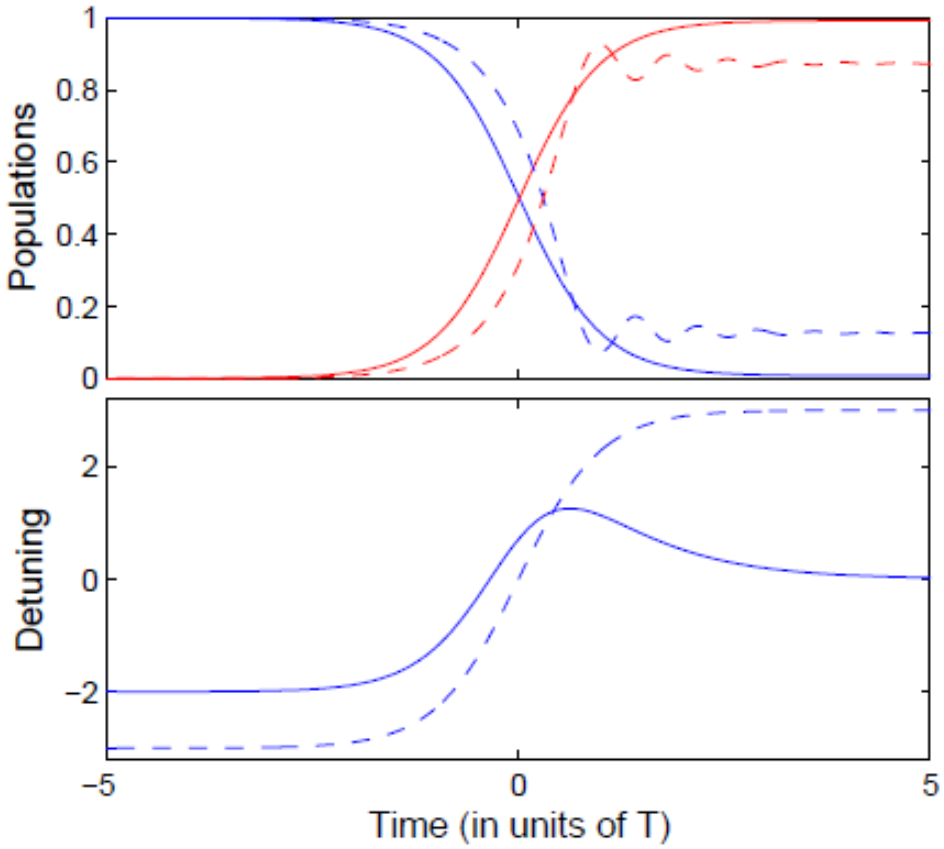

Figure 1.4: Numerical solution for (1) the DKAT model (solid line): $\Omega(t) = \Omega_0 \mathrm{sech}(t/T)$ with $\Omega_0 T = 6$ and $\Delta(t)$ (in units of $1/T$) determined from (1.15) with the tracked solution $P(t)$ (1.29), and (2) the standard nonlinear Demkov-Kunike model (dashed line), i.e. with $\Delta(t) = B \tanh(t/T)$, $BT = 9$ (both with $\Lambda_{ij} = 0$). Upper: Populations $P(t)$. Lower: Chirped detuning. The superiority of the asymmetric DKAT detuning is shown.

We consider the special choice $B = \frac{3\Omega_0}{2}$.

In the adiabatic limit $\Omega_0 T >> 1$ one has

$$P(t) = \sin^2 \left[\int_{t_i}^{t} \mathrm{sech}(s/T) ds/2T \right] \tag{1.33}$$

For the numerics, we use the above $\Omega(t)$, and the modified detuning $\Delta_{track}(t)$ from Eq. (2.20) (with $\alpha = 0$), which defines the corresponding nonlinear Demkov-Kunike adiabatic tracking model (DKAT).

Fig. 1.4 shows the detuning falling to zero near the end of the dynamics, when the pulse is switched off.

1.5 Analysis of robustness. Comparison with the Rabi model

In this section we compare the robustness of the Rabi model and of the adiabatic tracking technique. First we show that the Rabi solution is strongly non-robust with respect to the detuning or to the presence of third-order nonlinearities. Then we show that adiabatic tracking is robust with respect to the variation of these parameters.

The pulse ingredients are obtained by tracking the corresponding classical dynamics derived from a Hamiltonian formulation, in the adiabatic limit. This leads to a non-symmetric and non-monotonic chirp: the pulse parameters start, as in the linear case, out of resonance, but end at the resonance (these all are in the case of the absent of third-order nonlinearities).

The Rabi model (for $\Delta = 0$) gives the highest fidelity molecular BEC transfer for a given pulse.

The presence of a non-zero detuning, or of third-order nonlinearities, induces in general oscillations in the integral of (1.11) due to $\sin\alpha$, which ruins the fidelity of the Rabi model.

This can be seen in Fig. 1.5 displaying the transfer profile as a function of a constant detuning Δ_0 for a Rabi model. The excitation profile oscillates more and more for a larger pulse area.

The robustness of the tracking technique, with respect to the pulse area (as in traditional adiabatic techniques for linear problems) and with respect to a static detuning (see Fig. 1.5), is anticipated to be a decisive property for practical implementations.

Robustness for a particular implementation could necessitate optimizing the tracking

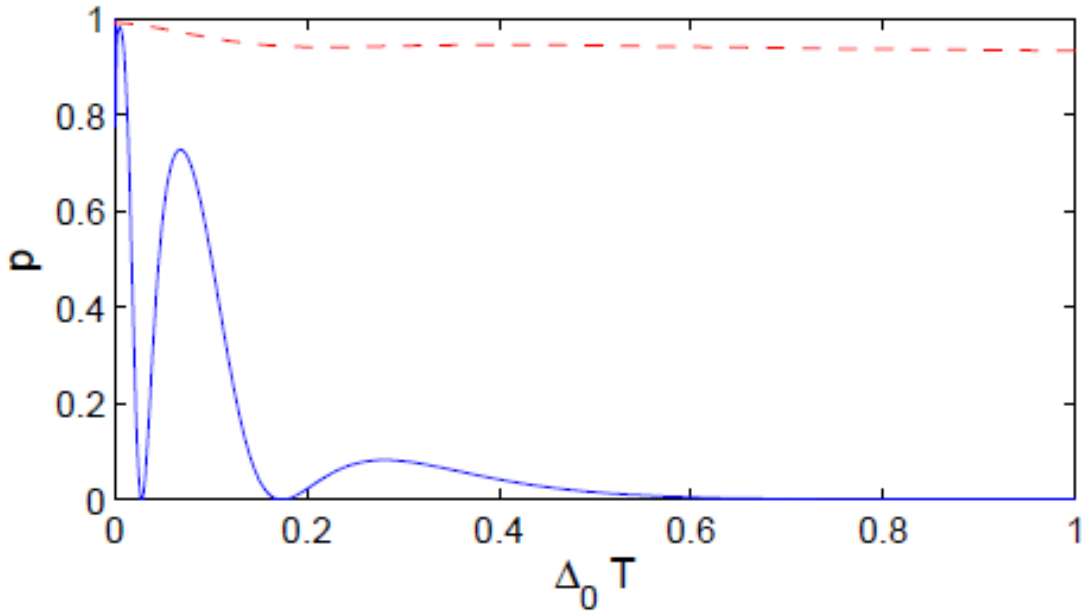

Figure 1.5: Robustness of the final transfer probability $P = 2|c_2(t_f)|^2 = 2I(t_f)$ as a function of a static detuning Δ_0 (in units of $1/T$) for $\Omega(t) = \Omega_0 \mathrm{sech}(t/T)$ with $\Omega_0 T = 3$, $\Lambda_{ij} = 0$ and the detuning $\Delta(t) + \Delta_0$ with (1) $\Delta(t) \equiv 0$ (the Rabi model, solid line) and (2) $\Delta(t)$ [(1.15) with $\alpha = 0$], $P(t)$ (1.33) (Demkov-Kunike nonlinear tracking model, dashed line).

specifically, as recently proposed for the linear case [91, 92].

1.6 Conclusion

In conclusion, we have studied the nonlinear dynamics of molecule formation by coherent photo- and magneto-association of an atomic Bose-Einstein condensate. We have studied a condensate initially in the all-atomic state, applying classical adiabatic theory. At first, we have discussed the classical phase space of the time-independent version of the problem in terms of the canonically conjugate variables α, I, that allow to describe the dynamics in a two-dimensional reduced phase space.

Taking into account that the considered initial condition corresponds to a fixed point, zero initial action, we obtain $P(t)$.

Further, we have derived an efficient and robust adiabatic passage technique based on the

tracking of a desired evolution scenario rather than imposing the parameters.

More generally, optimizing the tracking should be researched in order to improve the fidelity and/or the robustness. The proposed method can be applied for other types of nonlinearities, such as the ones described in [75] or in nonlinear optics [107]. One can also treat more complicated problems, such as Λ systems with stimulated Raman processes. The resulting non-monotonic chirps can be nowadays implemented in any timescale regime, even in the picosecond and subpicosecond regimes where the pulse has to be shaped in the spectral domain [94].

Thus, for a driven nonlinear quantum two-state system we present a technique of robust and efficient adiabatic passage, which provides the transfer to a molecular state from an atomic one by external optical fields. In the adiabatic limit we also obtained pulse parameters, by tracking the dynamics derived from a Hamiltonian formulation.

The robustness of the derived technique, with respect to the pulse area and with respect to a static detuning, is anticipated to be a decisive property for practical implementations. Robustness for a particular implementation could necessitate optimizing the tracking specifically, as proposed for the linear case [91]- [92]. The achievement of an ultrahigh fidelity with an optimal exponential efficiency (see, for instance, [95]) is an open question.

We have shown that this nonlinear system does not have any solution that leads exactly to the complete population transfer in a finite time. For an infinite pulse area it can be reached only asymptotically.

In [1] it was shown that in the model without Kerr terms the tracking solution can be chosen such, that there are no crossings with other fixed points at finite times when the laser amplitude is non-zero, and thus the adiabatic approximation is justified and one obtains an efficient tracking with the desired behaviour.

Chapter 2

Adiabatic tracking for molecule production in atomic Bose-Einstein condensates with Kerr nonlinearities

In this Chapter we consider the influence of the third-order nonlinearities on the nonlinear two-state dynamics. The third-order Kerr terms lead to a modified separatrix and fixed points.

We derive the equation for the probability $P(t)$ as a function of the Rabi frequency $\Omega(t)$ and an evolution phase $\alpha(t)$. The equation is of the same form as the equation for $P(t)$ from the previous Chapter, i.e. the Kerr terms do not modify this equation.

We show, that the inclusion of Kerr terms can produce qualitatively important modifications in the adiabatic dynamics, in which the trajectory that is being tracked losses its stability, so that the adiabatic theorem does not apply anymore. Thus, the adiabatic transfer can be strongly degraded. We show, however, that this degradation can either be compensated by using fields that are strong enough compared with the values of the Kerr nonlinearities if $\alpha = 0$ or can be avoided by taking a different branch of the tracking detuning corresponding to the choice $\alpha = \pi$.

Thus, the main result is that, despite the potentially detrimental features caused by the

Kerr nonlinearities, there always is a choice of the detuning that leads to an efficient adiabatic tracking, even for a relatively weak fields.

The details of the development are as follows: In the case $\alpha = 0$ there is an unavoidable crossing of the tracking fixed point with another fixed point, after which the tracking fixed point becomes hyperbolic, destroying the adiabaticity. In order to have a good transfer and suppress the oscillations one needs to take $\Omega_0 \gg \Lambda_s$, where Ω_0 is the peak Rabi frequency of the associating lase field and Λ_s is an effective Kerr coefficient standing for the combined action of the atom-atom, atom-molecule, and molecule-molecule elastic scattering described by the third-order nonlinear Kerr terms. In this case we have a crossing of the separatrix only at the end of the process, as it was in the model without Kerr nonlinearities. Thus, we have an efficient transfer, without oscillation and crossing.

A further important observation is that the other possible choice of the detuning for tracking, the one with $\alpha = \pi$, leads to a stable adiabatic transfer to the target state for arbitrary input parameters of the problem, that is, for the parameters involved in the Rabi frequency and in the Kerr nonlinearities.

In summary, the main result of this Chapter is that in the presence of the Kerr terms it is still possible to construct a detuning that leads to an efficient tracking for the chosen population dynamics.

2.1 Nonlinear two-level model with Kerr terms

In the present section, we consider a two-state model including the third-order nonlinearities given as [96]:

$$i\dot{a_1} = Ue^{-i\int^t \Delta(S)dS}\bar{a_1}a_2 + (\Lambda_{11}|a_1|^2 + \Lambda_{12}|a_2|^2)a_1, \tag{2.1}$$

$$i\dot{a_2} = \frac{U}{2}e^{i\int^t \Delta(S)dS}a_1a_1 + (\Lambda_{21}|a_1|^2 + \Lambda_{22}|a_2|^2)a_2 \tag{2.2}$$

with the first integral $J = |a_1|^2 + 2|a_2|^2 = 1$. Here a_1 and $\sqrt{2}a_2$ are the atomic- and molecular-state probability amplitudes, respectively, $U(t)$ is the Rabi frequency, which is chosen to be real and positive: $\Omega \geq 0$, and $\Delta(t)$ is the detuning of the field frequency from the frequency of the atom-molecule transition. The bar denotes complex conjugation and the Kerr coefficients Λ_{11}, $\Lambda_{12} = \Lambda_{21}$ and Λ_{22} describe the atom-atom, atom-molecule, and molecule-molecule elastic interactions, respectively. Some typical values for the Kerr coefficients, e.g. for a ^{87}Rb condensate with $4.3 \times 10^{20} m^{-3}$ density are presented in Refs. [97, 98].

We consider a condensate being initially in all-atomic state, hence, the initial condition at $t_i = -\infty$ is

$$|a_1(-\infty)| = 1, \qquad |a_2(-\infty)| = 0.$$

Using the transformation $a_1 = c_1 e^{-i\int \Delta(s)\frac{ds}{3}}$, $a_2 = c_2 e^{i\int \Delta(s)\frac{ds}{3}}$, and $\Omega(t) = \sqrt{2}U(t)$, we can rewrite Eqs. (2.1) and (2.2) as

$$i\dot{c_1} = \frac{\Omega}{\sqrt{2}}\bar{c_1}c_2 + \left[-\frac{\Delta}{3} + \Lambda_{11}|c_1|^2 + \Lambda_{12}|c_2|^2\right] c_1, \tag{2.3}$$

$$i\dot{c_2} = \frac{\Omega}{2\sqrt{2}}c_1 c_1 + \left[\frac{\Delta}{3} + \Lambda_{21}|c_1|^2 + \Lambda_{22}|c_2|^2\right] c_2. \tag{2.4}$$

2.1.1 Analysis of the model

A treatment of the nonlinear model in the adiabatic regime, which will allow the extension of the standard adiabatic passage in linear models, can be accomplished by a classical Hamiltonian formulation of the problem. For Eqs. (2.3) and (2.4) we can write the following equivalent classical equations of motion:

$$i\frac{\partial c_1}{\partial t} = \frac{\partial H}{\partial \bar{c_1}},$$

$$i\frac{\partial c_2}{\partial t} = \frac{\partial H}{\partial \bar{c_2}},$$

derived from a Hamiltonian, that includes the third-order nonlinearities, written as

$$H = \frac{\Delta}{3}(|c_2|^2 - |c_1|^2) + \frac{\Omega}{2\sqrt{2}}(c_1^2\bar{c_2} + \bar{c_1^2}c_2) + \frac{\Lambda_{11}}{2}|c_1|^4 + \frac{\Lambda_{22}}{2}|c_2|^4 + \Lambda_{12}|c_1|^2|c_2|^2. \tag{2.5}$$

The complex variables c_j can be written in terms of standard real canonical coordinates p_j, q_j as

$$c_j = \frac{q_j + ip_j}{\sqrt{2}}$$

We now define another pair of the canonical variables I_j and φ_j by the relation $c_j = \sqrt{I_j}e^{-i\varphi_j}$. Further, making the canonical transformation from $(I_1, \varphi_1, I_2, \varphi_2)$ to the new variables (I, α, J, γ) defined as

$$\gamma = \varphi_1,$$

$$J = I_1 + 2I_2,$$

$$\alpha = -2\varphi_1 + \varphi_2,$$

$$I = I_2,$$

we get the Hamiltonian

$$H = -\frac{\Delta}{3}J + \Delta I + \frac{\Omega}{\sqrt{2}}(J - 2I)\sqrt{I}\cos\alpha + \frac{\Lambda_{11}}{2}(J - 2I)^2 + \frac{\Lambda_{22}}{2}I^2 + \Lambda_{12}(J - 2I)I \tag{2.6}$$

Introducing the notations

$$\Lambda_s = 2\Lambda_{11} + \frac{\Lambda_{22}}{2} - 2\Lambda_{12}, \qquad \Lambda_a = 2\Lambda_{11} - \Lambda_{12}, \tag{2.7}$$

and considering the example of a *Rb* condensate, we have $\Lambda_s > 0$ [98, 99]. We remark that the equations of motion depend only on the combinations Λ_a and Λ_s. Thus, the Kerr terms produce two distinct effects: the constant Λ_a produces only a constant shift in the detuning, which can be trivially compensated in the adiabatic tracking, while Λ_s produces a nonlinear term in the coupling. Therefore, only one effective parameter Λ_s can be taken into account

in the analysis.

We explore in this Chapter a Rabi frequency up to the same order as the Kerr coefficients, which will allow using weak fields. We show that a specifically shaped detuning can lead to high-efficient transfer.

The Hamiltonian function is rewritten as

$$H = (\Delta - \Lambda_a J)I + \Lambda_s I^2 + \frac{\Omega}{\sqrt{2}}(J - 2I)\sqrt{I}\cos\alpha - C \tag{2.8}$$

where $C = \frac{\Delta}{3}J - \frac{\Lambda_{11}}{2}J^2$ is a constant, that can be omitted.

The Hamiltonian (2.8) leads to the following equations of motion ($J = 1$):

$$\dot{J} = -\frac{\partial H}{\partial \gamma} = 0,$$

$$\dot{\gamma} = \frac{\partial H}{\partial J} = -\frac{\Delta}{3} + \frac{\Omega}{\sqrt{2}}\sqrt{I}\cos\alpha - \Lambda_a I + \Lambda_{11}, \tag{2.9}$$

$$\dot{I} = -\frac{\partial H}{\partial \alpha} = \frac{\Omega}{\sqrt{2}}(1 - 2I)\sqrt{I}\sin\alpha, \tag{2.10}$$

$$\dot{\alpha} = \frac{\partial H}{\partial I} = (\Delta - \Lambda_a) + 2\Lambda_s I + \frac{\Omega}{2\sqrt{2}}\frac{(1 - 6I)}{\sqrt{I}}\cos\alpha \tag{2.11}$$

Since the Hamiltonian is independent of γ, we can define a reduced phase space of only two dimensions with the variables (I, α):

$$\dot{I} = \frac{\Omega}{\sqrt{2}}(1 - 2I)\sqrt{I}\sin\alpha, \tag{2.12}$$

$$\dot{\alpha} = (\Delta - \Lambda_a) + 2\Lambda_s I + \frac{\Omega}{2\sqrt{2}}\frac{(1 - 6I)}{\sqrt{I}}\cos\alpha. \tag{2.13}$$

We note that the angle α is not well-defined for $I = 0$ and $I = 1/2$. Denoting $P = 2I$, which has the physical interpretation of the probability for the system to be in the molecular state, the equations of motion are rewritten as follows

$$\dot{P} = \Omega(1 - P)\sqrt{P}\sin\alpha, \tag{2.14}$$

$$\dot{\alpha} = (\Delta - \Lambda_a) + \Lambda_s P + \frac{\Omega}{2}\frac{(1-3P)}{\sqrt{P}}\cos\alpha. \tag{2.15}$$

2.1.2 Achieving the targeted molecular state

We notice that the Kerr nonlinearities appear only in the Eq. (2.15). As a consequence, from Eq. (2.14) we can deduce the following result, that was derived for the model without Kerr terms [2] (for the initial condition $P(t_i) = 0$):

$$P(t) = 2I(t) = \tanh^2\left[\int_{t_i}^{t} \frac{\Omega(s)}{2}\sin\alpha(s)ds\right]. \tag{2.16}$$

It is seen that one cannot achieve a complete transfer with pulses of a finite area, as it was already established for the case without Kerr nonlinearitiess.

2.2 Adiabatic tracking of driven quantum nonlinear systems with Kerr terms

2.2.1 Determination of the fixed points with Kerr terms

The instantaneous fixed points in the reduced phase space, for a given Δ and Ω are obtained by setting $\dot{I} = 0$, and $\dot{\alpha} = 0$. We will start with fixed points determined from the Eqs. (2.12) and (2.13).

$$0 = \dot{I} = \frac{\Omega}{\sqrt{2}}(1-2I)\sqrt{I}\sin\alpha, \tag{2.17}$$

$$0 = \dot{\alpha} = \Omega\left(\mu + 2aI + \frac{(1-6I)}{2\sqrt{2}\sqrt{I}}\cos\alpha\right). \tag{2.18}$$

Thus, $\dot{I} = 0$, $\dot{\alpha} = 0$ are given by $\alpha = 0$ or $\alpha = \pi$. Introducing the notations $a = \frac{\Lambda_s}{\Omega}$ and $\mu = \frac{\Delta - \Lambda_a}{\Omega}$, one can determine I from the following equation, when $\alpha = 0$:

$$\mu = -2aI_0 - \frac{1}{2\sqrt{2}}\frac{(1-6I_0)}{\sqrt{I_0}} \tag{2.19}$$

$I = 1/2$ corresponds more precisely to an hyperbolic (unstable) fixed point.

The points $I = 0$ and $I = 1/2$ are also fixed points. The coordinate α is not defined for these points.

The dynamics is then realized if one assumes $\Delta(t)$ given by Eq. (2.19), which depends on the initial sign of $\Delta(t_i)$. For a given $P_{track}(t)$ and $\Omega(t)$, in the adiabatic limit $lim_{1/T\to 0}P(t) - P_{track}(t) = 0$, i.e. for $\Delta(t)$ from (2.19) the solution $P(t)$ will track $P_{track}(t)$ in the adiabatic limit, if there is no intersection with a separatrix.

Since $P_0 = 2I_0$, we can express Eq. (2.19) as:

$$\mu = -aP_0 - \frac{1}{2}\frac{(1-3P_0)}{\sqrt{P_0}} \tag{2.20}$$

where $P(t)$ is the probability of formation of a molecular state.

2.2.2 Adiabatic tracking with Kerr terms

The idea of adiabatic tracking is to choose a pulse shape $\Omega(t)$ and a molecular population evolution $P_{track}(t)$ that one wishes to follow, and then to determine a detuning $\Delta_{track}(t)$ such, that the exact solution corresponding to $\Omega(t)$, and $\Delta_{track}(t)$ approaches the desired $P_{track}(t)$ in the adiabatic limit. In order to achieve this, first we determine $\Delta_{track}(t)$ such that the instantaneous fixed point of (2.17) and (2.18) satisfies $P(t) = P_{track}(t)$. As in [1], we will use for illustration pulse shapes of the form

$$\Omega(t) = \Omega_0 \sec h(t/T), \tag{2.21}$$

and $P_{track}(t)$ of the form

$$P_{track}(t) = \sin^2 \frac{1}{2T}\int_{-\infty}^{t} \sec h(t'/T)dt' = \sin^2\big[\arctan(\tanh[t/2] + \pi/4)\big]. \tag{2.22}$$

The second step is to verify if the dynamics defined by this $\Omega(t)$, $\Delta_{track}(t)$ satisfies the conditions of validity of the adiabatic theorem. The main point is to verify whether there

is a crossing of the tracked fixed point (which starts out as a stable elliptic fixed point) and other fixed points of hyperbolic type. In references [100–103] it was shown that a crossings of a separatrix associated to a hyperbolic fixed point can produce a big deviation from the adiabatic approximation, and a strongly random behaviour (see also [104, 105] for further developments in the subject). General methods to analyse the crossing of separatrices are described in [80–82]. In [1] it was shown that in the model without Kerr terms the tracking solution can be chosen such that there are no crossings with other fixed points at finite times when the laser amplitude in non-zero, and thus the adiabatic approximation is justified and one obtains a good tracking with the desired behaviour.

In order to analyze the properties of the adiabatic tracking, when the Kerr nonlinearities are included, one should determine the instantaneous fixed points and the position of the instantaneous separatrices. The first Eq. (2.17) has two solutions: $\alpha = 0$ and $\alpha = \pi$. Inserting into Eq. (2.18) we get an algebraic equation for the corresponding fixed point populations P_0 and P_π. Thus, from the Eq. (2.20), we can get the solution for adiabatic tracking in the case of $\alpha = 0$:

$$\Delta = -\frac{\Omega}{2\sqrt{P_0}}(1 - 3P_0) + 2\Lambda_{11}(1 - P_0) - \frac{\Lambda_{22}}{2}P_0 - \Lambda_{12}(1 - 2P_0), \tag{2.23}$$

and for $\alpha = \pi$:

$$\Delta = \frac{\Omega}{2\sqrt{P_0}}(1 - 3P_0) + 2\Lambda_{11}(1 - P_0) - \frac{\Lambda_{22}}{2}P_0 - \Lambda_{12}(1 - 2P_0). \tag{2.24}$$

We try to use one of these equations to construct a detuning for the desired tracking of a given P_{track}. In the Fig. 2.2 we can show Demkov-Kunike $\Omega(t) = \Omega_0 \mathrm{sech(t/T)}$ [106] and detuning, defined from the Eq. (2.23), for $P_0 = \sin^2\left[\int_{t_i}^{t} \mathrm{sech(s/T)}ds/2T\right]$.

Thus, we can determine the fixed points for $\Omega(t)$ and $\Delta(t)$.

In the model without Kerr terms discussed in [1] the two choices (2.23) and (2.24) are essentially equivalent and they lead to the same quality of transfer. As we will show below,

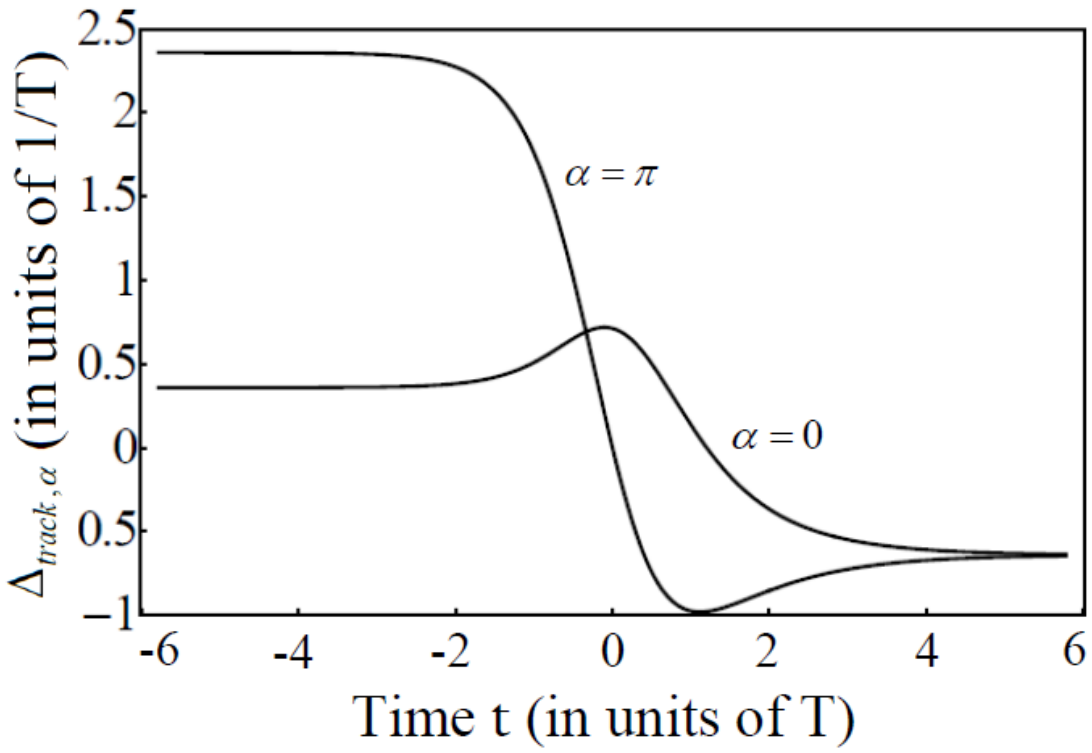

Figure 2.1: Detunings for $\alpha = 0$ and $\alpha = \pi$. $\Omega(t) = \Omega_0 \text{sech(t/T)}$, $\Delta(t)$ determined from the Eqs. (2.23) and (2.24) (in units of $1/T$, $T = 10$) with $\frac{\Omega_0}{\Lambda_s} = 0.5$, $\Lambda_{11} = 0.21328 s^{-1}$, $\Lambda_{12} = -0.27962 s^{-1}$, $\Lambda_{22} = 0.10664 s^{-1}$ and $\Lambda_s = 2\Lambda_{11} + \frac{\Lambda_{22}}{2} - 2\Lambda_{12} = 1.03912 s^{-1}$ parameters.

when Kerr terms are presented, the two choices lead to qualitatively different dynamics. In one of the cases of Fig. 2.1 we display an example of the two choices of Δ. The second choice (2.24) leads to significantly better transfer properties. We will show indeed that for (2.23) the tracking fixed point, which starts being elliptic, goes inevitably through an intersection with a hyperbolic fixed point, and its stability is lost by becoming hyperbolic. Once the tracking fixed point is hyperbolic the classical adiabatic theorem does not apply anymore, and thus the final stages of the process are non-adiabatic, which lead to an uncontrolled dynamics failing in general to reach the target state. We will show that this difficulty can be completely avoided by choosing the tracking (2.24) corresponding to the fixed point with $\alpha = \pi$ [2].

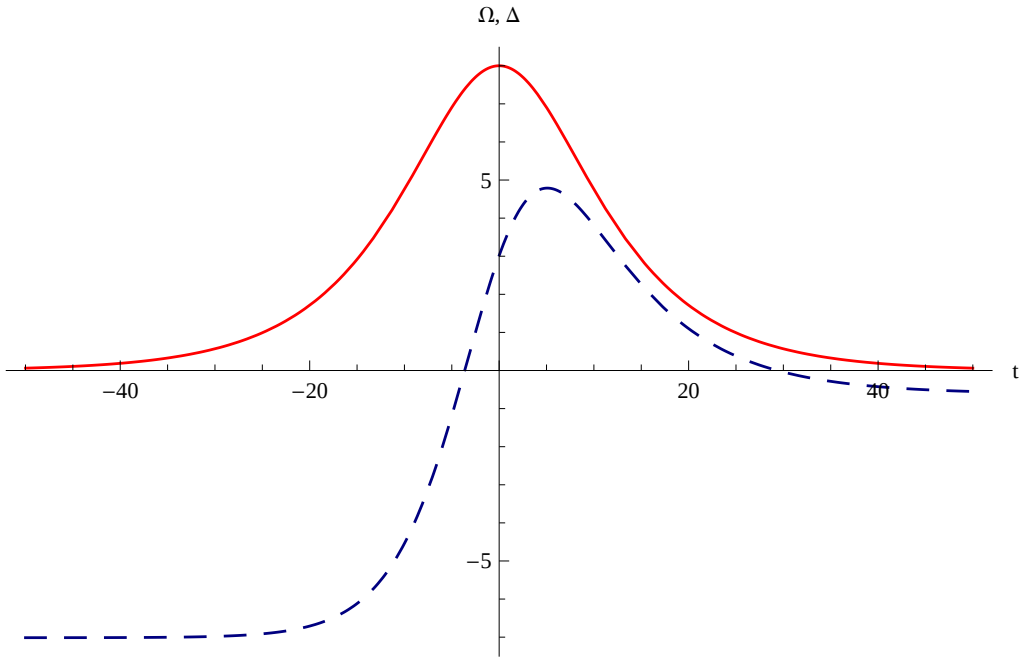

Figure 2.2: $\Omega(t) = \Omega_0 \mathrm{sech(t/T)}$ with red solid line, with $\Delta(t)$ determined from the Eq. (2.23) with blue dashed line (in units of $1/T$, $T = 9$). with $\Omega_0 = 8$, $\Lambda_{11} = 0.21328s^{-1}$, $\Lambda_{12} = -0.27962s^{-1}$, $\Lambda_{22} = 0.10664s^{-1}$ and $\Lambda_s = 2\Lambda_{11} + \frac{\Lambda_{22}}{2} - 2\Lambda_{12} = 1.03912s^{-1}$ parameters.

Apart from the restrictions of crossing imposed in the phase space described below, adiabatic passage needs a sufficiently large pulse area, i.e. $T >> 1$: we have determined numerically that the fidelity is already high ($P_{num.} \gtrsim 0.99$) for $T \gtrsim 5$. T determines the adiabatic scale.

2.2.3 Structure of the instantaneous phase portraits: fixed points and sepatrices

We choose one instantaneous fixed point $P_{track}(t)$ to construct the detuning by the adiabatic tracking formulas (2.23) or (2.24). The dynamics defined by $\Omega(t)$ and $\Delta_{track}(t)$, have other fixed points, that we have to determine in order to analyze their possible effect on the adiabatic evolution. In particular, when some other fixed points are hyperbolic, crossings with them (or with the associated separatrices) can be the main obstacle for the adiabatic following of the chosen P_{track}. Some general properties of the instantaneous phase portraits of a class of models including the present one were presented by Itin and Watanabe in [75].

We will present below the particular analysis required for the purpose of adiabatic tracking.

The main important point in this paragraph is that we remark that the continuity of the flow in the reduced phase space imposes some restrictions on possible crossings of fixed points: An elliptic fixed point can cross a hyperbolic fixed point, but not an elliptic one (unless it also crosses simultaneously a hyperbolic fixed point). Furthermore, an elliptic fixed point can cross a hyperbolic one, but it cannot cross any other part of the associated separatrix. In general, when an elliptic and a hyperbolic fixed points cross, they exchange their stability character, the elliptic one becomes hyperbolic and vice-versa [2].

2.2.4 Determination of the fixed points for given field configuration

In order to analyze the properties of the adiabatic tracking when the Kerr terms are included, we have to determine the instantaneous fixed points and the position of the instantaneous separatrices. From Eq. (2.20) we can find P as a function of detuning $\Delta(t)$ and the coupling $\Omega(t)$. For the fixed point (P_0, $\alpha = 0$) from (2.20) we can write

$$\mu + 2aI_0 + \frac{(1 - 6I_0)}{2\sqrt{2}\sqrt{I_0}} = 0. \tag{2.25}$$

From (2.25) the fixed points are the roots of the following third-order equation

$$2\Lambda_s P_0\sqrt{P_0} - 3\Omega P_0 + 2(\Delta - \Lambda_a)\sqrt{P_0} + \Omega = 0, \tag{2.26}$$

which can be written as

$$P_{0k} = \left(-\frac{1}{3A}\left(-\frac{3}{2}\Omega + u_k C + \frac{D_0}{u_k C}\right)\right)^2, \qquad k \in 1, 2, 3 \tag{2.27}$$

where $u_1 = 1, \qquad u_2 = \frac{-1+i\sqrt{3}}{2}, \qquad u_3 = \frac{-1-i\sqrt{3}}{2}$ are the three cube roots of unity, and

$$C = \left(\frac{D_1 + \sqrt{D_1^2 - 4D_0^3}}{2} \right)^{\frac{3}{2}},$$

$D_0 = \frac{9}{4}\Omega^2 - 3A(\Delta - \Lambda_a)$ and $D_1 = \frac{27}{4}\Omega^3 + \frac{27}{2}A(\Delta - \Lambda_a)\Omega + \frac{27}{2}A^2\Omega$.

For D we will get

$$D = \frac{-D_1^2 + 4D_0^3}{27A^2}$$

where D is the discriminant for cubic polynomial equation (2.27). From which we can get three values for fixed points, since $D > 0$.

We remark that the points $P = 1$ and for $\Omega = 0$, $P = 0$ are also fixed points. However, the coordinate α is not defined for these points, it has to be verified in the original coordinates.

Fig. 2.3 corresponds to a small value of Ω_0/Λ_S and Fig. 2.4 to a larger one. The black solid line is the exact solution $P(t)$ obtained by numerical solution of the differential Eqs. (2.3)-(2.4). The blue curve corresponds to the fixed point that has the same value of $\alpha = 0$ as the tracking fixed point, drawn in red, while the green curve corresponds to the other value; $\alpha = \pi$.

We observe that for any choice of the parameter Ω_0/Λ_s there is a crossing of P_{track} with the other fixed point for $\alpha = 0$. The fixed point with $\alpha = \pi$ is on the other side of the phase space, and thus it does not cross the tracking fixed point. Elliptic fixed points are displayed as continuous lines while hyperbolic ones are displayed with dashed lines.

Before the crossing P_{track} is elliptic, but after the crossing it becomes hyperbolic and the conditions for the adiabatic theorem are not satisfied anymore [80,83]. The end of the process is always non-adiabatic, which may lead to a deterioration of the transfer to the all-molecules state.

In numerical simulations we show when Ω_0/Λ_s is large enough the crossing happens when the population is close to $P = 1$ and in the end of the process there is still a good transfer without oscillations, despite the loss of adiabaticity. Since, it is known that after crossing of fixed points the adiabatic theorem is not valid anymore. If $\Omega_0/\Lambda_s >> 1$ the crossing can

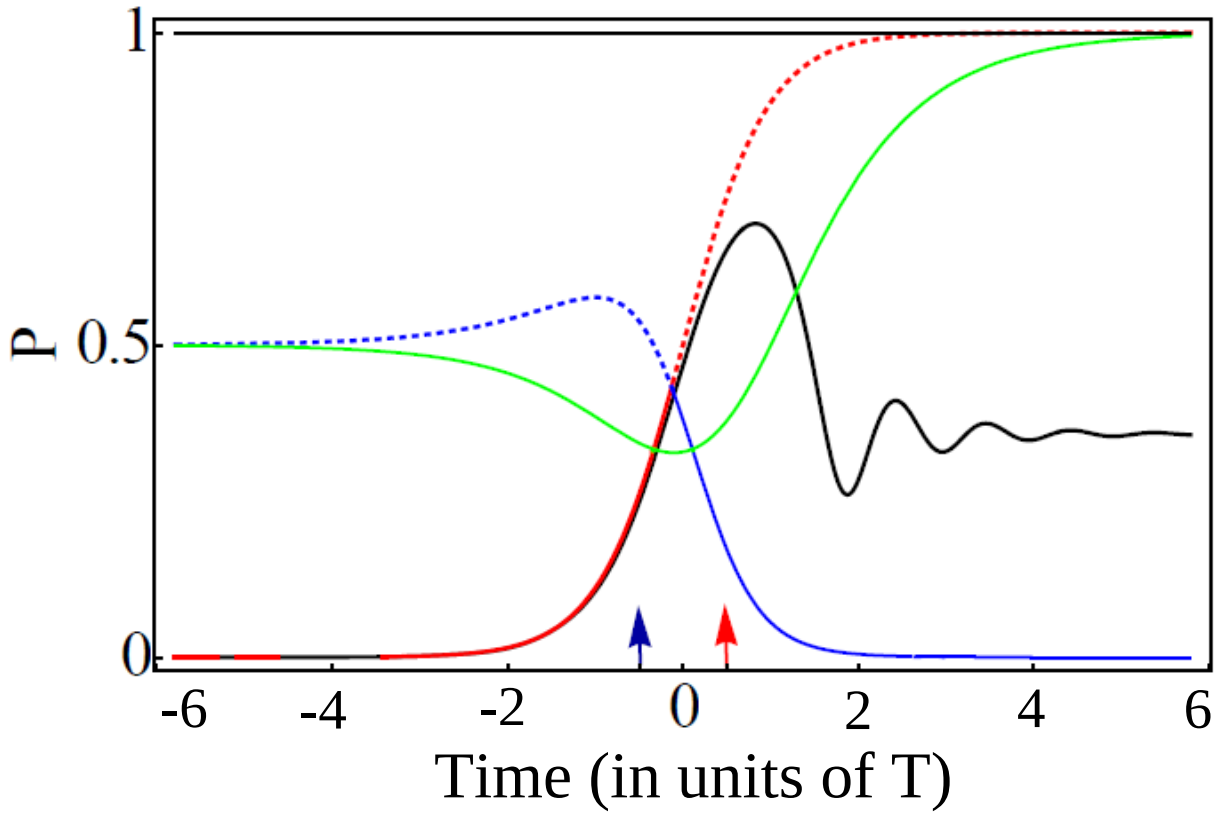

Figure 2.3: Tracking with $\Delta_{track,0}$, $\Omega_0/\Lambda_s = 0.5$, $\tau = 5$. Exact (numerical) solution (black solid line), and fixed points P_0 (elliptic: solid lines, hyperbolic: dashed lines). The red curve is the adiabatic tracking P_{track} and the blue and green curves are the two other fixed points. The red and the blue curves are on the same side of phase space, and they intersect, for the corresponding detuning [line $\alpha = 0$, Eq. (2.24)]: while the green one in this panel is on the opposite side, and corresponds to the other choice of detuning with $\alpha = \pi$, Eq. (2.24), at the times indicated by the arrows in panel. The colours of arrows correspond to the colours of fixed points. $\Lambda_{11} = 0.21328s^{-1}$, $\Lambda_{12} = -0.27962s^{-1}$, $\Lambda_{22} = 0.10664s^{-1}$ [97]. $\Lambda_s = 2\Lambda_{11} + \frac{\Lambda_{22}}{2} - 2\Lambda_{12} = 1.03912s^{-1}$.

be pushed toward the end of the transfer, where the equation of motion (2.14) shows that, because of the factor $(1-P)$, the population $P(t)$ stays constant when $(1-P) \to 0$, and thus the crossing has a negligible effect. This observation is consistent with the expected property that when Λ_s/Ω is small enough, one should observe a behaviour close to the one of model without Kerr terms. This is illustrated in Fig. 2.4.

$P = 0$ is an elliptic fixed point, and corresponds to the initial condition, which means the

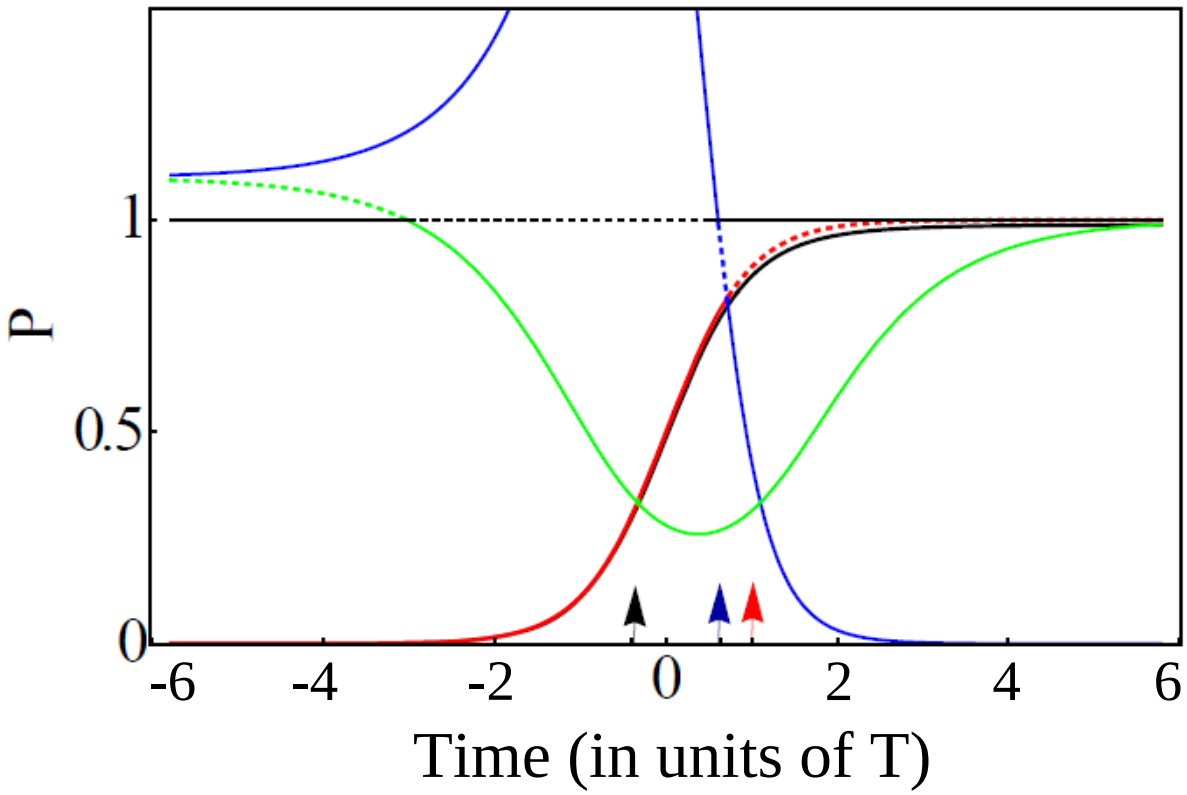

Figure 2.4: Tracking with $\Delta_{track,0}$, $\Omega_0/\Lambda_s = 1.1$, $\tau = 5.5$. Exact numerical solution (black solid line), and fixed points (elliptic: solid lines, hyperbolic: dashed lines). The red curve is the adiabatic tracking P_{track} and the blue and green curves are the two other fixed points. The red and the blue curves are on the same side of phase space, and they intersect, while the green one is on the opposite side, at the times indicated by the arrows in panel. The colours of arrows correspond to the colours of fixed points. $\Lambda_{11} = 0.21328s^{-1}$, $\Lambda_{12} = -0.27962s^{-1}$, $\Lambda_{22} = 0.10664s^{-1}$ [97]. $\Lambda_s = 2\Lambda_{11} + \frac{\Lambda_{22}}{2} - 2\Lambda_{12} = 1.03912s^{-1}$.

condensate is in all-atomic state. $P = 1$ corresponds to the target all-molecular state. Its stability character can change during the time evolution from elliptic to hyperbolic, as we will see below.

In Figs. 2.3 and 2.4 we display the time evolution of the instantaneous fixed points for two representative values of the parameter Ω_0/Λ_S. We can see the numerical exact solution $P(t)$, and positions of the three fixed points. These figures show, that if we take the line corresponding to the adiabatic tracking (red line), we have a curve that is close to the exact solution of $P(t)$.

2.2.5 Fixed points

$P = 1$ is always a fixed point, for any values of the parameters. This fixed point can be stable (elliptic) or unstable (hyperbolic) at different times of the process.

Once Δ_{track} is chosen, the fixed points other than $P = 1$ are solutions of the following equations, determined from Eqs. (2.23), (2.24):

$$\Delta_{track} = -\Lambda_s P_0 + \Lambda_a - \frac{\Omega}{2\sqrt{P_0}}(1 - 3P_0) \qquad \text{for } \alpha = 0. \tag{2.28}$$

or

$$\Delta_{track} = -\Lambda_s P_\pi + \Lambda_a + \frac{\Omega}{2\sqrt{P_\pi}}(1 - 3P_\pi) \qquad \text{for } \alpha = \pi. \tag{2.29}$$

These equations can be written as polynomial equation of degree 3 in the variable $y := \sqrt{P}$. Of the total of six roots, $\sqrt{P_{track}}$ is one of them, and among the others one has to select the ones that are real and are in the interval $[0, 1]$. The number of such solutions can be 0, 1 or at most 2, and vary as a function of time.

$P = 0$ is a fixed point at the beginning and at the end of the pulse, when $\Omega = 0$. Since $P_{track}(t_i) = 0$ and $P_{track}(t_f) \simeq 1$ the tracking is the adiabatic following of the family of fixed points that starts as $P = 0$. The tracking fixed point is at all times either at $\alpha = 0$ or at $\alpha = \pi$. The fixed points having the other value of α will thus never intersect it.

2.2.6 Separatrix

A separatrix is the energy curve that contains a hyperbolic fixed point. The energy of a hyperbolic fixed point (P, α), is given by

$$H = (\Delta - 2\Lambda_{11} + \Lambda_{12})\frac{P}{2} + \frac{\Lambda_s}{4}P^2 + \frac{\Omega}{2}(1 - P)\sqrt{P}\cos\alpha,$$

and thus, the points of the separatrix (P_s, α_s) associated to this hyperbolic fixed point are determined by the relation

$$H = (\Delta - 2\Lambda_{11} + \Lambda_{12})\frac{P}{2} + \frac{\Lambda_s}{4}P^2 + \frac{\Omega}{2}(1-P)\sqrt{P}\cos\alpha_s,$$

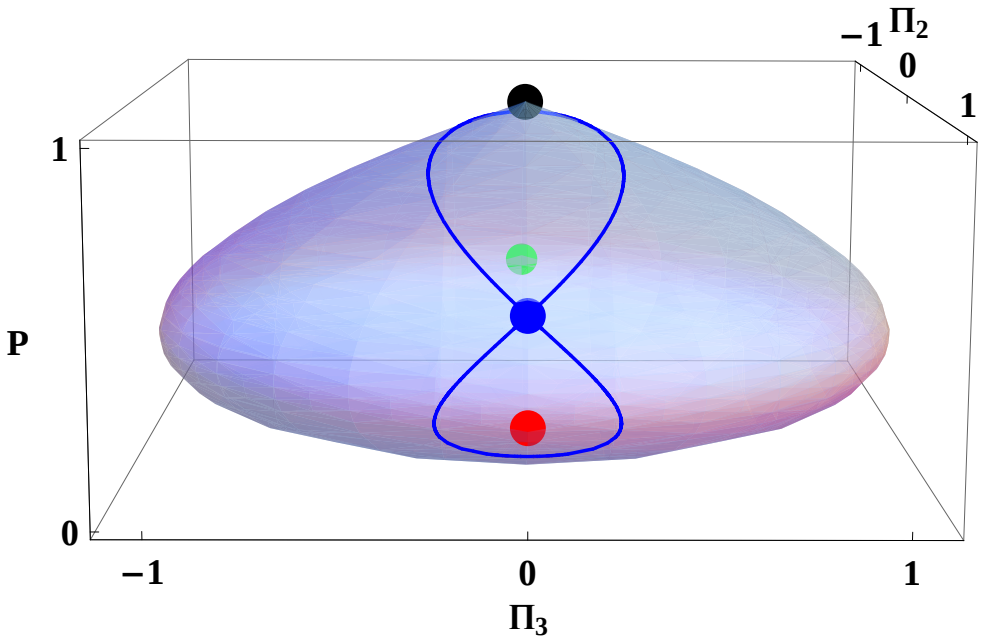

Figure 2.5: Tracking with $\Delta_{track,0}$, $\Omega_0/\Lambda_s = 0.5$, $\tau = 5$. Exact (numerical) solution (black line) and the adiabatic tracking P_{track} is with red line. Three values of fixed points for the adiabatic tracking $\Delta(t)$ from the Eq. (2.23). The red and the blue curves are on the same side of the phase space, and they intersect, while the green one is on the opposite side. Instantaneous phase portrait, with fixed points and separatrices, at times indicated by the arrows in the Fig. 2.3. The tracking fixed point (red dot) is elliptic for $t = -T/2$ (and hyperbolic for $t = T/2$) after the bifurcation by crossing with the blue fixed point. $\Lambda_{11} = 0.21328s^{-1}$, $\Lambda_{12} = -0.27962s^{-1}$, $\Lambda_{22} = 0.10664s^{-1}$ [97]. $\Lambda_s = 2\Lambda_{11} + \frac{\Lambda_{22}}{2} - 2\Lambda_{12} = 1.03912s^{-1}$.

one can obtain equation for separatrix:

$$\cos\alpha_s = \frac{H - (\Delta - 2\Lambda_{11} + \Lambda_{12})\frac{P}{2} - \frac{\Lambda_s}{4}P^2}{\frac{\Omega}{2}(1-P)\sqrt{P}}$$

In the Figs. 2.5 and 2.6 we show the time evolution of the instantaneous fixed points for $\Omega_0/\Lambda_s = 0.5$, in the case when $\alpha = 0$, at the times indicated by the arrows in panel of the Fig. 2.3. The position of the fixed points and of the separatrices associated with the hyperbolic

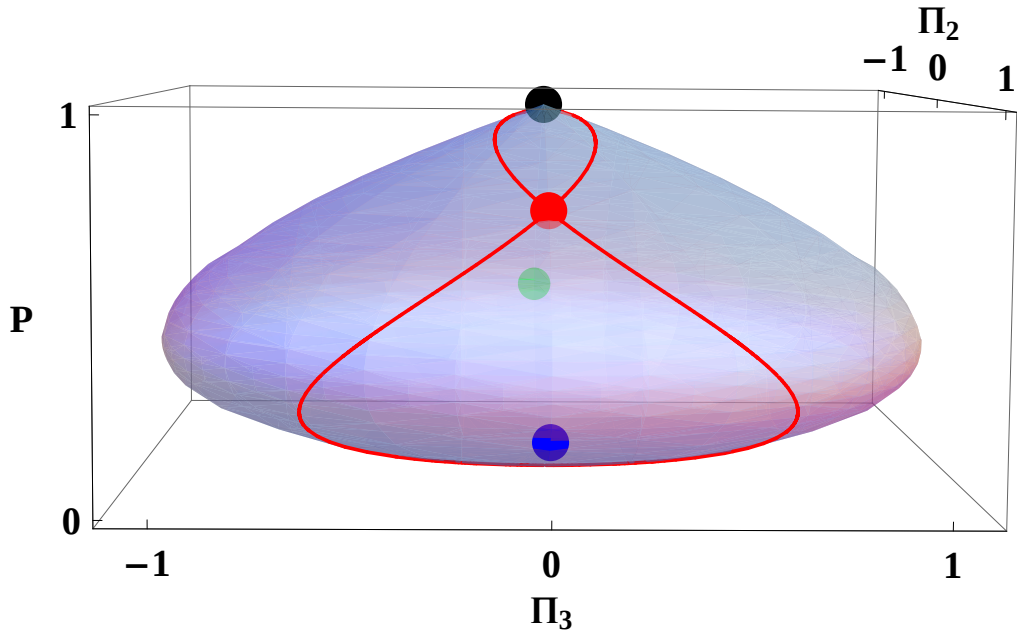

Figure 2.6: Same as in the Fig. 2.5, and $\tau = 5$.

one organize the global structure of the instantaneous phase portrait in the reduced phase space.

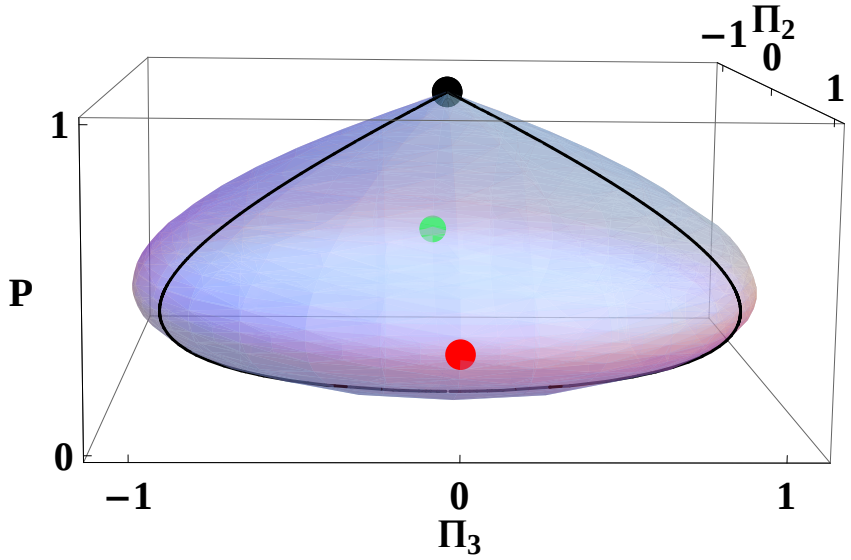

Figure 2.7: Same as in the 2.5, but for $\Delta_{track,0}$, $\Omega_0/\Lambda_s = 1.1$, and $\tau = 5.5$. The exact solution is almost indistinguishable from P_{track} (red line). The green and the blue curves are on the same side of the phase space and do not cross the red one, which is on the opposite side. The tracking fixed point (red) stays elliptic at all finite times.

One can see that in the phase portraits for $\Omega_0/\Lambda_s = 0.5$ and $\Omega_0/\Lambda_s = 1.1$, for any choice of the parameter Ω_0/Λ_s there is a crossing of P_{track} with the other fixed point, which corresponds

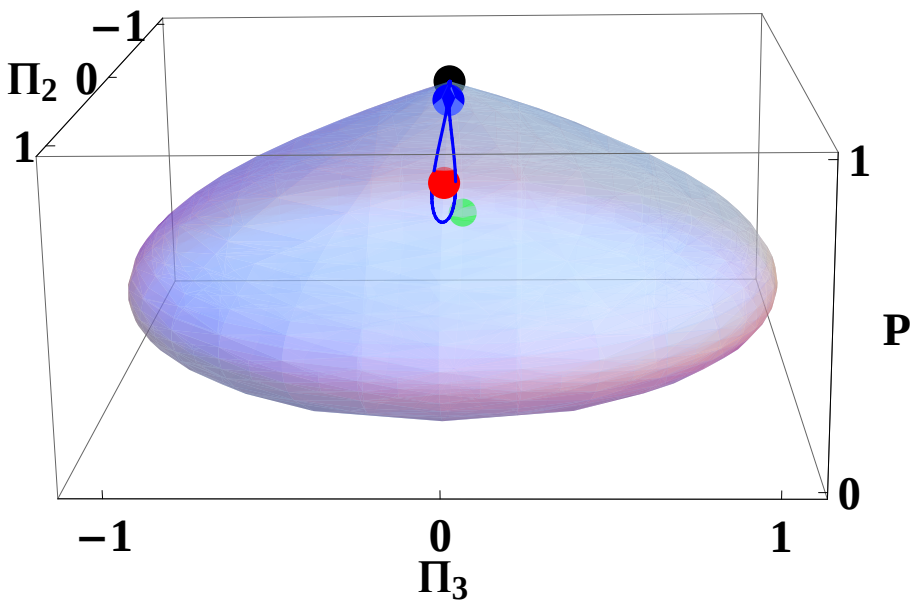

Figure 2.8: Same as in the Fig. 2.5, but for $\Delta_{track,0}$, $\Omega_0/\Lambda_s = 1.1$, and $\tau = 5.5$.

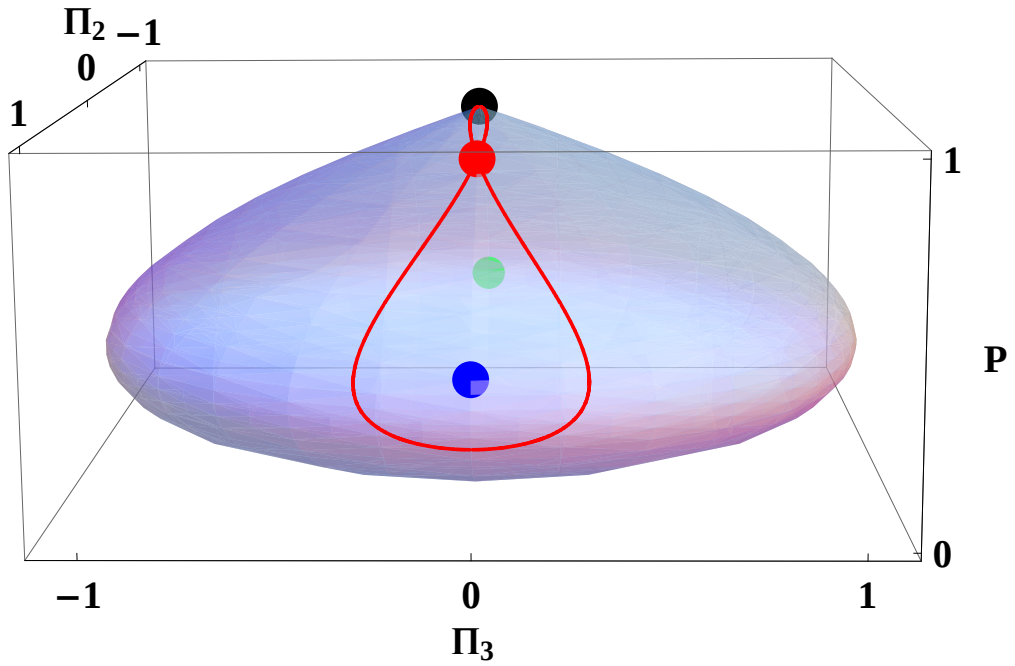

Figure 2.9: Same as in the Fig. 2.5, $\tau = 5.5$, $\Lambda_{11} = 0.21328s^{-1}$, $\Lambda_{12} = -0.27962s^{-1}$, $\Lambda_{22} = 0.10664s^{-1}$ [97], $\Lambda_s = 2\Lambda_{11} + \frac{\Lambda_{22}}{2} - 2\Lambda_{12} = 1.03912s^{-1}$.

to $\alpha = 0$. Before the crossing P_{track} is elliptic. However, after the crossing it becomes hyperbolic and the conditions for the adiabatic theorem are not satisfied anymore [80, 83]. The end of the process is thus always non-adiabatic, which may lead to a deterioration of the transfer to the all-molecules state. However, from the phase portraits for $\Omega_0/\Lambda_s = 1.1$ we show that by taking Ω_0/Λ_s larger we will have a good transfer without oscillations.

When $\Omega_0/\Lambda_s = 0.5$ the tracking fixed point (red dot) in the Fig. 2.5 is elliptic. Whereas, in the Fig. 2.6 it becomes hyperbolic, after the bifurcation by crossing with the blue fixed point.

In the case of $\alpha = 0$, when $\Omega_0/\Lambda_s = 1.1$ the tracking fixed point (red dot) in Figs. 2.7 and 2.8 is elliptic, then in the Fig. 2.9 it is hyperbolic.

2.2.7 Separatrix for $P = 1$

$I = \frac{1}{2}$ is a hyperbolic fixed point, and from the Hamiltonian with Kerr terms the corresponding energy is:

$$H_s = \Omega\left(\frac{\mu}{2} + \frac{a}{4}\right) - \frac{\Delta}{3} + \frac{\Lambda_{11}}{2}. \tag{2.30}$$

The curve corresponding to this energy is the solution of

$$\Omega\left(\frac{\mu}{2} + \frac{a}{4}\right) = \Omega\left(\mu I_S + a I_S^2 + \frac{(1-2I_S)}{\sqrt{2}}\sqrt{I_S}\cos\alpha_s\right) \tag{2.31}$$

(where $I_S \neq \frac{1}{2}$, $I_S \neq 0$).

Thus, the equation for the separatrix is

$$\cos\alpha_s = \frac{1}{\sqrt{P}_s(1-P_s)}\left(\mu + \frac{a}{2} - \mu P_s - \frac{a P_s^2}{2}\right), \tag{2.32}$$

$$\cos\alpha_s = \frac{1}{\sqrt{P}_s}\left(\mu + \frac{a}{2}(1+P_s)\right). \tag{2.33}$$

2.2.8 Conditions for crossing of separatrix and fixed points, $\alpha = 0$

In Figs. 2.10 we show exact solution $P(t)$ for $\Omega_0 > \Lambda_s$ and $\Omega_0 < \Lambda_s$.

Since $\Omega \to 0$ when $t \to \infty$ and P_0 tends to a finite value (~ 1), there is a crossing between fixed points and this crossing can not be avoided. We observe that for any choice of the parameter Ω_0/Λ_s there is a crossing of P_{track} at the end of the pulse, with the other fixed point with $\alpha = 0$, since the fixed point with $\alpha = \pi$ is on the other side of the phase space, and thus it does not cross the tracking fixed point.

From Figs. 2.10 one can see that there is no oscillation when $\Omega_0 > \Lambda_s$, and there are oscillations when $\Omega_0 < \Lambda_s$.

Thus, one can have a good transfer by taking Ω_0 bigger than Λ_s.

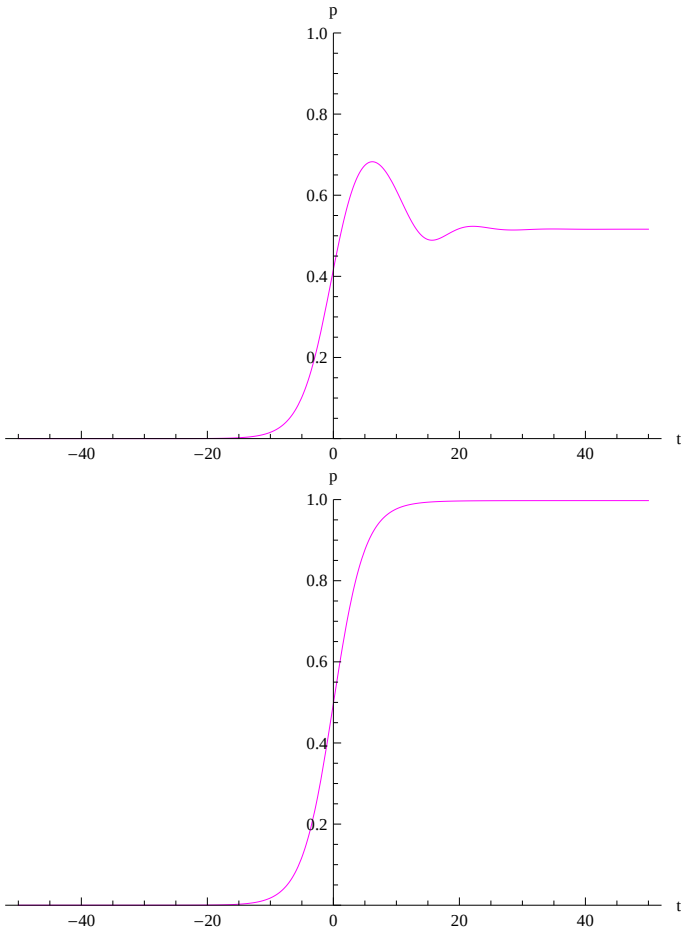

Figure 2.10: Exact numerical solution of $P(t)$, for the adiabatic tracking $\Delta(t)$ from Eq. (2.23). $T = 5$, $\Lambda_{11} = 0.21328s^{-1}$, $\Lambda_{12} = \Lambda_{21} = -0.27962s^{-1}$, $\Lambda_{22} = 0.10664s^{-1}$. [97]. $\Lambda_s = 2\Lambda_{11} + \frac{\Lambda_{22}}{2} - 2\Lambda_{12} = 1.03912s^{-1}$, $\Lambda_a = 2\Lambda_{11} - \Lambda_{12}$. In the first figure $\Omega_0 < \Lambda_s$, $\Omega_0 = 0.5$, whereas, in the second one $\Omega_0 \gg \Lambda_s$, $\Omega_0 = 2$.

2.3 Adiabatic tracking of driven quantum nonlinear systems with inter-particle elastic scattering Kerr terms, $\alpha = \pi$

2.3.1 Determination of fixed points if $\alpha = \pi$

In this paragraph for the fixed points we consider Eqs. (2.17) and (2.18). As it was mentioned before, for $I = 0,\ 1/2$, the angle α is not defined. $I = 1/2$ is hyperbolic (unstable) fixed point. The fixed points, corresponding to $\dot{I} = 0$ and $\dot{\alpha} = 0$ conditions for given values of Ω and Δ, can be given by $\alpha = 0$ or $\alpha = \pi$. In this paragraph, we will look at the case when $\alpha = \pi$.

With $P_0 = 2I_0$ we have

$$\mu = -aP_0 + \frac{1}{2}\frac{(1 - 3P_0)}{\sqrt{P_0}} \tag{2.34}$$

$P(t)$ is the molecular state probability, and the adiabatic tracking solution will be

$$\Delta = \frac{\Omega}{2\sqrt{P_0}}(1 - 3P_0) + 2\Lambda_{11}(1 - P_0) - \frac{\Lambda_{22}}{2}P_0 - \Lambda_{12}(1 - 2P_0). \tag{2.35}$$

One can obtain $\Delta(t)$ from the Eq. (2.35), using Demkov-Kunike $\Omega(t) = \Omega_0 \mathrm{sech(t/T)}$ [106] and $P_0 = \sin^2\left[\int_{t_i}^{t} \mathrm{sech(s/T)}ds/2T\right]$.

For these $\Omega(t)$ and $\Delta(t)$ we can determine the fixed points. One can obtain I as a function of the coupling $\Omega(t)$ and detuning $\Delta(t)$ from Eq. (2.19). From the Eq. (2.34), the fixed points are the roots of the following third-order equation:

$$2\Lambda_s P_0\sqrt{P_0} + 3\Omega P_0 + 2(\Delta - \Lambda_a)\sqrt{P_0} - \Omega = 0, \tag{2.36}$$

In Figs. 2.11 and 2.12 we show the time evolution of the instantaneous fixed points for two representative values of the parameter Ω_0/Λ_S. We can see the numerical exact solution $P(t)$, and three values of fixed points.

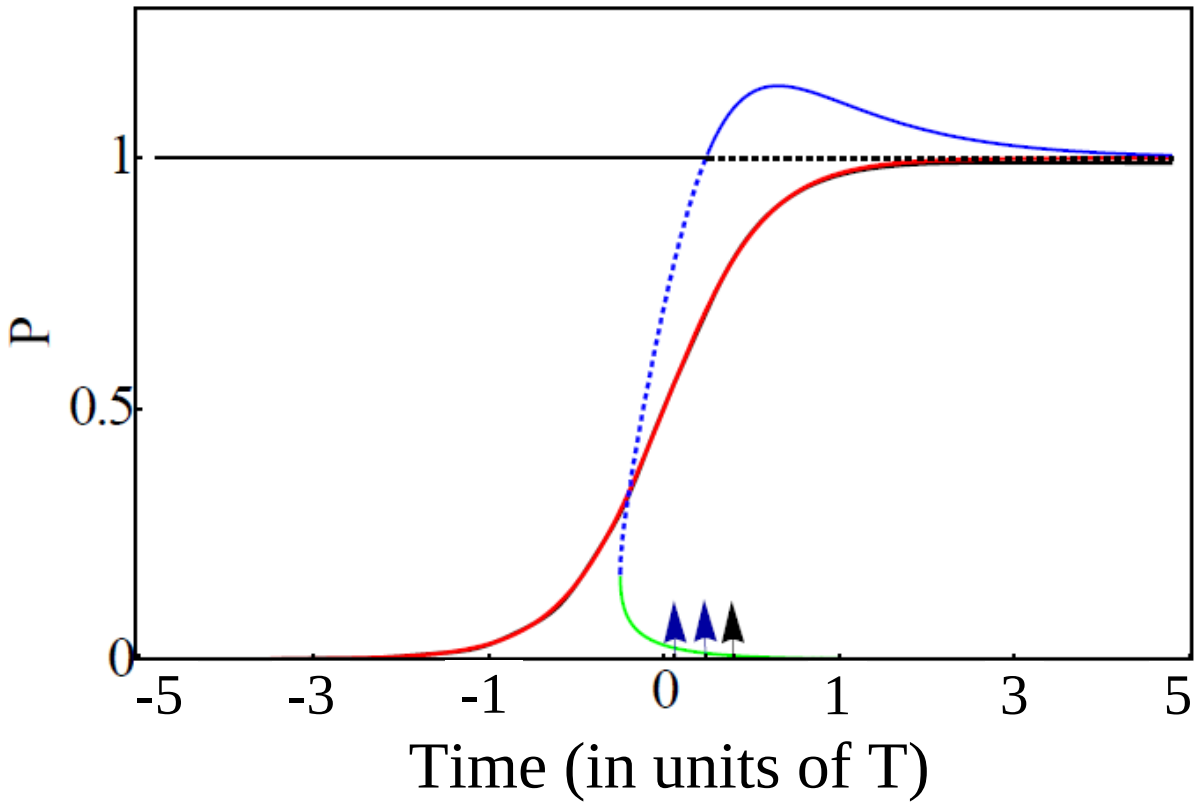

Figure 2.11: Tracking with $\Delta_{track,\pi}$, $\Omega_0/\Lambda_s = 0.2$: Exact numerical solution (blue solid line), $\tau = 6$, and fixed points (elliptic: solid lines, hyperbolic: dashed lines). The red curve is adiabatic tracking P_{track} and the orange and green curves are the two other fixed points. The green and the orange curves are on the same side of the phase space and do not cross the red one, which is on the opposite side. $\alpha = \pi$. $\frac{\Omega_0}{\Lambda_s} = 0.2$. $\Lambda_{11} = 0.21328s^{-1}$, $\Lambda_{12} = -0.27962s^{-1}$, $\Lambda_{22} = 0.10664s^{-1}$ [97]. $\Lambda_s = 2\Lambda_{11} + \frac{\Lambda_{22}}{2} - 2\Lambda_{12} = 1.03912s^{-1}$.

For any values of the parameters $P = 1$ is always a fixed point. At different times of the process it can be stable (elliptic) or unstable (hyperbolic).

The black full line is the exact solution $P(t)$ obtained by numerical solution of the differential equations (2.3), (2.4). In the early times of the process the tracking fixed point (shown in red) is the only fixed point (i.e. the only real root of the third-order polynomial equations in (2.23), (2.35). At a critical time there is a bifurcation in which two roots become real, one corresponding to an elliptic fixed point (shown as a full line) and the other to a hyperbolic one (shown as a dashed line). The blue curve corresponds to the fixed points that have the

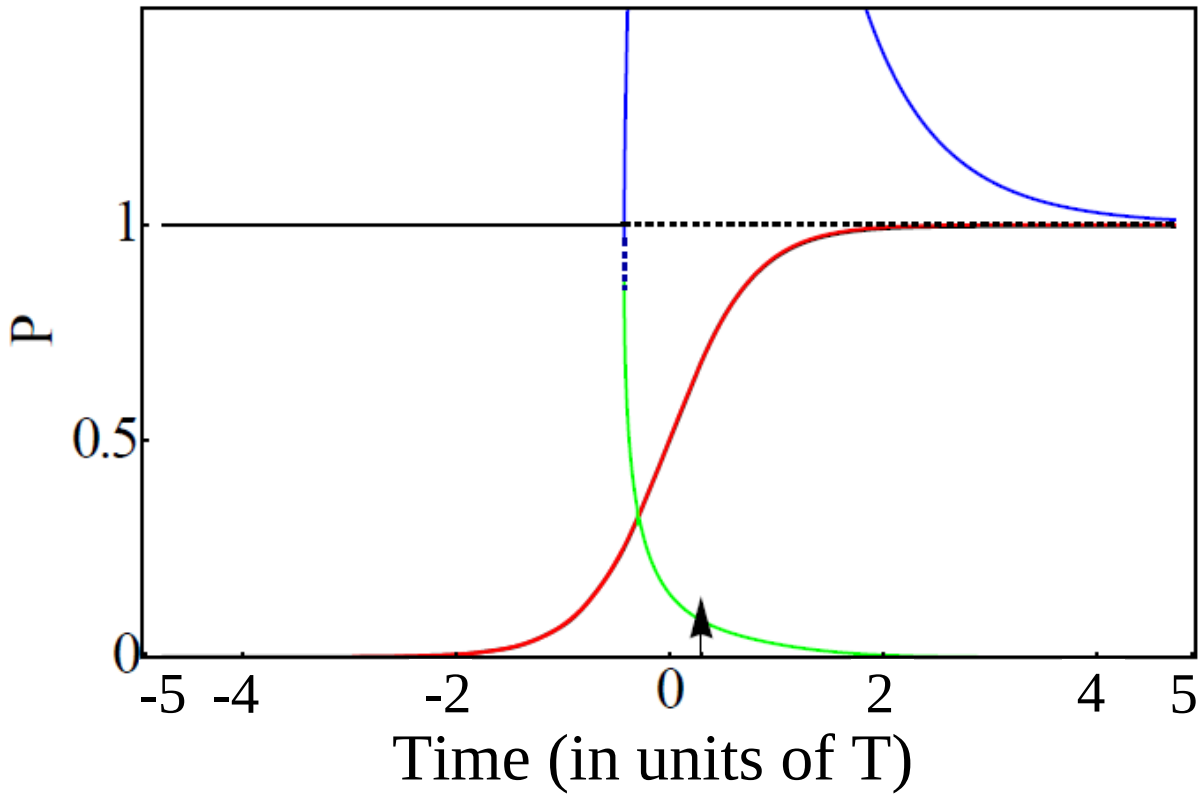

Figure 2.12: Tracking with $\Delta_{track,\pi}$, $\Omega_0/\Lambda_s = 0.2$: Exact numerical solution (blue solid line), $\tau = 9$, and fixed points (elliptic: solid lines, hyperbolic: dashed lines). The red curve is the adiabatic tracking P_{track} and the orange and green curves are the two other fixed points. The green and the orange curves are on the same side of phase space and do not cross the red one, which is on the opposite side. $\alpha = \pi$. $\frac{\Omega_0}{\Lambda_s} = 1.1$, $\Lambda_{11} = 0.21328s^{-1}$, $\Lambda_{12} = -0.27962s^{-1}$, $\Lambda_{22} = 0.10664s^{-1}$ [97]. $\Lambda_s = 2\Lambda_{11} + \frac{\Lambda_{22}}{2} - 2\Lambda_{12} = 1.03912s^{-1}$.

same value of $\alpha = \pi$ as the tracking fixed point. The green curve corresponds to the other value $\alpha = 0$, i.e. to the fixed point that is on the other side of the reduced phase space and thus does not cross the tracking fixed point. The full lines represent elliptic fixed points and the dashed lines hyperbolic ones. We observe that the tracking fixed point has no crossings at finite times, and it keeps its elliptic stable nature. Thus, the adiabatic theorem applies until the end of the process and we have an efficient adiabatic transfer even for relatively small values of Ω_0/Λ_s. This is illustrated in Fig. 2.11 and Fig. 2.12 corresponds to a larger value of Ω_0/Λ_s.

2.3.2 Determination of separatrix if $\alpha = \pi$

In this paragraph we consider the Hamiltonian with Kerr nonlinearities

$$H = (\Delta - 2\Lambda_{11} + \Lambda_{12})\frac{P}{2} + \frac{\Lambda_s}{4}P^2 + \frac{\Omega}{2}(1-P)\sqrt{P}\cos\alpha_s$$

and

$$\cos\alpha_s = \frac{H - (\Delta - 2\Lambda_{11} + \Lambda_{12})\frac{P}{2} - \frac{\Lambda_s}{4}P^2}{\frac{\Omega}{2}(1-P)\sqrt{P}}.$$

In the Figs. 2.13 - 2.16 the adiabatic tracking is with red line. One can define three values of fixed points for the adiabatic tracking $\Delta(t)$ from the Eq. (2.35). The green and the orange curves are on the same side of the phase space and do not cross the red one, which is on the opposite side. It is shown instantaneous phase portrait, with fixed points and separatrices. Red dot: tracking fixed point, which stays elliptic at all finite times. The values of the Kerr terms are: $\Lambda_{11} = 0.21328s^{-1}$, $\Lambda_{12} = -0.27962s^{-1}$, $\Lambda_{22} = 0.10664s^{-1}$ [97], $\Lambda_s = 2\Lambda_{11} + \frac{\Lambda_{22}}{2} - 2\Lambda_{12} = 1.03912s^{-1}$.

In Figs. 2.13 - 2.15 we show the time evolution of the instantaneous fixed points for $\Omega_0/\Lambda_s = 0.2$, in the case when $\alpha = \pi$, at the times indicated by the arrows in the panel of Fig. 2.11, colours correspond to the colour of the separatrix in the phase portraits, with fixed points and separatrix.

When $\alpha = \pi$ and $\Omega_0/\Lambda_s = 1.1$ the tracking fixed point (red dot) in the Fig. 2.16 is elliptic. The blue curve corresponds to the fixed point when $\alpha = \pi$, as for the tracking fixed point. They are in the same side of the phase space. In the figures where $\Omega_0/\Lambda_s = 0.2$ we show that the tracking fixed point keeps its elliptic stable nature, since at finite times there are no crossings, and the adiabatic theorem applies until the end of the process. Thus, we have an efficient adiabatic transfer for small values of $\Omega_0/\Lambda_s = 0.2$. The Fig. 2.16 corresponds to a larger value of Ω_0/Λ_S. Here also there is no crossing, since the blue and the adiabatic tracking (red) curves correspond to the fixed points, for which $\alpha = \pi$. The green curve corresponds to $\alpha = 0$, which is on the other side of the phase space. Thus, in the case of $\alpha = \pi$ we have an efficient transfer to the target state as in the case without Kerr terms.

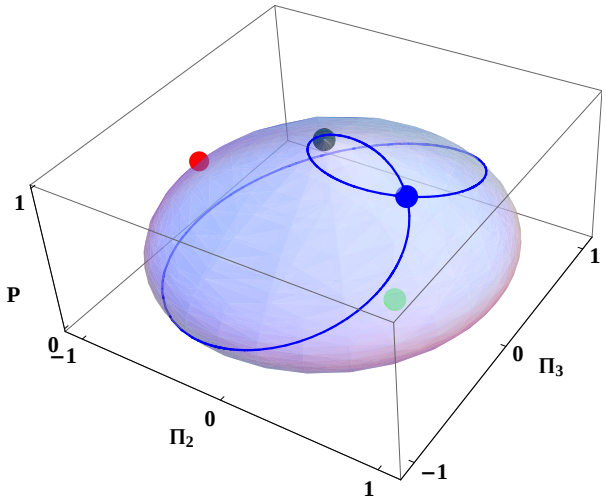

Figure 2.13: Tracking with $\Delta_{track,\pi}$. $\Omega_0/\Lambda_s = 0.2$, $\tau = 6$.

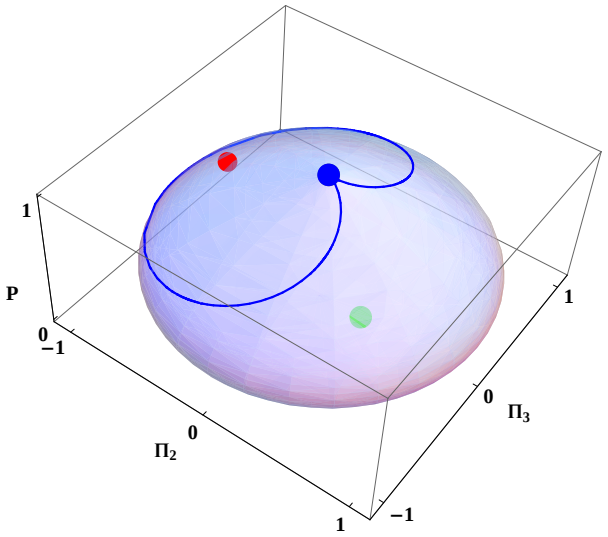

Figure 2.14: Tracking with $\Delta_{track,\pi}$. $\Omega_0/\Lambda_s = 0.2$, $\tau = 6$.

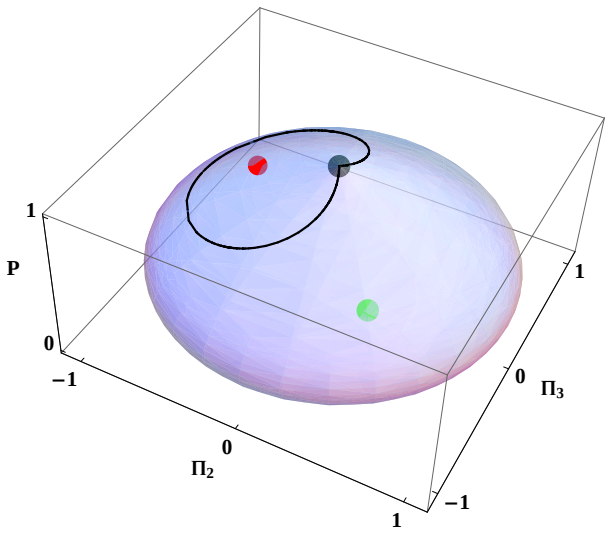

Figure 2.15: Tracking with $\Delta_{track,\pi}$. $\Omega_0/\Lambda_s = 0.2$, $\tau = 6$.

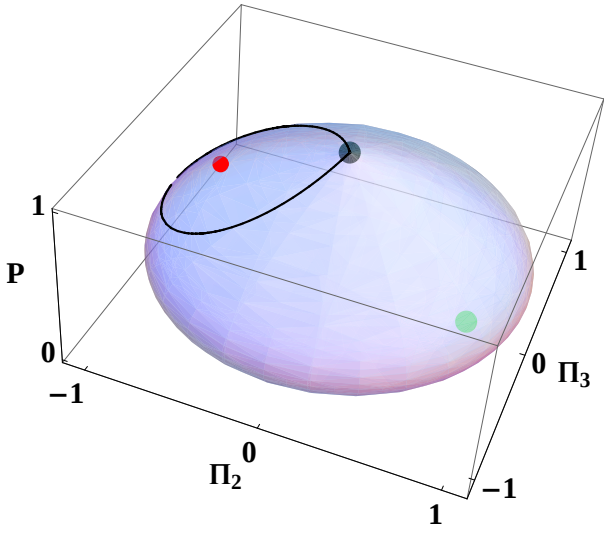

Figure 2.16: Tracking with $\Delta_{track,\pi}$. $\Omega_0/\Lambda_s = 1.1$, $\tau = 9$.

2.4 Exact tracking with Kerr nonlinearities

2.4.1 Determination of $\Delta(t)$ from $\Omega(t)$ and $P(t)$

We start with the Hamiltonian given by:

$$H = -\frac{\Delta}{3}J + \Delta I + \frac{\Omega}{\sqrt{2}}(J-2I)\sqrt{I}\cos\alpha + \frac{\Lambda_{11}}{2}(J-2I)^2 + \frac{\Lambda_{22}}{2}I^2 + \Lambda_{12}(J-2I)I \quad (2.37)$$

Introducing the notations

$$\Lambda_s = 2\Lambda_{11} + \frac{\Lambda_{22}}{2} - 2\Lambda_{12}, \qquad \Lambda_a = 2\Lambda_{11} - \Lambda_{12}, \quad (2.38)$$

$$f = \frac{1}{\sqrt{2}}(1-2I)\sqrt{I}, \quad (2.39)$$

and

$$g = \frac{\Lambda_{11}}{2}(1-2I)^2 + \frac{\Lambda_{22}}{2}I^2 + \Lambda_{12}(1-2I)I = -\Lambda_a I + \Lambda_s I^2 + const,$$

also adopting the normalization $J = 1$, instead of (2.37) we will have:

$$H = -\frac{\Delta}{3} + \Delta I + \Omega f(I)\cos\alpha + g(I) \quad (2.40)$$

from (2.40) one can obtain:

$$\dot{I} = -\frac{\partial H}{\partial \alpha} = \Omega f(I)\sin\alpha \quad (2.41)$$

$$\dot{\alpha} = \frac{\partial H}{\partial I} = \Delta + \Omega f'(I)\cos\alpha + g'(I). \quad (2.42)$$

where $\dot{\alpha}$ denotes the time derivative and $f'(I)$ the derivative with respect to I. Then, from (2.41) we can get

$$\sin\alpha = \frac{\dot{I}}{\Omega f}, \qquad \cos\alpha = \pm\sqrt{1 - \frac{\dot{I}^2}{\Omega^2 f^2}}$$

$$\alpha = \arcsin\frac{\dot{I}}{\Omega f}, \qquad \dot{\alpha} = \frac{1}{\pm\sqrt{1-\frac{\dot{I}^2}{\Omega^2 f^2}}}\frac{d}{dt}\left(\frac{\dot{I}}{\Omega f}\right).$$

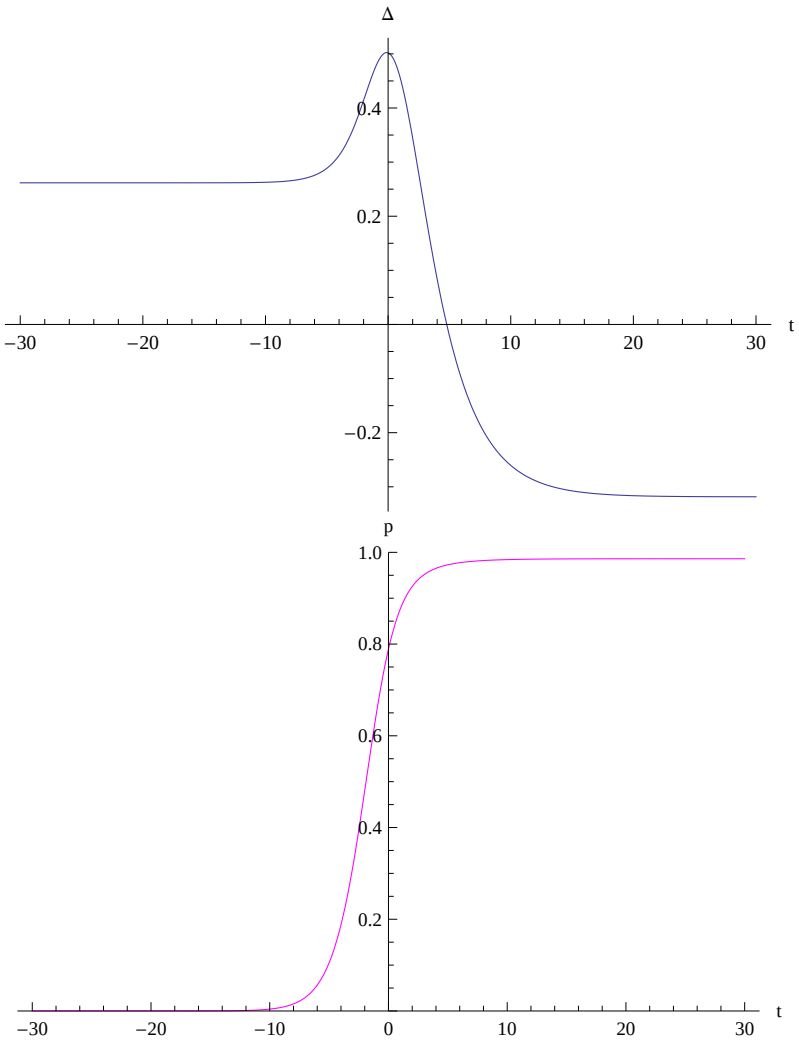

Figure 2.17: In the first figure $\Delta(t)$ constructed by exact tracking, by Eq. (2.45) with $P(t)$, since we have two exact solutions for $\Delta(t)$ Eq. (2.53) for the parameters $\Omega_0 = 1$, $T = 3$ and $r = 0.6$. In the second figure we present the exact tracking $P(t)$ with exact solution of $\Delta(t)$ from Eq. (2.45), for the parameters $\Omega_0 = 1$, $T = 3$.

Inserting into (2.42) one can write the exact tracking formula:

$$\Delta = \frac{1}{\pm\sqrt{1-\frac{\dot{I}^2}{\Omega^2 f^2}}}\left[\frac{\ddot{I}}{\Omega f} - \dot{I}^2\frac{f'}{f^2\Omega} - \frac{\dot{I}\dot{\Omega}}{\Omega^2 f}\right] - f'\Omega\left(\pm\sqrt{1-\frac{\dot{I}^2}{\Omega^2 f^2}}\right) - g' \tag{2.43}$$

$$\Delta = \frac{1}{\pm\sqrt{\Omega^2 f^2 - \dot{I}^2}}\left[\ddot{I} - \dot{I}\frac{\dot{\Omega}}{\Omega} - \dot{I}^2\frac{f'}{f} - ff'\Omega^2 + \frac{f'}{f}\dot{I}^2\right] - g' \tag{2.44}$$

For f given by Eq. (2.39), we will have

$$\Delta = \frac{1}{\pm\sqrt{\Omega^2 f^2 - \dot{I}^2}}\left[\ddot{I} - \frac{\dot{\Omega}}{\Omega}\dot{I} - \frac{\Omega^2}{4}(1 - 8I + 12I^2)\right] - g' \tag{2.45}$$

We obtain the formula for adiabatic tracking by neglecting $\dot{I} \sim \varepsilon \sim 0$, and $\ddot{I} \sim \varepsilon^2 \sim 0$, from which we will have $\Delta \approx -f'\Omega - g'$. Thus, we have a solution for exact tracking.

2.4.2 Conditions for the choice of $\Omega(t)$ and $P(t)$

From (2.45) we see that Δ will be well-defined (without divergence) if the denominator $\sqrt{\Omega^2 f^2 - \dot{I}^2} \neq 0$ for any t. This condition is equivalent, by integration to

$$I(t) < \frac{1}{2}\tanh^2\left[\int_{t_i}^{t}\frac{\Omega(s)}{2}ds\right] \tag{2.46}$$

since we have

$$I(t) = \frac{1}{2}\tanh^2\left[\int_{t_i}^{t}\frac{\Omega(s)}{2}\sin\alpha(s)ds\right] \tag{2.47}$$

one way to choose $I(t)$, is using $\Omega(t)$ and an arbitrary function $\sin\alpha(t)$.

For the example we will choose the simplest case, where

$$\sin\alpha(t) = \frac{r}{T} = const < 1$$

and $I(t)$ will be as we have in the Eq. (2.47). We cannot choose $I(t)$ and $\Omega(t)$ independently, but if we choose them such that they satisfy Eq. (2.46), then $\Omega^2 f^2 - \dot{I}^2 \neq 0$, we will have

the exact tracking formula, therefore, one can define Δ from Eq. (2.45).

We can prove this by taking $\Omega^2 f^2 - \dot{I}^2 = 0$ from which we get

$$\dot{I} = \frac{\Omega}{\sqrt{2}}(1 - 2I)\sqrt{I}$$

In this section we are doing the same calculations as we did in the paragraph 1.1.2 with $\alpha(t) = \frac{\pi}{2}$. We will obtain:

$$I(t) = \frac{1}{2}\tanh^2\left[\int_{t_i}^{t} \frac{\Omega(s)}{2} ds\right] \tag{2.48}$$

Thus, if

$$I(t) < \frac{1}{2}\tanh^2\left[\int_{t_i}^{t} \frac{\Omega(s)}{2} ds\right] \tag{2.49}$$

we will get

$$\Omega^2 f^2 - \dot{I}^2 \neq 0.$$

The condition for existence of exact tracking (non divergent $\Delta(t)$) is thus

$$P(t) < \tanh^2 \int_{t_0}^{t} \frac{\Omega(t')}{2} dt'. \tag{2.50}$$

On the other hand, from previous Chapter for $P(t)$ we have the relation:

$$P(t) = \tanh^2\left[\int_{t_0}^{t} \frac{\Omega(t')}{2} \sin\alpha(t') dt'\right]$$

Since $|\sin\alpha(t)| < 1$, from the last two equations we get

$$P(t) = \tanh^2\left[\int_{t_0}^{t} \frac{\Omega(t')}{2} \sin\alpha(t') dt'\right] \leq \tanh^2 \int_{t_0}^{t} \frac{\Omega(t')}{2} dt'. \tag{2.51}$$

2.4.3 An example

We choose $\Omega(t)$ as

$$\Omega(t) = \Omega_0 \text{sech}\left(\frac{t}{T}\right) \tag{2.52}$$

and $\sin\alpha(t) = \frac{r}{T\Omega_0} < 1$, where r is constant. Since

$$\frac{\Omega_0}{2}\int_{-\infty}^{t} \operatorname{sech}\left(\frac{t}{T}\right) dt = T\Omega_0\left[\arctan\left(\tanh\frac{t}{2T}\right) + \frac{\pi}{4}\right],$$

we can write

$$P(t) = \tanh^2\left(r\Omega_0\left[\arctan\left(\tanh\frac{t}{2T}\right) + \frac{\pi}{4}\right]\right) \tag{2.53}$$

where $r < 1$. In conclusion, the (2.52) and (2.53) provide a tracking solution, with a well-defined $\Delta(t)$, without singularities.

2.4.4 Exact tracking with $\alpha = const$ including Kerr nonlinearities

From the following equations

$$\dot{P} = \Omega(1-P)\sqrt{P}\sin\alpha \tag{2.54}$$

$$\dot{\alpha} = (\Delta - \Lambda_a) + \Lambda_s P + \frac{\Omega(1-3P)}{2\sqrt{P}}\cos\alpha \tag{2.55}$$

and with the initial condition $P(t_i) = 0$ the Eq. (2.54) we can present as

$$P(t) = \tanh^2\left[\int_{t_i}^{t}\frac{\Omega(t')}{2}\sin\alpha(t')dt'\right] \tag{2.56}$$

(assuming that $P(t) \geq 0$). Thus, by choosing $\alpha(t)$, for a given $\Omega(t)$ one can determine $P(t)$. One should choose $\sin\alpha(t)$ positive for small $t - t_i$ and for $\Omega(t) \geq 0$, to explain that $P \geq 0$.

A possible simple choice is $\sin\alpha(t) = \frac{S_0}{T\Omega_0} = const > 0$. Remark: for exact tracking we cannot choose $\alpha(t) = 0$ for any t, since $P(t) = 0$ and would have a divergence due to $\frac{\Omega(t)}{\sqrt{P}}$.

Note, that we choose $\alpha \in [0, \pi]$. Thus, $\sin\alpha(t) = const$, $\frac{d\alpha}{dt} = 0$, the exact tracking is determined by:

$$\Delta_{\pm} = \Lambda_a - \Lambda_s P \mp \frac{\Omega(1-3P)}{2\sqrt{P}}\sqrt{1 - \left(\frac{s_0}{T\Omega_0}\right)^2} \tag{2.57}$$

This exact tracking can be compared with the adiabatic tracking

$$\Delta_{\pm}^{ad} = \Lambda_a - \Lambda_s P \mp \frac{\Omega(1-3P)}{2\sqrt{P}} \tag{2.58}$$

Thus, the only thing that changes is the factor $\sqrt{1-\left(\frac{s_0}{T\Omega_0}\right)^2}$. This explains that after the crossing of fixed points one still obtains an efficient transfer (see [2]), although the adiabatic theorem is not valid.

2.5 Exact tracking with Kerr terms: a second approach

2.5.1 Determination of $\delta(t)$

We consider the following nonlinear system, which describes atomic and molecular condensates [96] and includes third-order nonlinearities:

$$i\dot{a_1} = Ue^{-i\delta(t)}\bar{a_1}a_2 + (\Lambda_{11}|a_1|^2 + \Lambda_{12}|a_2|^2)a_1 \tag{2.59}$$

$$i\dot{a_2} = \frac{U}{2}e^{i\delta(t)}a_1a_1 + (\Lambda_{21}|a_1|^2 + \Lambda_{22}|a_2|^2)a_2 \tag{2.60}$$

One can get an exact third-order nonlinear differential equation for molecular state probability $P = |a_2|^2$ [112]:

$$\left(\frac{d}{dt} - \frac{1}{G}\frac{dG}{dt}\right)\left[\frac{1}{U}\frac{d}{dt}\left(\frac{1}{U}\frac{dP}{dt}\right) - \frac{1}{2}(1 - 8P + 12P^2)\right] + G^2\frac{dP}{dt} = 0, \tag{2.61}$$

where

$$G = \frac{\delta_t - \Lambda_a + 2\Lambda_s P}{U}, \qquad \delta_t \equiv \frac{d\delta}{dt}. \tag{2.62}$$

$$\Lambda_s = 2\Lambda_{11} + \frac{\Lambda_{22}}{2} - 2\Lambda_{12}, \qquad \Lambda_a = 2\Lambda_{11} - \Lambda_{12} \tag{2.63}$$

From Eq. (2.61) after making some calculations, for δ_t one can obtain the following exact

equation

$$\delta_t = \Lambda_a - 2\Lambda_s P \pm \frac{\frac{d^2P}{dt^2} - \frac{1}{U}\frac{dU}{dt}\frac{dP}{dt} - \frac{U^2}{2}(1 - 8P + 12P^2)}{\sqrt{|\left(\frac{dP}{dt}\right)^2 - \frac{U^2}{2}(1-2P)^2 P + C_0 U^2|}}. \tag{2.64}$$

For the initial condition $P(-\infty) = 0$, we find $C_0 = 0$. If in Eq. (2.64) we put the derivatives of P equal to zero, we get an equation for adiabatic tracking.

2.6 Conclusion and discussion

In this Chapter we have analyzed the method of adiabatic tracking for nonlinear two-state models of photoassociation of Bose-Einstein atomic condensates, which include the Kerr type nonlinearities. The third-order nonlinearities result in a modified separatrix and fixed points, imposing different form for the instantaneous detuning.

We can summarize the main results as follows: We have first found an equation for $P(t)$, which is of the same form as the one which we obtained without Kerr terms. The formula shows that one cannot achieve a complete transfer with pulses of a finite area, one can only approach asymptotically, as it was already established for the models without Kerr terms.

The presented analysis shows that a good adiabatic transfer can be achieved by the adiabatic tracking approach also in the presence of the Kerr nonlinearities.

It is indeed still possible to construct a detuning that leads to an efficient tracking of the chosen population dynamics despite the strong modifications of the structure of the adiabatic phase portrait, through interfering fixed point trajectories, which induces bifurcation and loss of stability of the adiabatic dynamics.

To show this result, we have first reduced the two-level model in order to highlight two relevant combinations of Kerr terms Λ_a and Λ_s. They produce two distinct effects: The term Λ_a is a shift that can be easily compensated via a static detuning term. The Λ_s term leads to a behaviour qualitatively different from the nonlinear model without Kerr terms. We have analyzed the method of adiabatic tracking to design the detuning and to determine the range of pulse peaks, for a given pulse shape, allowing one to approach the complete transfer. We have found two qualitatively different forms for the detuning.

We have shown that if $\alpha = 0$, we always have an unavoidable crossing between the tracking and another fixed points that gives a hyperbolic character to the tracking fixed point. And once the tracking fixed point is hyperbolic, the classical adiabatic theorem does not apply anymore thus destroying the adiabaticity, and the final stage of the process is non-adiabatic. This can strongly degrade the quality of the transfer for small amplitudes of the driving pulse. However, we have shown that one can avoid oscillations by taking strong enough pulses compared with the magnitude of the Kerr terms. Thus, the effect of this non-adiabatic crossing can be made negligible [2].

The key result of this Chapter is that one can always design a path, i.e. a detuning for a given field, that leads to a very efficient association even for strong Kerr terms as large as the Rabi frequency.

Indeed, we found that the crossing of fixed points can be completely avoided by choosing the tracking corresponding to the fixed point with $\alpha = \pi$ [2]. This leads to a stable adiabatic transfer to the target molecular state as in the case without Kerr type nonlinearities [1].

From the practical point of view, in photo- and magneto-association of atomic BEC into molecular state, the Kerr terms are proportional to the density while the coupling scales as the square root of the density [99]. Some typical values, e.g. for a ^{87}Rb condensate, are [98]:

$$\Lambda_{11} = 4.96 \times 10^{-11}\rho(s^{-1}), \qquad \Lambda_{22} = 2.48 \times 10^{-11}\rho(s^{-1}) \qquad \Lambda_{12} = \Lambda_{21} = -6.44 \times 10^{-11}\rho(s^{-1}) \tag{2.65}$$

with ρ the density (in cm^{-3}), typically $\rho = \rho_0 \equiv 4.2 \times 10^{14}(cm^{-3})$, giving

$$\Lambda_s = 2.40 \times 10^{-10}\rho(s^{-1}), \qquad \Lambda_a = 1.64 \times 10^{-10}\rho(s^{-1}). \tag{2.66}$$

Using these numbers, we have numerically found that

✓Kerr terms as strong as $\Lambda_s \sim \Omega_0/2$ already lead to an infidelity of 10 % for the transfer if one does not take into account the compensating term proportional to Λ_s in the design of the detuning (2.23) or (2.24);

✓the distinction between the dynamics induced by the two respective detunings (2.23)

and (2.24) can be observed for Kerr terms as strong as $\Lambda_s \sim \Omega_0$;

✓one can compensate the Kerr terms with a high-fidelity transfer using the design (2.24) giving a high fidelity transfer for the peak Rabi frequency as low as $\Omega_0 \sim \Lambda_s/2$.

This opens the possibility to achieve the association at (1) larger densities than usually used (but not too large so that S-wave scattering is dominant) and (2) lower field amplitudes by designing the control detuning according to (2.24). Note that, in any case, the field duration T has to be adapted such that $\tau \equiv \Omega_0 T \gtrsim 5$ in order to maintain adiabaticity. For instance, typical coupling for photoassociation [98] $\Omega_0 = 2.1 \times 10^6 \sqrt{\rho/\rho_0} s^{-1}$, i.e. $\Omega_0/\Lambda_s \approx 10^{16}\sqrt{1/(\rho\rho_0)}$, allows one in principle to multiply the density of the condensate by up to 2500 or to divide the field amplitude by up to 50 (or any combination of these) to still reach a high fidelity transfer.

One can mention the Λ-photoassociation configuration which has the potential to strongly minimize loss and decoherence when the stimulated Raman adiabatic passage (STIRAP) process is considered [97,99]. It has been shown [98] that a low density of a ^{87}Rb condensate would in principle enhance the molecular conversion efficiency by reducing the Kerr nonlinearities compared to a standard density. However, it has been argued [99] that the reduction of the density causes in general several practical problems. Our alternative strategy to maintain or even increase the density appears thus in principle relevant in this configuration. Further, we will explore the extension of our results in Λ systems, taking into account the additional issue that the classical Hamitlonian for the three-state problem is non-integrable.

The language of photoassociation theory has been adopted in this Chapter, however, the derived results are general for nonlinear problems that are described by (2.1) and (2.2), arising also in other physical domains, for instance in nonlinear optics [93], such as frequency conversion beyond the undepleted pump approximation [108].

The adiabatic tracking ensures a certain robustness of the dynamics and a very good fidelity of the process. Achieving an ultrahigh fidelity comparable to the one obtained by optimized adiabatic passage of linear systems (see for instance [95]) or for shortcut to adiabaticity techniques [109] is an open question.

Chapter 3

Nonlinear stimulated Raman exact tracking

As it was already mentioned, the goal of the work is to present an analysis of the atom-molecule conversion dynamics in degenerate quantum gases. The atom-molecule conversion is performed within a two-step conversion process, which is known as the Raman transition.

A version of this kind of transition is the stimulated Raman adiabatic passage (STIRAP). The STIRAP, a field-matter interaction model, is a well established process widely used by the quantum physics community for more than 20 years. Here a counterintuitive sequence of two laser fields is applied to create a molecular Bose-Einstein condensate by means of connecting the initial free-atomic state and the final molecular ground state via a third excited state of weakly bound molecules. Remarkably, with the appropriate time-dependent pulse shapes, the STIRAP process permits the coherent transfer of the molecules to the ground state without essentially populating the excited state, thereby removing the possibility of losses because of spontaneous decay. In the considered model we obtain exact dynamics of quantum transfer by stimulated Raman processes for nonlinear systems controlled by pulsed fields. The external fields are designed by inverse-engineering construction, which allows to surpass the usual nonlinear STIRAP efficiency.

It is shown, that in order to have an efficient transfer for nonlinear stimulated Raman

exact tracking, one has to use a pump pulse stronger than the Stokes pulse, contrary to the ordinary linear STIRAP case.

To avoid the losses from the weakly bound molecular state, we propose a technique for stimulated Raman exact tracking including losses. We show how one can avoid these losses from the intermediate state in the case of one- and two-photon resonances.

Finally, we present an analysis of the robustness for linear and nonlinear STIRAP procedures.

3.1 Properties of the nonlinear model

The stimulated Raman processes for the nonlinear model are described by the equation

$$i\frac{\partial\psi}{\partial t} = H_{NL}\psi, \tag{3.1}$$

with

$$\psi = \begin{pmatrix} a_1 \\ a_2 \\ a_3 \end{pmatrix} \tag{3.2}$$

and

$$H_{NL} = \begin{bmatrix} 0 & 2\Omega_P\bar{a_1} & 0 \\ 2\Omega_P a_1 & 0 & \Omega_S \\ 0 & \Omega_S & 0 \end{bmatrix}, \tag{3.3}$$

where Ω_P and Ω_S are the pump and Stokes Rabi frequencies, respectively. We suppose that they are real and time-dependent. The normalization condition is:

$$|a_1|^2 + 2|a_2|^2 + 2|a_3|^2 = 1 \tag{3.4}$$

In the variables $a_1 = c_1$, $2a_2 = c_2$, $2a_3 = c_3$, and taking into account the detunings, Kerr

nonlinearities and losses, the governing equations are rewritten as

$$\begin{aligned} i\dot{c_1} &= \Omega_P \bar{c_1} c_2 + (\Lambda_{11}|c_1|^2 + \Lambda_{12}|c_2|^2 + \Lambda_{13}|c_3|^2)c_1 \\ i\dot{c_2} &= (-i\Gamma + \Delta)c_2 + \Omega_P c_1^2 + \Omega_S c_3 + (\Lambda_{21}|c_1|^2 + \Lambda_{22}|c_2|^2 + \Lambda_{23}|c_3|^2)c_2 \\ i\dot{c_3} &= \Omega_S c_2 + \delta c_3 + (\Lambda_{31}|c_1|^2 + \Lambda_{32}|c_2|^2 + \Lambda_{33}|c_3|^2)c_3 \end{aligned} \tag{3.5}$$

with the normalization condition now given as

$$|c_1|^2 + |c_2|^2 + |c_3|^2 = 1. \tag{3.6}$$

An important observation has to be highlighted: when starting with the initial condition $c_1(t_i) = 1$ at the initial time t_i, if the Rabi frequencies are real, from the form of the equations (3.5) we can conclude that $c_1(t)$ and $c_3(t)$ are real, and $c_2(t)$ is purely imaginary for all times. We will show that the nonlinear problem (3.3) is isomorphic to a modified nonlinear two-state problem (with $\psi_2 = [b_1\ b_2]^t$ and $|b_1|^2 + |b_2|^2 = 1$):

$$i\frac{\partial \psi_2}{\partial t} = H_{NL,2}\psi_2 \tag{3.7}$$

with the following Hamiltonian

$$H_{NL,2} = \frac{1}{2}\begin{bmatrix} -\Omega_S & \Omega_P(|b_1|^2 - |b_2|^2) \\ \Omega_P(|b_1|^2 - |b_2|^2) & \Omega_S \end{bmatrix}. \tag{3.8}$$

We note that the nonlinearlity which appears here is not the one usually encountered in the Bose-Einstein condensation or in nonlinear optics.

3.2 Isomorphism

The density matrix ρ corresponding to the system (3.8) is defined by

$$\rho_{ij} = \langle i|\psi_2\rangle \langle \psi_2|j\rangle .$$

and $|j>_{j=1,2}$. We introduce the corresponding Bloch variables ρ_x, ρ_y, ρ_z defined by

$$\begin{aligned} \rho_x &= \rho_{21} + \rho_{12} = b_2\bar{b_1} + b_1\bar{b_2}, \\ \rho_y &= i(\rho_{21} - \rho_{12}) = i(b_2\bar{b_1} - b_1\bar{b_2}), \\ \rho_z &= \rho_{22} - \rho_{11} = |b_2|^2 - |b_1|^2, \end{aligned} \tag{3.9}$$

The isomorphism is shown with the use of the density matrix formulation on the Bloch sphere. Thereby, the system (3.7) expressed in these variables leads to the following differential equations:

$$\frac{d}{dt}\begin{bmatrix} \rho_z \\ \rho_y \\ \rho_x \end{bmatrix} = \begin{bmatrix} 0 & \Omega_P\rho_z & 0 \\ -\Omega_P\rho_z & 0 & \Omega_S \\ 0 & -\Omega_S & 0 \end{bmatrix}\begin{bmatrix} \rho_z \\ \rho_y \\ \rho_x \end{bmatrix} \tag{3.10}$$

The population difference (or equivalently the coefficient $\overline{c_1}$ in the original three-state representation) in front of Ω_P can be expected to reduce the efficiency of the pump near the end of the transfer while the transfer is being accomplished, $\mid a_1 \mid \longrightarrow \mid a_2 \mid$ (or equivalently $c_1 \longrightarrow 0$). We thus anticipate that a stronger pump pulse is needed, in contrast to the ordinary linear STIRAP.

By comparing (3.10) with (3.3) we see that the equations are the same if we make the identification

$$c_1 = -\rho_z, \qquad c_2 = -i\rho_y, \qquad c_3 = \rho_x$$

(under the condition that c_1 and c_3 are real and c_2 is imaginary). Note, that in the current Chapter for our calculations we consider $\hbar = 1$. Thus, from each solution of (3.8) we obtain a solution of Eq. (3.10).

We thus recover the initial three-state problem with the initial condition $c_1(t_i) = 1$. As a consequence, the resonant nonlinear STIRAP equation can be mapped to a nonlinear two-level model. From the definition of the variables (3.9) we see that a complete transfer of the 3 level system $|c_3(t_f)| = 1$, i.e. $\rho_x(t_f) = \pm 1$ at the final time t_f, corresponds in the two-state problem (3.8) to the passage from the initial state $\rho_{11}(t_i) = 1$, to the superposition of states:

$\rho_{12}(t_f) = \rho_{21}(t_f) = \pm\frac{1}{2}$, (which is the maximal coherence in the density matrix formulation).

This shows a similar qualitative behaviour as for its linear analog.

3.3 Analysis of the model

We can rewrite the general solution of the two-state problem Eq. (3.8) parameterized by three angles:

$$\begin{bmatrix} b_1 \\ b_2 \end{bmatrix} = \begin{bmatrix} \cos(\theta/2) \\ \sin(\theta/2)e^{-i\varphi} \end{bmatrix} e^{-i\gamma} \tag{3.11}$$

In terms of these three angles the time-dependent Schrödinger equations lead to the equations

$$\begin{aligned} \dot{\theta} &= 2\Omega_P \cos\theta \sin\varphi, \\ \dot{\varphi} &= 2\Omega_S + 2\Omega_P \tfrac{\cos^2\theta}{\sin\theta} \cos\varphi, \\ \dot{\gamma} &= -\Omega_S + \Omega_P \cos\theta \tan(\theta/2) \cos\varphi. \end{aligned} \tag{3.12}$$

One can solve the first equation of (3.12) exactly [for any $\Omega_P(t)$ and $\Omega_S(t)$]:

$$\tanh(\theta/2) = \tanh\left[2\int_{t_i}^{t} \Omega_P(s)\sin\varphi(s)ds\right]. \tag{3.13}$$

This relation implies that in order to have a complete transfer from the first state to the third one, in the original model, i.e. $\theta(t_i) = 0$ and $\theta(t_f) = \pi/4$, we need an infinite pulse area of $\Omega_P(t)$.

This contrasts with the linear model where a complete population transfer is possible for finite pulse area. It can be achieved for a so-called intuitive sequence, i.e. with the pump pulse switched on first, or for a counterintuitive sequence in which the Stokes pulse is switched on first. With the intuitive sequence the pump pulse transfers first the population from state 1 to state 2, and next the Stokes pulse leads the population from state 2 to state 3. However, an overlap optimizes the time of interaction as shown in Ref. [110]. A counterintuitive sequence requires larger pulse areas but allows a smaller transient on the intermediate state, which is desirable since in practice this state is in general lossy. For the nonlinear model, we

derive below solutions for finite pulse areas which lead to an *approximate* population transfer.

3.4 Derivation of an ordinary differential equation for $c_3(t)$

We now derive a second-order differential equation for c_3. For convenience, we rewrite here the equations (3.5) without detunings, Kerr nonlinearities and losses

$$\begin{aligned} i\dot{c_1} &= \Omega_P \bar{c_1} c_2 \\ i\dot{c_2} &= \Omega_P c_1 c_1 + \Omega_S c_3 \\ i\dot{c_3} &= \Omega_S c_2 \end{aligned} \tag{3.14}$$

Since c_2 is imaginary we can denote $c_2 = ib_2$ and insert it into the second equation of (3.14) to obtain

$$-(\dot{b_2}) = \Omega_P c_1 c_1 + \Omega_S c_3 \tag{3.15}$$

Further, from the normalization condition we can write $c_1^2 = 1 - c_2^2 - c_3^2$. Inserting this into equation (3.15) we obtain

$$-(\dot{b_2}) = \Omega_P(1 - |c_2|^2 - |c_3|^2) + \Omega_S c_3 = \Omega_P(1 - b_2^2 - c_3^2) + \Omega_S c_3 \tag{3.16}$$

Dividing Eq. (3.16) by Ω_S, we get

$$-\frac{db_2}{\Omega_S dt} = \frac{\Omega_P}{\Omega_S}(1 - b_2^2 - c_3^2) + c_3 \tag{3.17}$$

The advanches result is that here by introducing the notations $\tilde{c}_3 \equiv \tilde{c}_3(z) = c_3(t)$, $z \equiv z(t) = \int_{t_i}^{t} \Omega_S(t')$, and also using the shortcut notations $\tilde{c}_{3,z} \equiv \frac{d\tilde{c}_3}{dz}$, $\tilde{c}_{3,zz} \equiv \frac{d^2\tilde{c}_3}{dz^2}$, for the third state probability amplitude we obtain the nonlinear ordinary differential equation of the second-order

$$\tilde{c}_3, zz + \tilde{c}_3 + \frac{\Omega_P}{\Omega_S}[1 - \tilde{c}_{3,z}^2 - \tilde{c}_3^2] = 0. \tag{3.18}$$

From this equation one can easily derive the values for pump or Stokes pulses for an exact tracking.

3.5 An exact tracking: determination of the pump- and Stokes-pulses

From Eq. (3.18) for any $\Omega_S(t)$ and $c(z)$ we have

$$\frac{\Omega_P}{\Omega_S} = \frac{-\tilde{c}_{3zz} - \tilde{c}_3}{1 - \tilde{c}_{3,z}^2 - \tilde{c}_3^2} = \frac{\tilde{c}_{3zz} + \tilde{c}_3}{\tilde{c}_3^2 + \tilde{c}_{3z}^2 - 1}. \tag{3.19}$$

Thus, it is seen that we can determine $\Omega_P(t)$ corresponding to a chosen $\Omega_S(t)$ and $c_3(t)$:

$$\Omega_P(t) = -\Omega_S(t)\frac{c_{3,tt} - c_{3,t}\Omega_{St}/\Omega_S + \Omega_S^2 c_3}{(1 - c_3^2)\Omega_S^2 - c_{3,t}^2}. \tag{3.20}$$

(since $z(t) = \int_{t_i}^{t} \Omega_S(t')$). This is the tracking solution.

We remark that in order to obtain a finite $\Omega_P(t)$, $\Omega_S(t)$ and $c_3(t)$ have to satisfy a compatibility condition, that can be expressed by requiring that the denominator in (3.20) is not zero: $(1 - c_3^2)\Omega_S^2 - c_{3,t}^2 \neq 0$.

Further, we choose an alternative parametrization, which is convenient to present as follows:

$$\begin{aligned} c_1 &= \cos\Theta\cos\phi, \\ c_2 &= i\sin\Theta, \\ c_3 &= -\cos\Theta\sin\phi \end{aligned} \tag{3.21}$$

where $\Theta(t_i) = \Theta(t_f) = 0$ and $\phi(t_i) = 0$, $\phi(t_f) = \pm\frac{\pi}{2}$.

One can derive the form of the pump and Stokes pulses using the time-dependent Schrödinger equations. Inserting the values of c_1, c_2, and c_3 from the Eq. (3.21) into the Eq. (3.3) we

obtain

$$\begin{aligned} i\Omega_P \sin\Theta \bar{c_1} &= i(-\dot{\Theta}\sin\Theta\cos\phi - \dot{\phi}\cos\Theta\sin\phi) \\ \dot{\Theta}\cos\Theta &= -\Omega_P \cos\Theta\cos^2\phi + \Omega_S \sin\phi \\ i\Omega_S \sin\Theta &= i(\dot{\Theta}\sin\Theta\sin\phi - \dot{\phi}\cos\Theta\cos\phi) \end{aligned} \tag{3.22}$$

The last equation of (3.22) for the Stokes pulse gives

$$\Omega_S = -\dot{\Theta}\sin\phi + \dot{\phi}\frac{\cos\phi}{\tan\Theta} \tag{3.23}$$

Further, inserting (3.23) into the second equation of (3.22) we obtain

$$\Omega_P = \dot{\Theta}\frac{1}{\cos\Theta}\left(-\frac{1}{\cos^2\phi} + \frac{\sin^2\phi}{\cos^2\phi}\right) - \dot{\phi}\frac{\tan\phi}{\sin\Theta} \tag{3.24}$$

and thus

$$\Omega_P = -\dot{\Theta}\frac{1}{\cos\Theta} - \dot{\phi}\frac{\tan\phi}{\sin\Theta}. \tag{3.25}$$

For the nonlinear case, only the form of the pump pulse differs from the one of the linear case, which has the form

$$\Omega_P = \dot{\Theta}\cos\phi + \dot{\phi}\frac{\sin\phi}{\tan\Theta}. \tag{3.26}$$

3.6 Parametrization of the tracking solution for two angles

We can choose in the mentioned two cases the following simple parametrization $\tilde{\Theta}(\phi) = \Theta(t)$:

$$\tilde{\Theta}(\phi) = \epsilon\frac{4}{\pi}\sqrt{\phi\left(\pm\frac{\pi}{2} - \phi\right)}, \tag{3.27}$$

which satisfies the boundary condition $\tilde{\Theta}(0) = \tilde{\Theta}(\pm\frac{\pi}{2}) = 0$, and has the maximum value $\tilde{\Theta}_{max} = \tilde{\Theta}\left(\phi = \pm\frac{\pi}{4}\right) = \epsilon$. Thus, the quantity ϵ allows the control of the maximum transient

population in the upper state 2:

$$max|c_2|^2 = \sin^2(\epsilon). \tag{3.28}$$

For $\phi(t)$ one finally chooses the time parametrization as, for instance:

$$\phi(t) = \eta\frac{\pi}{4}\left[1 + \tanh\left(\frac{t}{T}\right)\right], \tag{3.29}$$

where $\phi(t_i = -\infty) = 0$, $\phi_f = \phi(t_f = +\infty) = \eta\frac{\pi}{2}$. T is a normalized time, and $0 \leq \eta \leq 1$ allows the control of the final transfer:

$$|c_3(t_f)|^2 = \cos^2(\tilde{\Theta}(\phi_f))\sin^2\left(\eta\frac{\pi}{2}\right). \tag{3.30}$$

For the nonlinear case, η can be exactly one only for an infinite pump pulse area. In practice, one thus takes it being less than one.

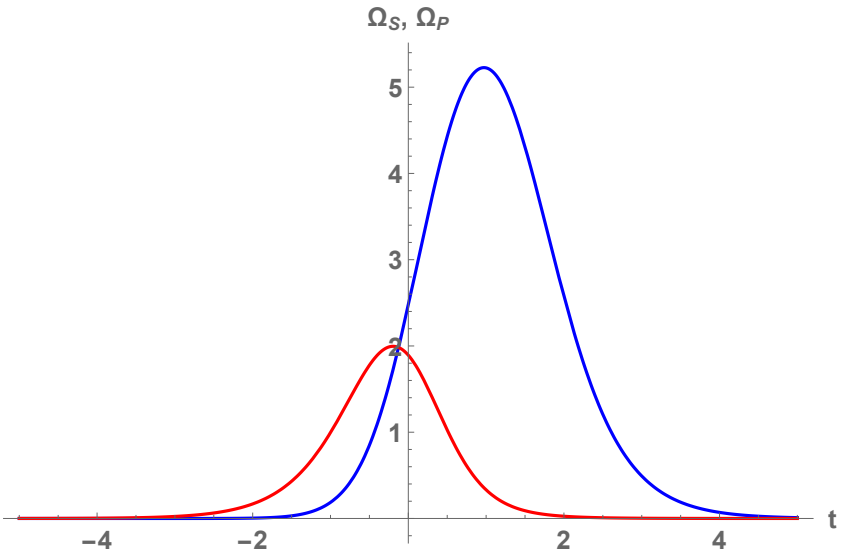

Figure 3.1: Nonlinear-system dynamics for the three-state problem, the Rabi frequencies: Stokes (first) and pump (second). $T = 1$, $\epsilon = 0.2$, $\eta = 0.96$, $\Delta = 0.1$. Kerr nonlinearities: $\Lambda_{11} = 0.212328\nu$, $\Lambda_{13} = \Lambda_{31} = -0.27962\nu$, $\Lambda_{33} = 00.10664\nu$, $\Lambda_{12} = \Lambda_{21} = 0$, $\Lambda_{22} = 0$, $\Lambda_{23} = \Lambda_{32} = 0$, where $\nu = 0,01$.

In Figs. 3.1 and 3.3 we display the dynamics of the nonlinear model for $\epsilon = 0.2$ and $\eta = 0.96$, leading to a very efficient transfer $|c_3|^2(t_f) \approx 0.99$ with a low transient population

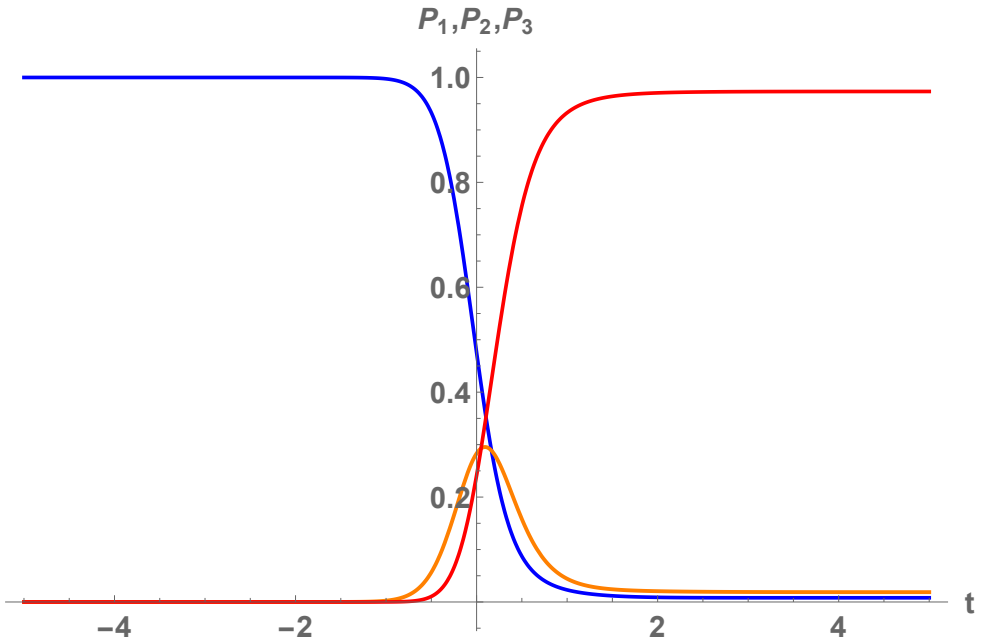

Figure 3.2: Nonlinear-system dynamics. The populations for three levels. $T = 1$, $\epsilon = 0.2$, $\eta = 0.96$, $\Delta = 0.1$. Kerr nonlinearities: $\Lambda_{11} = 0.212328\nu$, $\Lambda_{13} = \Lambda_{31} = -0.27962\nu$, $\Lambda_{33} = 00.10664\nu$, $\Lambda_{12} = \Lambda_{21} = 0$, $\Lambda_{22} = 0$, $\Lambda_{23} = \Lambda_{32} = 0$, where $\nu = 0, 01$.

in state 2. Here we consider Eqs. (3.5), where $\Gamma = 0$ and $\delta = 0$.

We notice the counterintuitive sequence (Stokes pulse first) for both linear and nonlinear models which results from this parametrization when a low transient transfer to the intermediate state is imposed.

3.7 Comparison with the dynamics by delayed Gaussian pulses

The results given by the tracking solution suggests to test the efficiency of the population transfer for standard shapes, such as delayed Gaussian pulses.

The pump Rabi frequency amplitude is adapted for a given Stokes Rabi frequency. In Fig. 3.3 we can see the transfer efficiency to state 3 for a counterintuitive Gaussian pulse sequence with delay $\tau > 0$ and pulse half-width T:

$$\Omega_P = \Omega_{Pmax} e^{-[(t-\tau)/T]^2}, \qquad \Omega_S = \Omega_{Smax} e^{-[(t+\tau)/T]^2}.$$

As expected, we retain a very good efficiency when the pump area is stronger than the Stokes area with the use of Gaussian pulses as well. In Fig. 3.3 we can see the same dynamics as in Fig. 3.2.

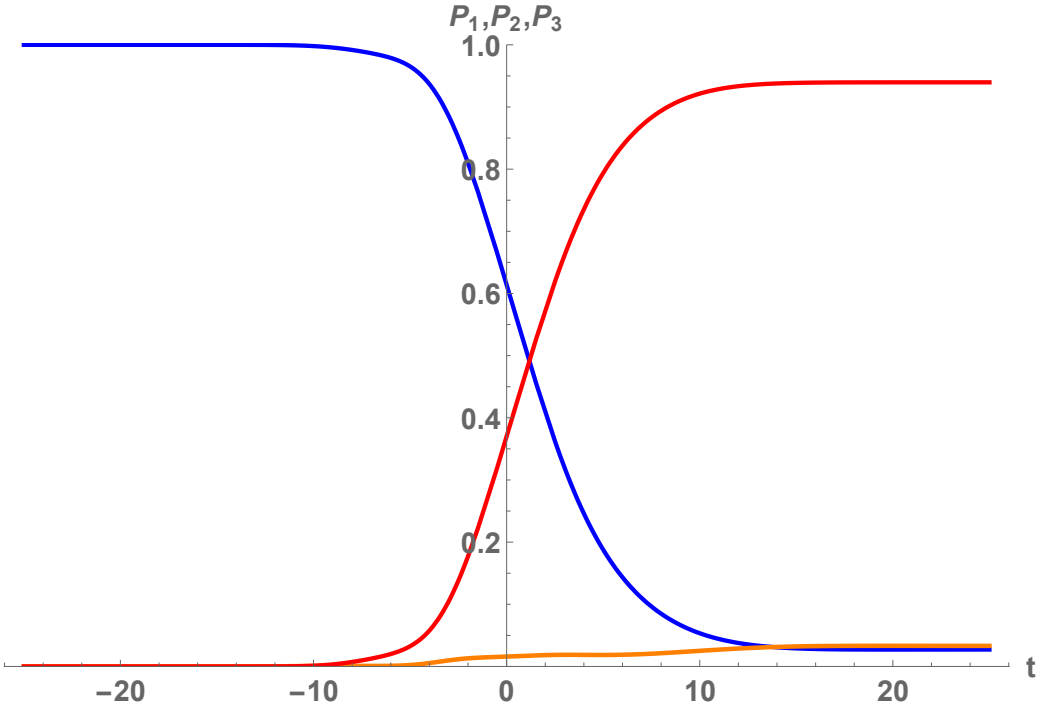

Figure 3.3: Nonlinear system dynamics for the three-state problem with $\tau_P = \tau_S = 5$, $T_P = T_S = 8$, $\Omega_{Pmax} = 5.1$, $\Omega_{Smax} = 2$, $\Delta = 0.1$. Kerr nonlinearities: $\Lambda_{11} = 0.212328\nu$, $\Lambda_{13} = \Lambda_{31} = -0.27962\nu$, $\Lambda_{33} = 00.10664\nu$, $\Lambda_{12} = \Lambda_{21} = 0$, $\Lambda_{22} = 0$, $\Lambda_{23} = \Lambda_{32} = 0$, where $\nu = 0, 01$.

Thus, we observe a very good efficiency when Ω_{Pmax} is stronger than Ω_{Smax} and for a relatively wide region of τ. This efficiency appears robust with respect to the peak amplitudes and the delay, similarly to the linear STIRAP.

We have derived an exact dynamics of quantum transfer by stimulated Raman processes for nonlinear systems. This technique describes the transient from an atomic to a molecular Bose-Einstein condensate. The main point is, that unlike in the linear stimulated Raman adiabatic passage, for nonlinear systems the technique features the need of a pump pulse stronger than the Stokes pulse.

3.8 Nonlinear stimulated Raman exact tracking with detuning and Kerr nonlinearities

We consider a nonlinear three-level system, without losses, including detuning and Kerr nonlinearities:

$$\begin{aligned} i\dot{c_1} &= \Omega_P \bar{c_1} c_2 + (\Lambda_{11}|c_1|^2 + \Lambda_{12}|c_2|^2 + \Lambda_{13}|c_3|^2)c_1 \\ i\dot{c_2} &= \Delta c_2 + \Omega_P c_1^2 + \Omega_S c_3 + (\Lambda_{21}|c_1|^2 + \Lambda_{22}|c_2|^2 + \Lambda_{23}|c_3|^2)c_2 \\ i\dot{c_3} &= \Omega_S c_2 + (\Lambda_{31}|c_1|^2 + \Lambda_{32}|c_2|^2 + \Lambda_{33}|c_3|^2)c_3 \end{aligned} \tag{3.31}$$

We took the values for the third-order nonlinearities as [97]:

$$\Lambda_{11} = 0.212328\nu, \qquad \Lambda_{13} = \Lambda_{31} = -0.27962\nu, \qquad \Lambda_{33} = 0.10664\nu$$

$$\Lambda_{12} = \Lambda_{21} = 0, \qquad \Lambda_{23} = \Lambda_{32} = 0, \qquad \Lambda_{22} = 0.$$

where $\nu = 0.01$, $\Delta = 0.1$, $\delta = 0$.

As we did without Kerr terms, we can choose the Rabi frequencies as Gaussian or via mentioned parametrization.

We choose the parametrization:

$$\tilde{\Theta}(\phi) = \epsilon \frac{4}{\pi} \sqrt{\phi \left(\pm \frac{\pi}{2} - \phi \right)} \tag{3.32}$$

The time parametrization for $\phi(t)$:

$$\phi(t) = \eta \frac{\pi}{4} \left[1 + \tanh\left(\frac{t}{T} \right) \right], \tag{3.33}$$

where T is a normalized time.

Thus, we can choose the Rabi frequencies as:

$$\Omega_P = \dot{\tilde{\Theta}}(t) \frac{1}{\cos(\tilde{\Theta}(t))} + \dot{\Phi}(t) \frac{\tan(\Phi(t))}{\sin(\tilde{\Theta}(t))} \tag{3.34}$$

$$\Omega_S = -\dot{\tilde{\Theta}}(t)\sin(\Phi(t)) + \dot{\Phi}(t)\frac{\cos(\Phi(t))}{\tan(\tilde{\Theta}(t))} \tag{3.35}$$

As a result, we can achieve an efficient transfer with third-order Kerr nonlinearities and the second intermediate state can be less populated. Note, that here we do not take into account losses: $\Gamma = 0$. Thus, in this paragraph we consider the three-level system with Kerr nonlinearities and detuning Eqs. (3.31).

3.9 Nonlinear stimulated Raman exact tracking with losses. Determination of $c_3(t)$

In this paragraph we consider the dynamics of a nonlinear three-state system at one- and two-photon resonance at the presence of irreversible losses from the intermediate second level.

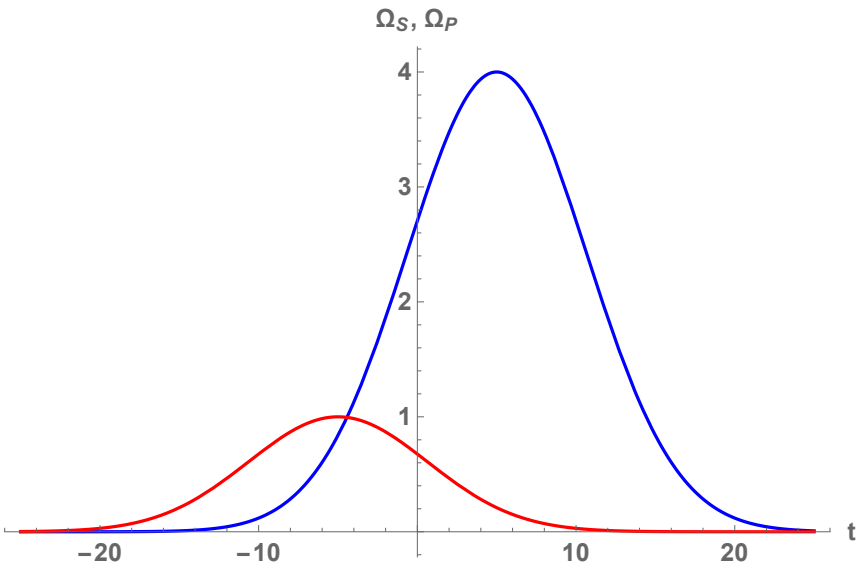

Figure 3.4: Nonlinear stimulated Raman exact tracking. The Rabi frequencies, which are taken as Gaussian. $\Omega_{Pmax} = 4$, $\Omega_{Smax} = 1$, $\tau_P = \tau_S = 5$, $T_P = T_S = 8$, and $\Gamma = 0.2$.

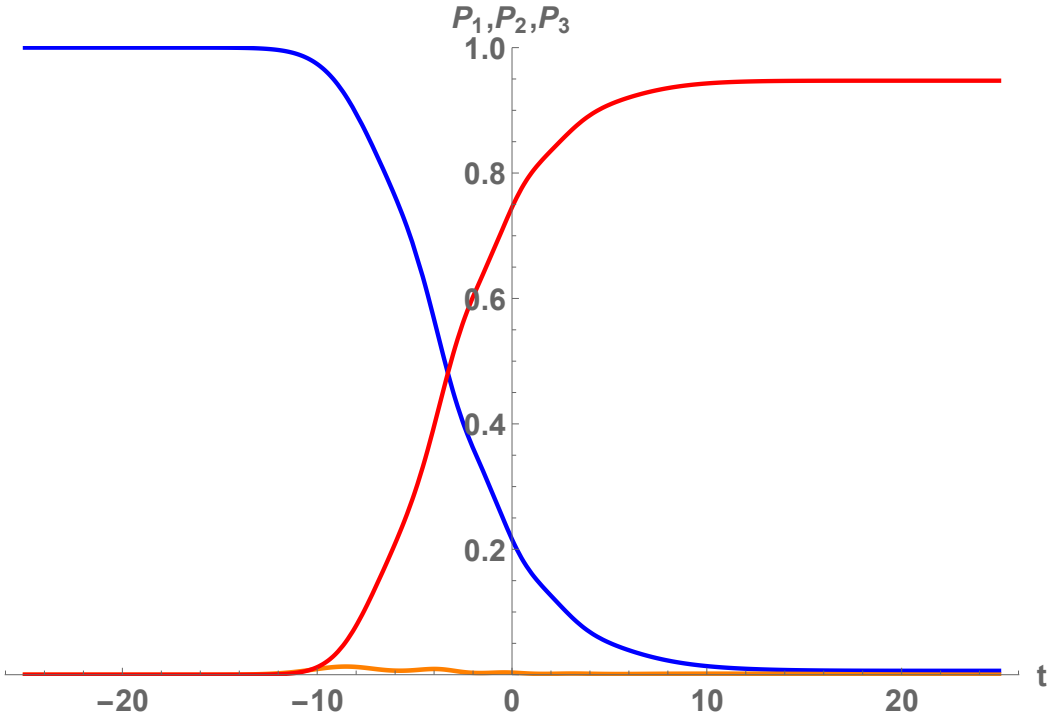

Figure 3.5: Nonlinear stimulated Raman exact tracking. Populations for three levels. $\Omega_{Pmax} = 4$, $\Omega_{Smax} = 1$, $T_P = T_S = 8$, $\tau_P = \tau_S = 5$, and $\Gamma = 0.2$.

In this case the governing Eqs. (3.5) are written as

$$\begin{aligned} i\dot{c_1} &= \Omega_P \bar{c_1} c_2 \\ i\dot{c_2} &= -i\Gamma c_2 + \Omega_P c_1^2 + \Omega_S c_3 \\ i\dot{c_3} &= \Omega_S c_2 \end{aligned} \tag{3.36}$$

where $\Gamma > 0$ presents the losses from the state 2.

As it was already mentioned, c_1 and c_3 can be chosen real, whereas c_2 is imaginary. Using the normalization condition and multiplying first equation of the Eq. (3.36) by c_1 we get

$$\frac{i}{2}\dot{c_1}^2 = \Omega_P(1 - |c_2|^2 - |c_3|^2)c_2 \tag{3.37}$$

Also, from the second equation of the Eq. (3.36) we have

$$c_1^2 = \frac{i}{\Omega_P}\dot{c_2} - \frac{\Gamma}{\Omega_P}c_2 - \frac{\Omega_S}{\Omega_P}c_3 \tag{3.38}$$

and from the third equation of the Eq. (3.36):

$$c_2 = \frac{i\dot{c}_3}{\Omega_S} \tag{3.39}$$

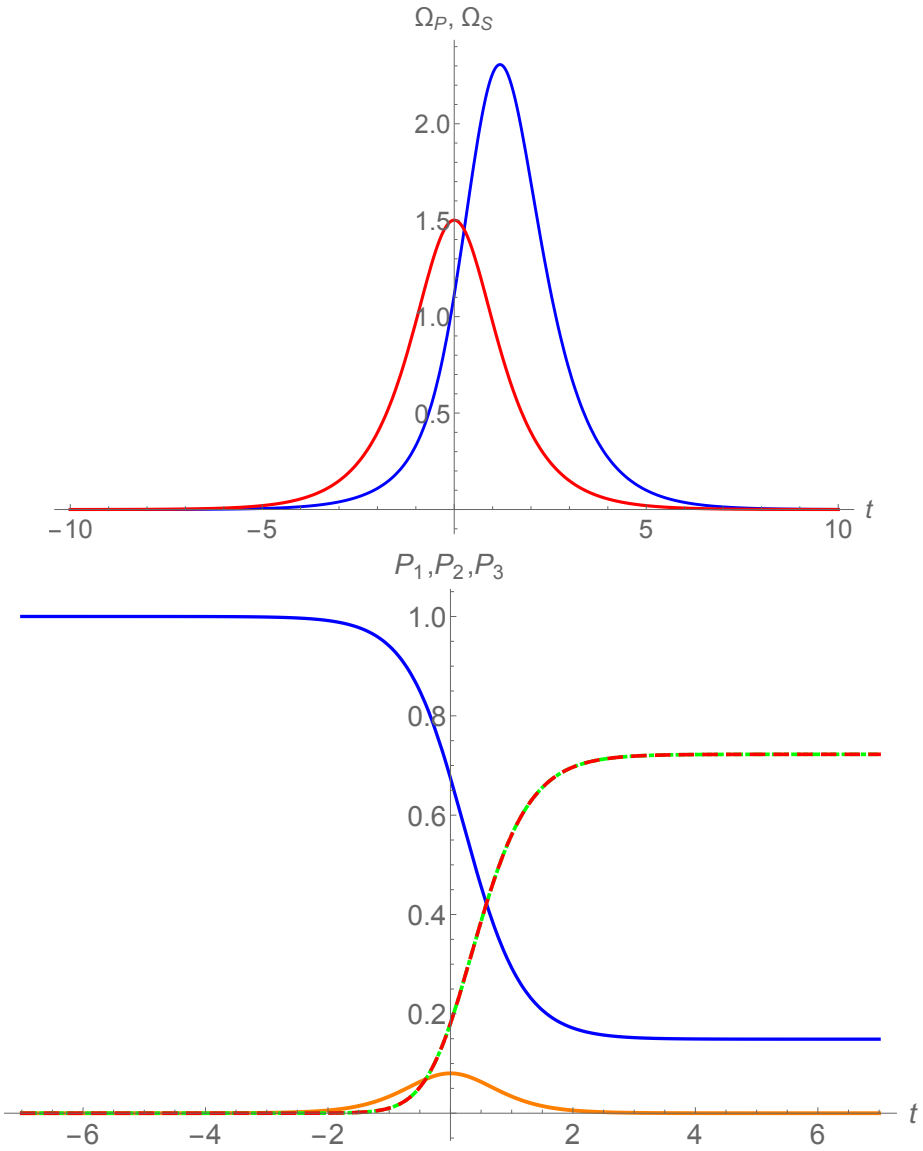

Figure 3.6: Nonlinear stimulated Raman exact tracking. The first figure presents the Rabi frequencies and the second one plots the populations for three levels. $\Omega_S = \Omega_{S0}\,\mathrm{sec}\,h(t)$, $c_3 = \frac{c}{2}(1 + \tanh(t))$ with $\Omega_{S0} = 1.5$, $\Gamma = 0.4$, $c = -0.85$.

Inserting the normalization condition, Eqs. (3.38), and (3.39) into Eq. (3.37), one gets

$$\frac{i}{2}\dot{c_1}^2 = \Omega_P \left(1 - \left(\frac{i\dot{c_3}}{\Omega_S}\right)^2 - |c_3|^2\right)\frac{i\dot{c_3}}{\Omega_S} \tag{3.40}$$

or

$$\frac{i}{2}\left(\frac{i}{\Omega_P}\dot{c_2} - \frac{\Gamma c_2}{\Omega_P} - \frac{\Omega_S}{\Omega_P}c_3\right)_t = \Omega_P \left(1 - \left(\frac{i\dot{c_3}}{\Omega_S}\right)^2 - |c_3|^2\right)\frac{i\dot{c_3}}{\Omega_S}.$$

Further, substituting Eqs. (3.38) and (3.39) into the Eq. (3.37) we obtain the equation for c_3:

$$c_{3t} = \frac{\Omega_S}{2\Omega_P}\frac{d}{dt}ln\left(\frac{1}{\Omega_P}\left(\left(\frac{c_{3t}}{\Omega_S}\right)_t + \Gamma\frac{c_{3t}}{\Omega_S} + \Omega_S c_3\right)\right) \tag{3.41}$$

The important remark is that Eq. (3.41) involves only the first derivative of Ω_P and the second derivative of Ω_S (respectively, the equation for c_1 involves only the first derivative of Ω_S and the second derivative of Ω_P). One can further check that, owing to this circumstance, Ω_P can be determined from this equation for any given c_3 and Ω_S. This is the idea of tracking. We note that in the similar way one may take the corresponding equation for c_1 and this time determine Ω_S for a given c_1 and Ω_P.

Thus, we have presented a stimulated Raman exact tracking model that takes into account the irreversible losses from the intermediate second state. We have shown how to avoid these losses in the one- and two-photon resonance case.

3.10 Nonlinear stimulated Raman robust exact tracking with detuning

The stimulated Raman processes for the nonlinear model we can present as:

$$i\frac{d}{dt}\begin{bmatrix} c_1 \\ c_2 \\ c_3 \end{bmatrix} = \begin{bmatrix} K_1 & \Omega_P\bar{c_1} & 0 \\ \Omega_P c_1 & -i\gamma + \Delta + K_2 & \Omega_S \\ 0 & \Omega_S & \delta + K_3 \end{bmatrix}\begin{bmatrix} c_1 \\ c_2 \\ c_3 \end{bmatrix} \tag{3.42}$$

and then using anzats

$$c_1 = |c_1|e^{-i\phi(t)}e^{i\Theta_1}, c_{2,3} = |c_{2,3}|e^{i\Theta_{2,3}}e^{-2i\phi(t)}$$

where $\Theta_{1,2,3}$ are constant, and the Kerr terms are

$$K_1 = \Lambda_{11}|c_1|^2 + \Lambda_{12}|c_2|^2 + \Lambda_{13}|c_3|^2$$

$$K_2 = \Lambda_{22}|c_2|^2 + \Lambda_{12}|c_1|^2 + \Lambda_{13}|c_3|^2$$

$$K_3 = \Lambda_{33}|c_3|^2 + \Lambda_{13}|c_1|^2 + \Lambda_{23}|c_2|^2.$$

We get the following set of equations

$$i\begin{bmatrix} \dot{|c_1|}e^{i\Theta_1} \\ \dot{|c_2|}e^{i\Theta_2} \\ \dot{|c_3|}e^{i\Theta_3} \end{bmatrix} = \begin{bmatrix} -\dot{\Phi} + K_1 & \Omega_P\bar{c_1}e^{-i\Theta_1} & 0 \\ \Omega_P|c_1|e^{i\Theta_1} & -i\gamma + \Delta - 2\dot{\Phi} + K_2 & \Omega_S \\ 0 & \Omega_S & \delta - 2\dot{\Phi} + K_3 \end{bmatrix} \begin{bmatrix} |c_1|e^{i\Theta_1} \\ |c_2|e^{i\Theta_2} \\ |c_3|e^{i\Theta_3} \end{bmatrix} \tag{3.43}$$

Further, we impose

$$\dot{\Phi} = K_1 \tag{3.44}$$

$$\Delta = 2\dot{\Phi} - K_2 = 2K_1 - K_2 \tag{3.45}$$

$$\delta = 2\dot{\Phi} - K_3 = 2K_1 - K_3 \tag{3.46}$$

From the last equation we obtain:

$$\delta = 2\Lambda_{11}|c_1|^2 + 2\Lambda_{12}|c_2|^2 + 2\Lambda_{13}|c_3|^2 = (2\Lambda_{11} - \Lambda_{13})|c_1|^2 + (2\Lambda_{12} - \Lambda_{23})|c_2|^2 + (2\Lambda_{13} - \Lambda_{33})|c_3|^2 \tag{3.47}$$

Using the last equations we get

$$i\begin{bmatrix} \dot{|c_1|}e^{i\Theta_1} \\ \dot{|c_2|}e^{i\Theta_2} \\ \dot{|c_3|}e^{i\Theta_3} \end{bmatrix} = \begin{bmatrix} 0 & \Omega_P\bar{c_1}e^{-i\Theta_1} & 0 \\ \Omega_P|c_1|e^{i\Theta_1} & -i\gamma & \Omega_S \\ 0 & \Omega_S & 0 \end{bmatrix} \begin{bmatrix} |c_1|e^{i\Theta_1} \\ |c_2|e^{i\Theta_2} \\ |c_3|e^{i\Theta_3} \end{bmatrix} \tag{3.48}$$

Eg. $\Theta_1 = 0$, $\Theta_2 = \frac{\pi}{2}$ and $\Theta_3 = 0$.

$$i\begin{bmatrix} \dot{|c_1|} \\ i\dot{|c_2|} \\ \dot{|c_3|} \end{bmatrix} = \begin{bmatrix} 0 & \Omega_P|c_1| & 0 \\ \Omega_P|c_1| & -i\gamma & \Omega_S \\ 0 & \Omega_S & 0 \end{bmatrix} \begin{bmatrix} |c_1| \\ i|c_2| \\ |c_3| \end{bmatrix} \tag{3.49}$$

Now we can do the same calculations. Considering the last equation, in the two-photon resonance case we will have

$$i\begin{bmatrix} i\dot{|c_1|} \\ i\dot{|c_2|} \\ i\dot{|c_3|} \end{bmatrix} = \begin{bmatrix} 0 & \Omega_P|c_1| & 0 \\ \Omega_P|c_1| & -i\gamma + \Delta & \Omega_S \\ 0 & \Omega_S & \delta \end{bmatrix} \begin{bmatrix} |c_1| \\ i|c_2| \\ |c_3| \end{bmatrix} \tag{3.50}$$

Eg. $\Theta_1 = 0$, $\Theta_2 = \frac{\pi}{2}$ and $\Theta_3 = 0$ one can come to the following equation:

$$i\dot{c_1} = c_1\dot{\phi}(t) - c_1\dot{\theta}_1 + \Omega_P c_1 c_2 + (K_1 - \dot{\phi})c_1$$

$$i\dot{c_2} = -c_2\dot{\theta}_2 + 2c_2(i\dot{\phi}(t)) + (\Delta - i\gamma)c_2 + \Omega_P c_1^2 + \Omega_S c_3 + (K_2 - 2\dot{\phi})c_2$$

$$i\dot{c_3} = 2c_3 i\dot{\phi}(t) - c_3(i\dot{\theta_3}) + \delta c_3 + \Omega_S c_2 + (K_3 - 2\dot{\phi})c_3$$

and using Eqs. (3.44)-(3.46) one can get:

$$i\dot{c_1} = \Omega_P\bar{c_1}c_2 + K_1 c_1$$

$$i\dot{c_2} = \Omega_P c_1^2 + \Omega_S c_3 + (K_2 - i\gamma + \Delta)c_2$$

$$i\dot{c}_3 = \Omega_S c_2$$

which coincides with our starting equations.

3.11 Robustness for linear and nonlinear cases including detuning

For a three-level system we have:

$$\begin{aligned} i\dot{c}_1 &= \Omega_P e^{-i\Delta t} c_2 \\ i\dot{c}_2 &= \Omega_P e^{i\Delta t} c_1^2 + \Omega_S e^{i(\Delta-\delta)t} c_3 \\ i\dot{c}_3 &= \Omega_S e^{i(-\Delta+\delta)t} c_2 \end{aligned} \tag{3.51}$$

Our technique is numerically examined for the robustness with respect to the pulse area, to the detuning, or to both parameters.

From the previous paragraphs it is seen that the most efficient transfer takes place when both the Stokes- and pump-pulses are in resonance. But, however hard the experimenter tries to achieve it, there will always be an inevitable failure to do it strictly, because δ and Δ are constant throughout the experiment and thereby do not cross zero. For this reason, we are interested in investigating the influence of incorrect settings of detuning on the experimental results.

Note, that in the current paragraph we do not consider the effect of fluctuations in temperature, pressure, and other extraneous parameters. Thus, we confine ourselves in choosing though incorrect but still constant parameters, say, δ, Δ, Ω_{P0}, Ω_{S0}.

In the figures of 3.7 for the linear and nonlinear STIRAP we present contour plots, and lines of equal probability versus δ and Δ.

It is seen that above the value $P = 0.9$ there exists a plateau in the graph, which indicates the region of P-insensitivity to changes in δ and Δ. Thus, it is named robustness region, which is marked white. We have the exact resonance case when δ and Δ are equal to zero.

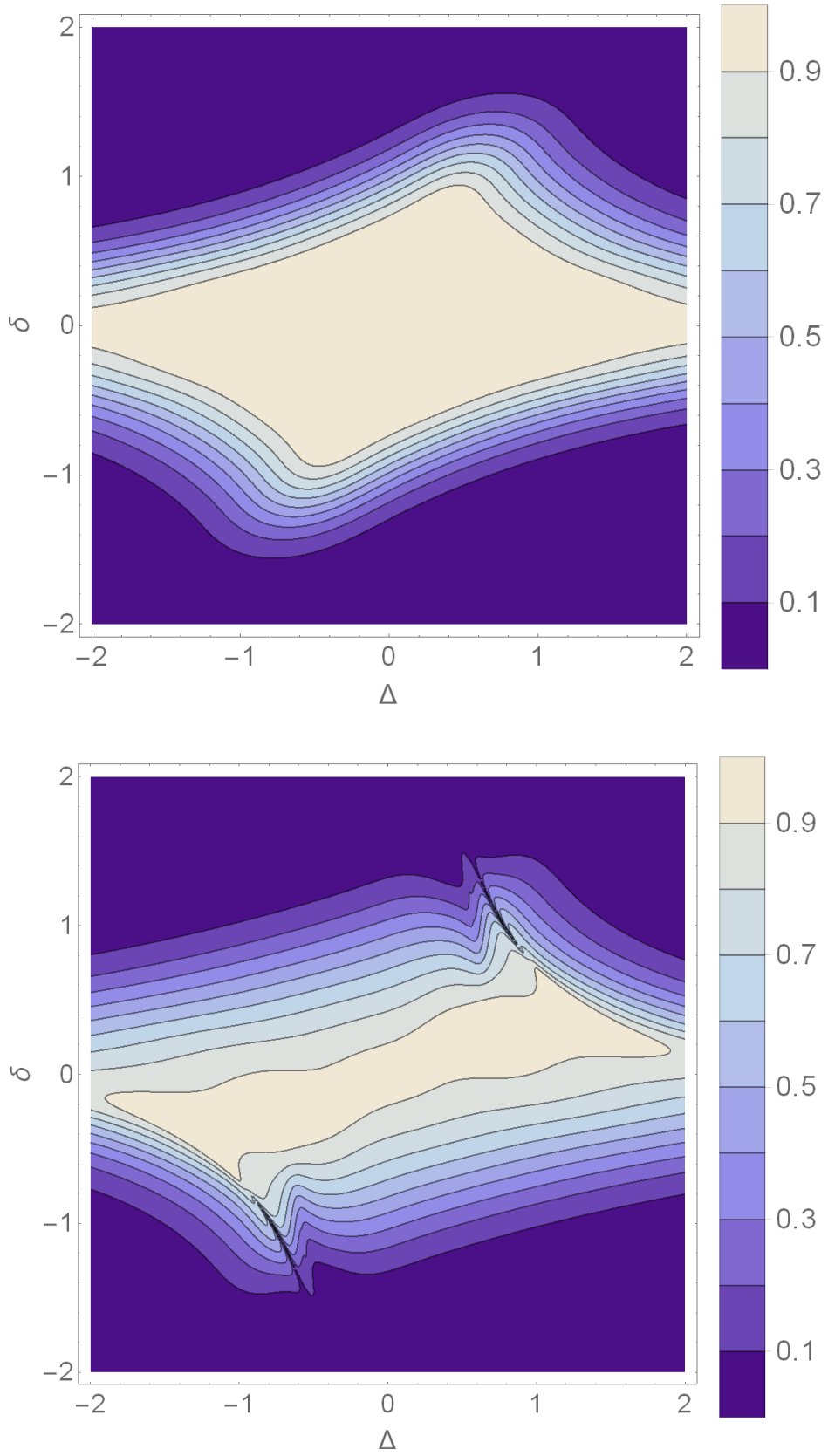

Figure 3.7: Two-photon resonance case where $T = 8$ and $\tau = 5$. In the first figure presented is the linear STIRAP and in the second figure nonlinear STIRAP, $\Omega_{Pmax} = \Omega_{Smax} = 1$ and $\Omega_{Pmax} = 3$, $\Omega_{Smax} = 1$, respectively.

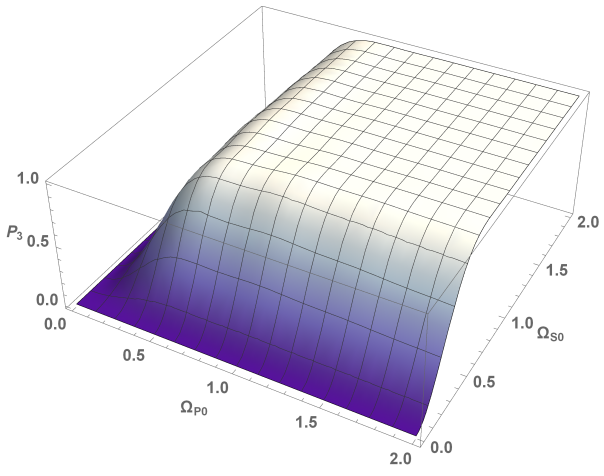

Figure 3.8: Linear STIRAP for two-photon resonance case.

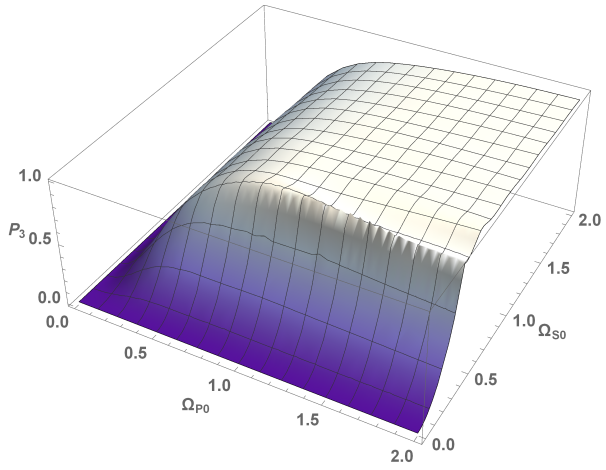

Figure 3.9: Nonlinear STIRAP for two-photon resonance case.

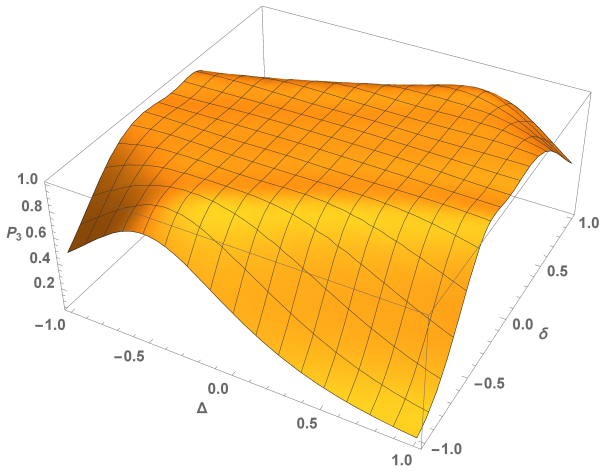

Figure 3.10: Linear STIRAP for two-photon resonance case.

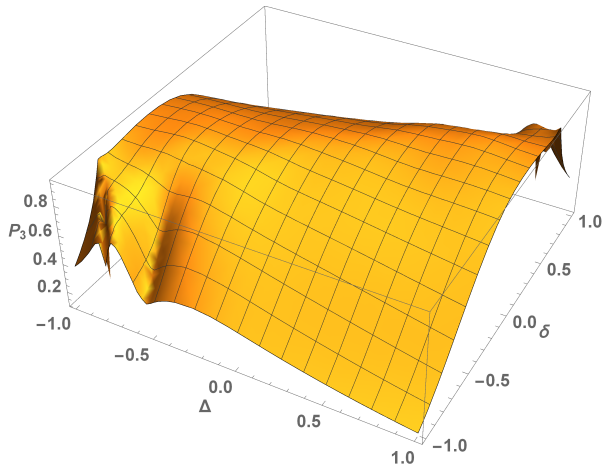

Figure 3.11: Nonlinear STIRAP for two-photon resonance case.

Figs. 3.8 - 3.11 give a view as a 3-D plots of the plateau shown in the figures of 3.7 for $T = 8$ and $\tau = 5$ parameters.

Thus, our scheme can be a powerful tool for coherent control in degenerate systems, because of its robustness when the selective addressing of the states is not required or impossible.

3.12 Summary

In this Chapter we have discussed the nonlinear stimulated Raman exact tracking. The idea is to create stable molecules in the ground state by coupling the initial pure-atomic state and the final molecular ground state by using a third excited state of weakly bound molecules.

As it was already mentioned, by transfering atoms to the weakly bound molecular state we do not have a molecular Bose-Einstein condensate. For that, one needs to transfer molecules to the ground molecular state.

We have shown that in the nonlinear case for an efficient transfer one needs the pump pulse to be stronger than the Stokes one, in contrast to the ordinary linear case.

We have presented a field configuration, which provides an effective Raman transition to the ground molecular state by exactly tracking the prescribed population dynamics. The latter is implied to be such that the population of the unstable intermediate state is negligible during the whole time evolution of the system.

In addition, there are irreversible losses from the weakly bound state. Hence, one needs to suppress this dissipation. We have presented a stimulated Raman exact tracking model that takes into account the irreversible losses from the intermediate second state. We have shown how to avoid these losses in the one- and two-photon resonance case.

Finally, for both linear and nonlinear stimulated Raman exact tracking procedures, we have shown their robustness. The most robust regime is achieved in the vicinity of the one- and two-photon resonances.

Chapter 4

Linear time-dependent level-crossing two-state models described by the bi-confluent Heun functions

The starting observation for this Chapter is that the nonlinear mean-field dynamics of coherent (photo- or magneto-) association of ultracold atoms within the one-color two-state approximation for any configuration of the associating optical or magnetic field is rather accurately described by a two-term variational ansatz written as [111–113]

$$p = p_0(A,t) + C^* \frac{p_L(U_0^*, \delta_0^*, t)}{p_L(U_0^*, \delta_0^*, \infty)}. \tag{4.1}$$

Here $p_0(A,t)$ is the solution of an *augmented limit* nonlinear equation, C^* is a variational scaling factor, $p_L(U_0^*, \delta_0^*, t)$ is the solution of the corresponding *linear* problem with *modified* parameters U_0^* and δ_0^*, which are considered as variational parameters standing for the effective Rabi frequency and effective detuning, respectively. The possibility to make such a decomposition is quite surprising since the Hamiltonian of the system is essentially nonlinear. The ansatz provides a highly accurate approximation for the whole time domain for any set of the input parameters involved in the associating field configuration. The absolute error of the formula is less than 10^{-4} for the final transition probability, and for arbitrary times the

absolute error is commonly of the order of $10^{-3} - 10^{-4}$.

If the molecule formation is performed through a level-crossing excitation scheme, it has been shown that in the strong coupling limit the process is effectively described by the first term of the approximation (4.1), while the second term, being a scaled solution of the linear problem, describes the oscillations which come up some time after the system has passed through the resonance. From this observation, one can conclude that in the strong coupling limit the time dynamics of the atom-molecule conversion consists of an essentially nonlinear process of resonance crossing followed by atom-molecular coherent oscillations that are principally of linear nature [111–113].

The ansatz (4.1) is developed by application of the *exact* nonlinear ordinary differential equation of the third order obeyed by the molecular state probability $p(t) = |a_2|^2$. For any model with varying field amplitude $U(t)$ and detuning $\delta_t(t)$ this equation is conveniently written through an equivalent effectively constant Rabi frequency field configuration achieved via the transformation of the independent variable

$$z(t) = \int_{t_0}^{t} \frac{U(t')}{U_0} dt' \tag{4.2}$$

with an effective U_0 (a convenient choice here is $U_0 = \max[U(t)]$). The equation for the molecular state probability then reads

$$\left(\frac{d}{dz} - \frac{\delta^*_{zz}}{\delta^*_z}\right)\left[p_{zz} - \frac{U_0^2}{2}\left(1 - 8p + 12p^2\right)\right] + \delta^{*2}_z p_z = 0\,. \tag{4.3}$$

The approximate solution of this equation for the large coupling and fast sweeping regime is constructed by neglecting the two higher-order derivate terms originating from the second derivative p_{zz} and adding to the term in the square brackets an adjustable constant A. It has been further shown that the exact solution $p_0(A,t)$ of the resultant augmented limit equation is given by the solution of the following *quartic* algebraic equation:

$$\frac{U_0^2}{\delta^{*2}_z(z(t))} = \frac{c_0 + p_0(p_0 - \beta_1)(p_0 - \beta_2)}{9(p_0 - \alpha_1)^2(p_0 - \alpha_2)^2}, \tag{4.4}$$

where c_0 is an integration constant and the parameters $\alpha_{1,2}$ and $\beta_{1,2}$ are defined through the variational constant A [111–113].

Since the solution $p_0(A,t)$ of equation (4.4) is known for any field configuration, we conclude that in order to construct an accurate description for the molecule formation dynamics within the one-color two-state approach one should look for an appropriate second term of the ansatz (4.1), that is, for the solution of the associated *linear* problem. For this reason, we now proceed to the discussion of the solutions of the two-state problem in terms of the Heun functions, which present the direct generalizations of the functions of the hypergeometric class.

The Heun functions are the solutions of the equations of the Heun class [114–116]. There are five Heun equations - the general Heun equation having four regular singularities [114] and its four confluent reductions achieved by coalescence of the singularities of this equation: single-confluent, double-confluent, bi-confluent and tri-confluent Heun equations [115, 116]. We focus here on the particular case of the bi-confluent Heun equation.

The bi-confluent Heun equation is widely involved in different domains of contemporary pure and applied sciences such as quantum mechanics, general relativity, solid state physics, atomic, molecular and optical physics, chemistry, etc. (see, e.g., [115, 116]). A recent example is the inverse square root potential [117], a member of the bi-confluent Heun class of potentials, which describes a less singular interaction than the Coulomb potential.

Though the properties of the bi-confluent Heun equation have been studied by many authors, however, there are many open problems in the theory of this equation. Among these, an important challenge is the construction of non-polynomial solutions [118]. Here we make a step in this direction by constructing an expansion of the solutions of the bi-confluent Heun equation in terms of the incomplete Beta functions. Further, we present the solution of the bi-confluent Heun equation as a series in terms of the Hermite functions. We note that the latter functions have an alternative representation through the Kummer or Tricomi confluent hypergeometric functions. The coefficients of the expansion obey a three-term recurrence relation between successive coefficients. We discuss the conditions for both

left- and right-hand side terminations of the series. Finally, we apply the two-term Hermite function solution achieved by means of such a termination to a particular dissipative level-crossing field configuration. In general, the involved Hermite functions are of non-integer order so that they do not reduce to polynomials.

The structure of this Chapter is as follows: The first task is to explore the reduction of the linear quantum time-dependent two-state problem to the bi-confluent Heun equation [119]. Discussing the solutions of the latter equation, we construct expansions of the bi-confluent Heun functions in terms of the incomplete Beta functions [3] and Hermite functions of non-integer order [120]. We then apply the constructed expansions to identify the field configurations for which the solution of the two-state problem (that is, the involved bi-confluent Heun function) is written as a linear combination of two Hermite functions. Finally, we present a conditionally integrable level-crossing model for the linear quantum time-dependent two-state problem involving irreversible losses from the second level [4].

The model is given by an exponentially varying Rabi frequency and a level-crossing detuning that starts from the exact resonance, then crosses the resonance at some finite time point, and further exponentially diverges at the infinity. The model includes irreversible losses from the second level, while the spontaneous relaxation to the first level is neglected. We derive the exact solution of the two-level problem for this field configuration in terms of two Hermite functions of a shifted and scaled argument and discuss the dynamics of levels' populations under different regimes of excitation described by this model.

4.1 Two-state models solvable in terms of the bi-confluent Heun functions

The bi-confluent Heun equation is a linear second-order ordinary differential equation having two singularities: a regular singularity conventionally located at $z = 0$ and an irregular singularity of rank 2 at infinity.

According to the general theory [115, 116, 121], this equation has four irreducible param-

eters. A canonical form of the equation adopted in [115] is written as

$$\frac{d^2u}{dz^2}+\frac{1+\alpha-\beta z-2z^2}{z}\frac{du}{dz}+\frac{(\gamma-\alpha-2)z-(\delta+(1+\alpha)\beta)/2}{z}u=0. \tag{4.5}$$

A different form also involving four independent parameters is adopted in [121]:

$$\frac{d^2u}{dz^2}-\left(\frac{\gamma}{z}+\delta+\varepsilon\, z\right)\ \frac{du}{dz}+\frac{\alpha\ z-q}{z}u=0. \tag{4.6}$$

Depending on the particular developments of interest and corresponding theoretical background, other canonical forms may be suitable, as stated in [115]. For the sake of generality, here we adopt the following form of this equation:

$$\frac{d^2u}{dz^2}+\left(\frac{\gamma}{z}+\delta+\varepsilon z\right)\ \frac{du}{dz}+\frac{\alpha\ z-q}{z}u=0, \tag{4.7}$$

where $\gamma,\delta,\varepsilon,\alpha,q$ are arbitrary complex parameters. It is readily seen that the above two forms as well as other forms applied in literature are derived from this form by straightforward specifications of the involved parameters.

A few remarks concerning some elementary cases of the bi-confluent Heun equation are relevant. First of all, we note that equation (4.3) is immediately reduced to the Kummer confluent hypergeometric equation if $\varepsilon=0$ and $\alpha=0$. Furthermore, in fact, the case $\varepsilon=0$ is always reducible, irrespective of the value of α, because in this case equation (4.3) is reduced to the confluent hypergeometric equation by a simple transformation of the dependent variable $u=e^{sz}\nu(z)$. The general solution of the equation is then written as

$$u=e^{sz}\left[C_1\cdot{}_1F_1\left((q-\gamma s)/s_0;\,\gamma;\,s_0z\right)+C_2\cdot U\left((q-\gamma s)/s_0;\,\gamma;\,s_0z\right)\right], \tag{4.8}$$

where ${}_1F_1$ and U are the Kummer and the Tricomi confluent hypergeometric functions, respectively, $C_{1,2}$ are constants and

$$s=-(\delta+s_0)/2,\qquad s_0=\pm\sqrt{\delta^2-4\alpha}. \tag{4.9}$$

Another known case when the solution of equation (4.3) is written in terms of the confluent hypergeometric functions (this time, of the argument $-\varepsilon z^2/2$) is the case $\delta = q = 0$ [111]. Finally, a simple case, in a sense degenerate, is the case $\alpha = 0$ and $q = 0$, when the general solution of the bi-confluent Heun equation is readily written in quadratures:

$$u = C_1 + C_2 \int e^{-\delta z - \varepsilon z^2/2} z^{-\gamma} dz, \qquad C_{1,2} = \text{const.} \tag{4.10}$$

Taking into account above observations, below we suppose that $\varepsilon \neq 0$, as well as α and q are not simultaneously zero.

To consider the reduction of the quantum time-dependent two-state problem

$$i\, a_{1t} = U(t)\, e^{-i\delta(t)}\, a_2 \tag{4.11}$$

$$i\, a_{2t} = U(t)\, e^{i\delta(t)}\, a_1 \tag{4.12}$$

to the bi-confluent Heun equation (4.7), we eliminate a_1 from this system thus arriving at a second-order linear differential equation for the second state‘s probability amplitude a_2:

$$a_{2tt} + (-i\delta_t - U_t/U) a_{2t} + U^2\, a_2 = 0. \tag{4.13}$$

According to the class property of the integrable models of the two-state problem, if the function $a_2^*(z)$ is a solution of this equation rewritten for an auxiliary argument z for some functions $U^*(z)$, $\delta^*(z)$ then the function $a_2(t) = a_2^*(z(t))$ is the solution of equation (4.13) for the field configuration defined as

$$U(t) = U^*(z)\frac{dz}{dt}, \tag{4.14}$$

$$\delta_t(t) = \delta_z^*(z)\frac{dz}{dt} \tag{4.15}$$

for arbitrary complex-valued transformation function $z(t)$. The pair of functions $U^*(z)$ and $\delta^*(z)$ is referred to as a basic integrable model.

Transformation of variables $a_2 = \varphi(z)u(z)$, $z = z(t)$ together with (4.14)-(4.15) reduces equation (4.13) to the following equation for the new dependent variable $u(z)$:

$$u_{zz} + \left(2\frac{\varphi_z}{\varphi} - i\delta_z^* - \frac{U_z^*}{U^*}\right) u_z + \left(\frac{\varphi_{zz}}{\varphi} + \left(-i\delta_z^* - \frac{U_z^*}{U^*}\right)\frac{\varphi_z}{\varphi} + U^{*2}\right) u = 0, \tag{4.16}$$

This equation is the bi-confluent Heun equation if

$$\frac{\gamma}{z} + \delta + \varepsilon z = 2\frac{\varphi_z}{\varphi} - i\,\delta_z^* - \frac{U_z^*}{U^*} \tag{4.17}$$

and

$$\frac{\alpha\, z - q}{z} = \frac{\varphi_{zz}}{\varphi_z} + \left(-i\,\delta_z^* - \frac{U_z^*}{U^*}\right)\frac{\varphi_z}{\varphi} + U^{*\,2}. \tag{4.18}$$

These equations compose an under-determined system of two nonlinear equations for three unknown functions, $U^*(z)$, $\delta^*(z)$ and $\varphi(z)$. The general solution of this system is not known. However, many particular solutions can be found starting from specific forms of the involved functions. We here present the known solutions following the approach of [119, 122, 123].

We search for the solutions of equations (4.17), (4.18) in the following form:

$$\frac{\varphi_z(z)}{\varphi(z)} = \frac{\alpha_1}{z} + \alpha_0 + \alpha_2\, z \;\Leftrightarrow\; \varphi = z^{\alpha_1}\, e^{\alpha_0\, z + \frac{\alpha_2}{2}\, z^2}, \tag{4.19}$$

$$\frac{U_z^*}{U^*} = \frac{k}{z} \;\Leftrightarrow\; U^* = U_0^*\, z^k, \tag{4.20}$$

$$\delta_z^* = \frac{\delta_1}{z} + \delta_0 + \delta_2\, z. \tag{4.21}$$

Multiplying equation (4.18) by z^2 we get that for arbitrary $\delta_{0,\,1,\,2}$ the product $U_0^{*\,2}\, z^{2\,k+2}$ should be a polynomial in z of the fourth degree at most. Hence, k is an integer or half-integer obeying the inequalities $0 \le 2\,k + 2 \le 4$. This leads to five admissible cases of k, namely, $k = -1,\ -1/2,\ 0,\ 1/2,\ 1$, generating five classes of two-state models solvable in terms of the bi-confluent Heun functions.

The amplitude modulation functions for these classes are

$$\frac{U_z^*}{U^*} = \frac{1}{z}\,,\ \frac{1}{\sqrt{z}},\ 1,\ \sqrt{z},\ z\,. \tag{4.22}$$

According to equations (4.14)-(4.15), the field configurations, for which the solution of the two-state problem is written in terms of the bi-confluent Heun functions, are then given as

$$U(t) = U_0^*\ z^k\,\frac{dz}{dt}, \tag{4.23}$$

$$\delta_t(t) = \left(\frac{\delta_1}{z} + \delta_0 + \delta_2\,z\right)\,\frac{dz}{dt} \tag{4.24}$$

with $k = -1,\ -1/2,\ 0,\ 1/2,\ 1$, and $U_0^*\,,\ \delta_{0,\,1,\,2}$ being complex constants which should be chosen so that the functions $U(t)$ and $\delta(t)$ are real for the chosen complex-valued $z(t)$. Since these parameters are arbitrary, all 5 classes are four-parametric. The classes are listed in Table 4.1, where for completeness we also present the field configurations for which the two-state problem is solvable in terms of other Heun functions (there are in total 61 Heun classes of basic integrable models) [119, 122, 123].

The solution of the initial two-state problem (4.11)-(4.12) is explicitly written as

$$\alpha_2 = z^{\alpha_1}\,e^{\alpha_0\,z+\frac{\alpha_2}{2}\,z^2}\,H_B(\gamma,\,\delta,\,\varepsilon;\,\alpha,\,q;\,z), \tag{4.25}$$

where the parameters of the bi-confluent Heun function γ, δ, ε, α, q are given as

$$\gamma = 2\,\alpha_1 - i\delta_1 - k, \qquad \delta = 2\,\alpha_0 - i\,\delta_0, \qquad \varepsilon = 2\,\alpha_2 - i\,\delta_2, \tag{4.26}$$

$$\alpha = \alpha_0\ (\alpha_0 - i\,\delta_0) + \alpha_1\,(2\,\alpha_2 - i\,\delta_2) + \alpha_2\,(1 - k - i\,\delta_1) + Q''(0)/2, \tag{4.27}$$

$$q = \alpha_0\ (k + i\,\delta_1) - \alpha_1\,(2\,\alpha_0 - i\,\delta_0) - Q'(0), \tag{4.28}$$

Heun Eqs.	Field configurations		Classes		Solution $a_2(z)=\varphi(z)\,u(z)$		Expansion functions
	$U^*(z)/U_0^*$	$\delta_z^*(z)$			$\varphi(z)$	$u(z)$	
GHE	$z^{k_1}(z-1)^{k_2}(z-a)^{k_3}$	$\frac{\delta_0}{z}+\frac{\delta_1}{z-1}+\frac{\delta_2}{z-a}$	35	$k_{1,2,3}\in\{-1,-1/2,\,0,\,1/2,\,1\}$	$z^{\alpha_1}(z-1)^{\alpha_2}(z-a)^{\alpha_3}$	H_G	${}_2F_1$
CHE	$z^{k_1}(z-1)^{k_2}$	$\frac{\delta_0}{z}+\frac{\delta_1}{z-1}+\delta_2$	15	$k_{1,2}\in\{-1,-1/2,\,0,\,1/2,\,1\}$	$z^{\alpha_1}(z-1)^{\alpha_2}\,e^{\alpha_3 z}$	H_C	${}_1F_1$
DHE	z^{k_1}	$\frac{\delta_0}{z^2}+\frac{\delta_1}{z}+\delta_2$	5	$k=-2,-3/2,-1,-1/2,\,0$	$z^{\alpha_1}\,e^{\alpha_0 z-\frac{\alpha_2}{z}}$	H_D	J_ν
BHE	z^{k_1}	$\frac{\delta_1}{z}+\delta_0+\delta_2 z$	5	$k=-1,-1/2,\,0,\,1/2,\,1$	$z^{\alpha_1}\,e^{\alpha_0 z+\frac{\alpha_2}{2}z^2}$	H_B	H_ν
THE	1	$\delta_0+\delta_1 z+\delta_2 z^2$	1	$k=0$	$e^{\alpha_1 z+\alpha_2 z^2+\alpha_3 z^3}$	H_T	---

Table 4.1: The 61 classes of basic models $(U^*(z),\delta_z^*(z))$ for which the quantum time-dependent two-state problem is integrable in terms of the Heun functions.

with $Q(z)=U_0^{*\,2}\,z^{2\,k+2}$, and

$$\alpha_0\,\varepsilon-i\,\alpha_2\,\delta_0+Q'''(0)/3!=0, \tag{4.29}$$

$$\alpha_1^2-\alpha_1\,(1+k+i\,\delta_1)+Q(0)=0, \tag{4.30}$$

$$\alpha_2^2-i\,\alpha_2\,\delta_2+Q^{(4)}(0)/4!=0. \tag{4.31}$$

4.2 Expansion of the solutions of the bi-confluent Heun equation in terms of the incomplete Beta functions

The approach we apply for construction of series solutions of the bi-confluent Heun equation is as follows: We consider the following representation of the first derivative of a solution $u(z)$ of the bi-confluent Heun equation:

$$\frac{du}{dz} = z^{-\gamma}\nu(z). \tag{4.32}$$

If now the function $\nu(z)$ allows an expansion of the form

$$v(z) = \sum_{n=0}^{+\infty} c_n (z-s)^{\mu+n}, \tag{4.33}$$

then the term-by-term integration of equation (4.7) produces the following expansion in terms of incomplete Beta functions ($\mid z \mid \leq \mid z_0 \mid$):

$$u = C_0 + \sum_{n=0}^{+\infty} c_n \left(-s\right)^n B\left(1-\gamma, 1+n+\mu; \frac{z}{s}\right). \tag{4.34}$$

A more elaborate example is constructed using a possible expansion for the function $\nu(z)$ of the form:

$$v(z) = C_1 + \sum_{n=0}^{+\infty} c_n B(a_n, b_n;\, z/s). \tag{4.35}$$

Then, the term-by-term integration produces an expansion in terms of combinations of incomplete Beta functions:

$$u(z) = C_0 + C_1 \frac{z^{1-\gamma}}{1-\gamma} + \sum_{n=0}^{+\infty} \frac{c_n}{1-\gamma} \left(z^{1-\gamma} B(a_n, b_n;\, z/s) - s^{1-\gamma} B(a_n+1-\gamma, b_n;\, z/s)\right). \tag{4.36}$$

Note that the integration constants C_0 and C_1 in above expansions are not arbitrary; rather, they should be appropriately chosen in order to achieve a consistent solution.

In the force of the presented approach, it is understood that the task now is to look at

different equations obeyed by functions involving the derivatives of the bi-confluent Heun function and to construct expansions for the latter functions based on these equations.

To be more specific, consider, e.g., the details of derivation of the expansion (4.34). It is readily shown, e.g., by dividing equation (4.7) by $(\alpha z - q)/z$ and further differentiating, that a differential equation obeyed by the function $\nu(z) = z^{\gamma} du/dz$ is written as:

$$\frac{d^2v}{dz^2} + \left(\frac{1-\gamma}{z} + \delta + \varepsilon\, z - \frac{\alpha}{\alpha\, z - q} \right) \frac{dv}{dz} + \frac{\Pi(z)}{z(\alpha z - q)} v = 0, \tag{4.37}$$

where $\Pi(z)$ is a quadratic polynomial in z:

$$\Pi(z) = \alpha(\alpha\ + \varepsilon - \gamma\varepsilon) z^2 - (\alpha(2q + \gamma\delta) + q\varepsilon(2-\gamma)) z + q(q + (\gamma - 1)\delta). \tag{4.38}$$

As compared with equation (4.7), it is seen that this equation has an additional regular singularity at $z_0 = q/\alpha$. Let us now have $\alpha \neq 0$ and $q \neq 0$ so that the additional singular point is a finite point of the complex z-plane, not located at the origin: $z_0 \neq 0$. Then, taking the Frobenius solution of equation (4.37) in the neighborhood of this singularity:

$$v = (z - z_0)^{\mu} \sum_{n=0}^{+\infty} a_n^{(z_0)} (z - z_0)^n, \tag{4.39}$$

we get the expansion (4.33), and further term-by-term integrating equation (4.32) we arrive at the expansion (4.34) finally written as ($|\ z\ | \leq |\ z_0\ |$)

$$u = C_0 + \sum_{n=0}^{+\infty} a_n^{(z_0)}\, (-z_0)^n\, B\left(1-\gamma,\ 1+n+\mu;\ \frac{z}{z_0}\right). \tag{4.40}$$

Substituting this expansion into equation (4.7) and taking the limit $z \to 0$ we readily find that $C_0 = 0$ if $Re(1-\gamma) > 0$. The successive coefficients of the constructed expansion obey a four-term recurrence relation:

$$S_n a_n^{(z_0)} + R_{n-1} a_{n-1}^{(z_0)} + Q_{n-2} a_{n-2}^{(z_0)} + P_{n-3} a_{n-3}^{(z_0)} = 0, \tag{4.41}$$

where

$$S_n a_n^{(z_0)} + R_{n-1} a_{n-1}^{(z_0)} + Q_{n-2} a_{n-2}^{(z_0)} + P_{n-3} a_{n-3}^{(z_0)} = 0, \tag{4.42}$$

$$S_n = z_0(n+\mu)(n+\mu-2), \tag{4.43}$$

$$R_n = z_0(\delta + z_0\varepsilon)(n+\mu-1) + (n+\mu)(n+\mu-1-\gamma), \tag{4.44}$$

$$Q_n = -\gamma(\delta + z_0\varepsilon) + (\delta + 2z_0\varepsilon)(n+\mu), \tag{4.45}$$

$$P_n = \alpha + \varepsilon(n+\mu+1-\gamma). \tag{4.46}$$

The series is left-hand side terminated at $n = 0$ if $S_0 = 0$, i.e., if $\mu = 0$ or $\mu = 2$. These exponents differ in an integer, and it is readily checked that only the greater exponent $\mu = 2$ produces a consistent power-series expansion; the second independent solution requires a logarithmic term. The series terminates from the right-hand side if three successive coefficients vanish for some $N = 1, 2, \ldots :$ $\alpha_N \neq 0,$ $\alpha_{N+1} = \alpha_{N+2} = \alpha_{N+3} = 0.$ From the condition $\alpha_{N+3} = 0$ we find that the termination is possible if $P_N = 0$, i.e., if

$$\alpha = -\varepsilon(N+\mu+1-\gamma), \qquad \mu = 2. \tag{4.47}$$

The remaining two equations, $\alpha_{N+1} = 0$ and $\alpha_{N+2} = 0$, then impose two more restrictions on the parameters of the bi-confluent Heun equation.

4.3 Series solutions of the bi-confluent Heun equation in terms of the Hermite functions

Following the lines of [120] we present the expansion of the solutions of the bi-confluent Heun equation (4.7) in terms of the Hermite functions of a shifted and scaled argument:

$$u = \sum_n c_n u_n, \qquad u_n = H_{\alpha_0+n}\left(s_0(z+z_0)\right), \tag{4.48}$$

where α_0, s_0 and z_0 are complex constants to be defined afterwards. The involved Hermite functions satisfy the following second-order linear differential equation:

$$\frac{d^2u_n}{dz^2} - 2s_0^2(z+z_0)\,\frac{du_n}{dz} + 2s_0^2\alpha_n\,u_n = 0, \qquad \alpha_n = \alpha_0 + n. \tag{4.49}$$

Substituting equations (4.48) and (4.49) into equation (4.7) and multiplying the result by z we get

$$\sum_n c_n\left[\left(\gamma + z(\delta+\varepsilon\,z) + 2s_0^2 z(z+z_0)\right)u_n' + \left(\alpha\,z - q - 2s_0^2\alpha_n\,z\right)\,u_n\right] = 0. \tag{4.50}$$

By putting $s_0 = \pm\sqrt{-\varepsilon/2}$ and $z_0 = \delta/\varepsilon$, the terms proportional to $z\,u_n'$ and z^2u_n' are cancelled so that using the recurrence identities

$$u_n' = 2s_0\,\alpha_n u_{n-1}, \qquad s_0(z+z_0)\,u_n = \alpha_n u_{n-1} + u_{n+1}/2, \tag{4.51}$$

we arrive at a three-term recurrence relation for coefficients c_n:

$$R_n c_n + Q_{n-1}c_{n-1} + P_{n-2}\,c_{n-2} = 0, \tag{4.52}$$

where

$$R_n = \frac{\sqrt{2}}{\sqrt{-\varepsilon}}\,(\alpha_0+n)\;(\alpha + (\alpha_0+n-\gamma)\,\varepsilon)\,, \tag{4.53}$$

$$Q_n = \mp\frac{\alpha\,\delta + (q + (\alpha_0+n)\,\delta\,)\varepsilon}{\varepsilon}, \tag{4.54}$$

$$P_n = \frac{\alpha + (\alpha_0+n)\,\varepsilon}{\sqrt{-2\,\varepsilon}}. \tag{4.55}$$

Here the signs $\mp$ in the equation for Q_n refer to the choices $s_0 = \pm\sqrt{-\varepsilon/2}$, respectively.

For left-hand side termination of the developed series at $n = 0$ provided that the initial conditions $c_{-1} = c_{-2} = 0$ are fulfilled it should be $R_0 = 0$. This is the case if $\alpha_0 = 0$ or $\alpha_0 = \gamma - \alpha/\varepsilon$. The first choice leads to the known polynomial solutions [115]. Hence, we

discuss the second case

$$\alpha_0 = \gamma - \frac{\alpha}{\varepsilon}, \tag{4.56}$$

which is applicable for non-zero ε. The final expansion is then written as

$$u = \sum_{n=0}^{\infty} c_n H_{n+\gamma-\alpha/\varepsilon}\left(\pm\sqrt{-\varepsilon/2}\,(z+\delta/\varepsilon)\right). \tag{4.57}$$

N	γ	q-equation	Restrictions
0	0	$q = 0$	$\alpha \neq \varepsilon$
1	-1	$q^2 - \delta q + \alpha = 0$	$\alpha \neq 0, \varepsilon$
2	-2	$q^3 - 3\delta q^2 + 2(2\alpha + \delta^2 + \varepsilon)q - 4\alpha\delta = 0$	$\alpha \neq 0, \pm\varepsilon$
3	-3	$q^4 - 6\delta q^3 + (10\alpha + 11\delta^2 + 10\varepsilon)q^2$ $-6\delta(5\alpha + \delta^2 + 3\varepsilon)q + 9\alpha(\alpha + 2(\delta^2 + \varepsilon) = 0$	$\alpha \neq 0, \pm\varepsilon, -2\varepsilon$
4	-4	$q^5 - 10\delta q^4 + 5(4\alpha + 7\delta^2 + 6\varepsilon)q^3 - 2\delta(60\alpha + 25\delta^2 + 69\varepsilon)q^2$ $+(64\alpha^2 + 8\delta^2(26\alpha + 3\delta^2) + 8\varepsilon(24\alpha + 18\delta^2 + 9\varepsilon))q$ $-32\alpha\delta(4\alpha + 3\delta^2 + 9\varepsilon) = 0$	$\alpha \neq 0, \pm\varepsilon, -2\varepsilon, -3\varepsilon$

Table 4.2: Equations for the accessory parameter q resulting from the condition $c_{N+1} = 0$.

The series will terminate from the right-hand side if two successive coefficients vanish for some $N = 1, 2, ...,$, i.e., if $c_N \neq 0$ and $c_{N+1} = c_{N+2} = 0$. From the last equation $c_{N+2} = 0$ we find that the termination is possible if $P_N = 0$. This condition is satisfied if

$$\gamma = -N. \tag{4.58}$$

Since ε is non-zero, the remaining equation $c_{N+1} = 0$ presents a polynomial equation of the

degree $N+1$ for the accessory parameter q, defining, in general, $N+1$ values of q for which the termination of the series occurs (we refer to this equation as q-equation). For the first five cases, that is for $\gamma = 0, -1, -2, -3, -4$ the corresponding q-equations are listed in Table 4.2. We note that the case $\gamma = q = 0$ is trivial since the bi-confluent Heun equation (4.7) directly reduces to the Hermite equation (4.49). Starting from $N = 1$, however, the results become highly non-trivial. Supporting this is the recent solution of the Schrödinger equation for the inverse square root potential, which is achieved by applying the two-term Hermite function solution of the bi-confluent Heun equation provided by the q-equation for $N = 1$: $q^2 - \delta\, q + \alpha = 0$ [117]. We will now apply the latter equation to obtain a conditionally integrable level-crossing model for the quantum time-dependent two-state problem involving irreversible losses from the second level [4].

4.4 Constant-amplitude two-state models solvable in terms of the Hermite functions

Consider the excitation of an effective two-state quantum system by a constant-amplitude laser field for which the two-state problem is solved in terms of the bi-confluent Heun functions. The corresponding field configurations are derived from those presented in Table 4.1 if one requires $U(t) = U_0 = const.$ We then get from equation (4.23) that such field configurations are achieved if the transformation of the time is chosen as

$$z(t) = e^t, \frac{t^2}{4}, t, \left(\frac{3\,t}{2}\right)^{2/3}, \sqrt{2\,t} \tag{4.59}$$

for the classes with $k = -1, -1/2, 0, 1/2, 1$, respectively (without loss of the generality, we put the time scale equal to unity). Equation (4.24), that is $\delta_t(t) = (\delta_1/z + \delta_0 + \delta_2\, z)\; dz/dt$, then leads to the corresponding detuning modulation functions presented in Table 4.3.

Discussing now the question if the bi-confluent Heun function involved in the solution of a two-state problem for these field configurations may allow a finite-sum expansion in

terms of the Hermite functions, one should note the following. For a given field configuration with input parameters U_0^* and $\delta_{0,1,2}$ the parameters of the bi-confluent Heun function and those of the pre-factor $\varphi(z)$ involved in solution (4.25) are calculated through the equations (4.26)-(4.31). According to the above presented expansion, in order that the bi-confluent Heun function could be written as a finite-sum linear combination of the Hermite functions, the parameters of the bi-confluent Heun function should necessarily satisfy the condition $\gamma = -N$ with a non-negative integer N and the corresponding q-equation. Obviously, the latter equations cannot be satisfied for arbitrary parameters U_0^* and $\delta_{0,1,2}$ involved in the field configuration. The necessary conditions for termination of the series (4.57) are satisfied only for some special sets of U_0^* and/or $\delta_{0,1,2}$.

Field configurations			$z(t)$	$\delta_t(t)$	**Conditions from q-equation for $N=1$**
k	U^*/U_0	$\delta_z^*(z)$			
-1	$1/z$	$\delta_1/z+\delta_0+\delta_2 z$	e^t	$\delta_0 e^t+\delta_1+\delta_2 e^{2t}$	$\delta_2-\forall,\ \delta_1=-2i$ Particular case of the Nikitin model
$-\frac{1}{2}$	$1/\sqrt{z}$		$\frac{t^2}{4}$	$\delta_0\frac{t}{2}+\delta_1\frac{2}{t}+\delta_2\frac{t^3}{8}$	$\delta_2-\forall,\ \delta_1=-\frac{3i}{2}$ Dissipative case
0	1		t	$\delta_0+\frac{\delta_1}{t}+\delta_2 t$	$\delta_2=0,\ \delta_1=-i$ Dissipative case
$\frac{1}{2}$	$\sqrt{z}$		$(3t/2)^{2/3}$	$\delta_0\left(\frac{3t}{2}\right)^{-1/3}+\delta_1\frac{2}{3t}+\delta_2\left(\frac{3t}{2}\right)^{1/3}$	$\delta_2-\forall,\ \delta_1=-\frac{i}{2}$ Dissipative case
1	z		$\sqrt{2t}$	$\frac{\delta_0}{\sqrt{2t}}+\frac{\delta_1}{2t}+\delta_2$	$\delta_{0,2}-\forall,\ \delta_1=0$ New level-crossing model

Table 4.3: Detuning modulation functions for the bi-confluent Heun constant-amplitude field configurations $U(t) = U_0 = const.$ The conditions for the two-state problem to be solved through a two-term Hermite function expansion are presented in the last column.

For the constant-amplitude field configurations the conditions for the two-state problem to be solved through a *two-term* Hermite-function expansion are presented in the last column

of Table 4.3. We note that the first model corresponding to $k = -1$ is a particular case of the Nikitin exponential level-crossing field configuration [124], while the fifth detuning modulation function with $k = +1$ presents a new level-crossing model. A notable feature of the three remaining detuning modulation functions for which $k = -1/2,\ 0,\ 1/2$ is that they involve an imaginary term. This may correspond to a dissipative two-state model with irreversible losses included. However, because the imaginary terms are not constants, these models seem to have a limited applicability.

4.5 A time-dependent dissipative level-crossing two-state model solvable in terms of the Hermite functions

There exist non-constant amplitude models for which the involved bi-confluent Heun function reduces to a sum of a finite number of Hermite functions. It turns out, however, that the termination conditions in many cases are such that some parameters of the field configuration are expressed through other parameters. Since the amplitude- and detuning-modulation functions do not vary independently, in these cases we meet *conditionally* integrable two-state models. We will now present an example of such a non-constant amplitude conditionally integrable model.

Consider the case of the two-term termination of the series (4.57), so that the solution of the initial two-state problem is written as a sum of two Hermite functions. In this case $\gamma = -1$ and the q-equation is a second-degree polynomial equation (see Table 4.2):

$$q^2 - \delta\, q + \alpha = 0. \tag{4.60}$$

Consider the class with $k = 1/2$. For this case equation (4.60) leads to just one possible value for the parameter δ_1:

$$\delta_1 = -\frac{i}{2}. \tag{4.61}$$

The field amplitude- and detuning-modulation functions are then written as

$$U(t) = U_0^* \sqrt{z(t)} \frac{dz(t)}{dt}, \tag{4.62}$$

$$\delta_t(t) = \left(-\frac{i}{2\,z} + \delta_0 + z\,\delta_2 \right) \frac{dz(t)}{dt}. \tag{4.63}$$

In order to make the imaginary term constant in equation (4.63), as an independent variable transformation we take the real valued function $z = \exp(2\,\Gamma\,t)$ and arrive at the following three-parametric level-crossing field configuration:

$$U(t) = U_0\, e^{3t}, \tag{4.64}$$

$$\delta_t(t) = \tilde{\delta}_t(t) - i\Gamma = 2\left(\delta_0 e^{2t} + \delta_2 e^{4t}\right) - i. \tag{4.65}$$

where U_0, δ_0 and δ_2 are arbitrary real parameters. We have here put $U_0 = 2\,U_0^*$ and $\Gamma = 1$. The last condition implies that hereafter all the involved parameters are supposed dimensionless. Equations (4.64), (4.65) define a field configuration with a detuning-modulation function $\tilde{\delta}_t(t)$ describing an asymmetric-in-time level-crossing dissipative process. The field configuration is presented in Fig. 4.1.

The crossing of the resonance occurs at the time point

$$t_0 = \ln(-\delta_0/\delta_2)/2. \tag{4.66}$$

We note that in the vicinity of the resonance crossing point the behaviour of the detuning $\tilde{\delta}_t(t)$ is approximately modeled by the linear crossing law of the Landau-Zener type:

$$\delta_t = \frac{4\delta_0^2}{\delta_2} t + O(t^2), \tag{4.67}$$

so that the resonance crossing rate is mostly defined by the combined parameter δ_0^2/δ_2.

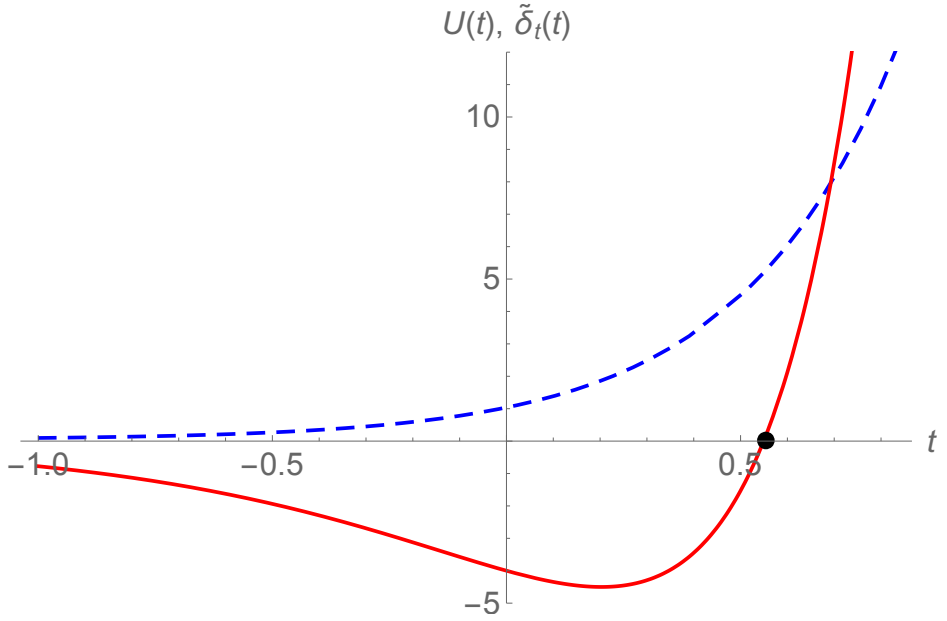

Figure 4.1: Conditionally integrable dissipative two-state level-crossing model (4.63)-(4.64). The blue dashed line is the Rabi frequency ($U_0 = 1$), the red solid line stands for the detuning ($\delta_2 = 1$, $\delta_0 = -3$). The filled circle indicates the level-crossing time point $t_0 = \ln(-\delta_0/\delta_2)/2$.

4.6 Population dynamics of the dissipative two-state system

We consider the semiclassical time-dependent two-state problem with a decaying upper level. Let the probability amplitudes of the ground and excited states be $a_1(t)$ and $b_2(t)$, respectively. If the decay of the excited state is supposed to be a third state, the equations for the probability amplitudes read [125]

$$i\frac{da_1}{dt} = U(t)\, b_2, \tag{4.68}$$

$$i\frac{db_2}{dt} = U(t)\, a_1 + \left(\tilde{\delta}_t(t) - i\Gamma\right) b_2, \tag{4.69}$$

where the Rabi frequency $U(t)$ and the frequency modulation function $\tilde{\delta}(t)$ (the derivative of this function $\tilde{\delta}_t(t)$ is the detuning of the transition frequency from the field frequency) are arbitrary real functions of time, and the parameter Γ defines the rate of the losses from the upper level.

By change of the variable $b_2 = a_2(t)\, e^{-i\,\delta(t)}$ and further elimination of a_1, system (4.68), (4.69) is reduced to the following second-order linear differential equation for $a_2(t)$:

$$a_{2tt} + \left(-i\,\delta_t - \frac{U_t}{U}\right) a_{2t} + U^2 a_2 = 0, \tag{4.70}$$

$$\delta_t = \tilde{\delta}_t - i\Gamma, \tag{4.71}$$

where (and hereafter) the lowercase alphabetical index denotes differentiation with respect to the corresponding variable.

According to the expansion (4.57), a fundamental solution of the initial two-state problem (4.68), (4.69) is written through a linear combination of two Hermite functions:

$$b_2^F(t) = z^{\alpha_1} e^{\alpha_0 z + \alpha_2 z^2/2}\, e^{i\,\delta(t)} \left(c_0 H_{\alpha/\varepsilon - 1}(y) + c_1 H_{\alpha/\varepsilon}(y)\right), \tag{4.72}$$

where

$$y = s\sqrt{\frac{-\varepsilon}{2}} \left(z + \frac{\delta}{\varepsilon}\right), \qquad z(t) = e^{2\Gamma t}. \tag{4.73}$$

The expansion coefficients $c_{0,1}$ are conveniently written through the parameters of the bi-confluent Heun function, which are readily calculated through the amplitude and detuning modulation functions' parameters and the auxiliary parameter $s = \pm 1$. The result reads

$$c_0 = 1, \qquad c_1 = s\sqrt{\frac{-\varepsilon}{2}} \left(\frac{\delta - q}{\alpha}\right). \tag{4.74}$$

We note that $s = +1$ and $s = -1$ produce linearly independent fundamental solutions. This is readily verified by checking the Wronskian of the two solutions. Hence, the linear combination of these fundamental solutions

$$b_2(t) = C_1\, b_2^F\big|_{s\to+1} + C_2\, b_2^F\big|_{s\to-1}. \tag{4.75}$$

with arbitrary constant coefficients $C_{1,2}$ presents the general solution of the problem.

We consider the situation when the system initially starts from the ground state, that is,

we impose the initial conditions

$$a_1(-\infty) = 1, \quad b_2(-\infty) = 0. \tag{4.76}$$

In the Fig. 4.2 we present the graphs for the probability $p_1 = |a_1(t)|^2$ for the atom to stay on the first level and the probability $p_2 = |b_2(t)|^2$ for the atom to be occupying the excited state during the interaction. As it is clearly seen, for the chosen field parameters the result of the dissipation is the complete removal of the population from both levels. It is understood that this is because the chosen field parameters provide a sufficiently intensive interaction with the field accompanied with a strong decay rate from the excited state. The analysis of the asymptotes of the solution reveals that the physical parameter defining the interaction regime is $\lambda \sim U_0^2/(\delta_0\delta_2)$. The strong interaction regime corresponds to large $\lambda \gg 1$, while the weak interaction regime applies to small $\lambda \ll 1$.

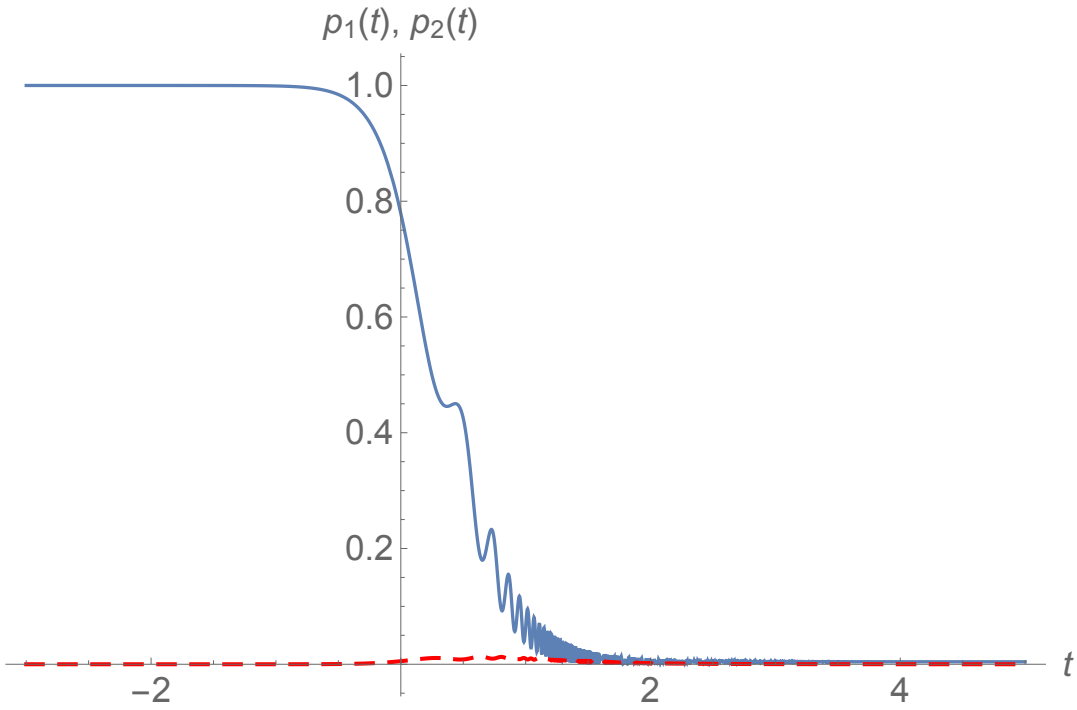

Figure 4.2: Probabilities $p_1 = |a_1(t)|^2$ and $p_2 = |b_2(t)|^2$ (blue solid and red dashed lines, respectively) for the field configuration parameters $U_0 = 1$, $\delta_0 = -3$, $\delta_2 = 1$.

As the field amplitude increases, the excitation of the atom intensifies, the second level becomes more populated, hence, the losses from the second level become more pronounced

(Fig. 4.3). In contrast, if the field amplitude decreases, the excitation process slows down, the excited state becomes less populated so that the losses from the second level wash out from the system a lesser population and, as a result, the system may end up with a not depleted population in the ground state (Fig. 4.4).

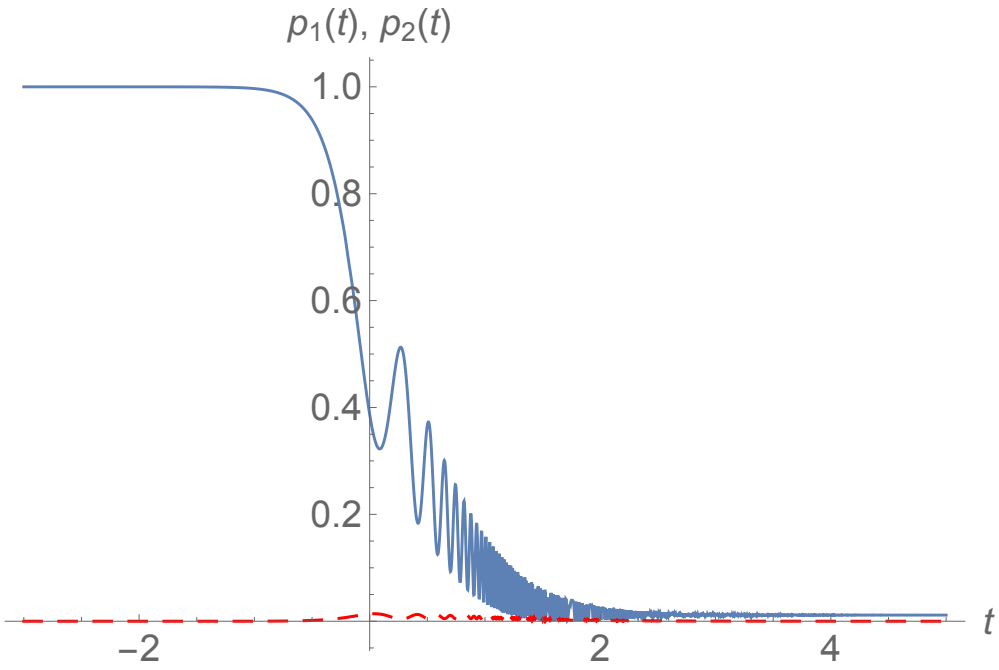

Figure 4.3: Occupation probabilities for the ground and excited states (blue solid and red dashed lines, respectively) for the field configuration parameters $U_0 = 2$, $\delta_0 = -3$, $\delta_2 = 1$.

From the Figs: 4.3 and 4.4 we conclude that if the field amplitude is small, then during the interaction the population of the first level decreases, because of the resonance crossing; however, at the end of the process the first level still possesses a remnant population, while the second level always completely empties because of the losses. In other words, if the coupling is weak (that is the Rabi frequency is small), then the interaction is not very intensive (compared to the case presented in the Fig. 4.2), so that by the effective time of the resonance crossing the population of the first level manages not to get fully exhausted.

Finally, even for a weak coupling (small Rabi frequency), complete transition to the second level is possible if δ_2 is sufficiently small (Fig. 4.5). In this case the system remains near the resonance for a sufficiently long time period, hence, the second level may be well populated thus resulting in complete decay of its population to a third state.

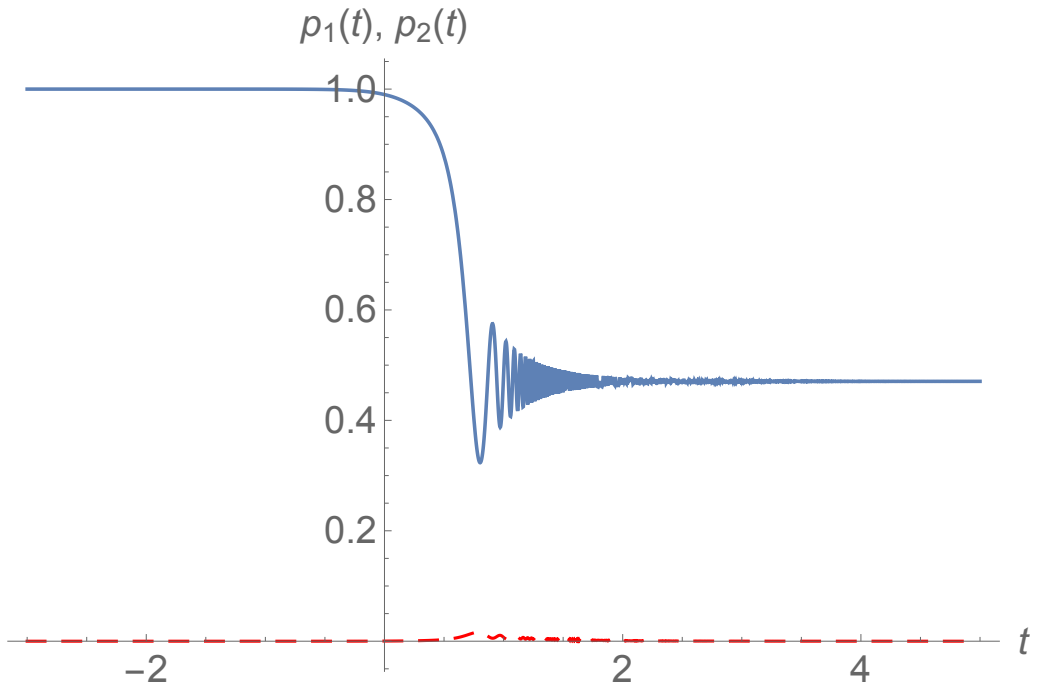

Figure 4.4: Occupation probabilities for the ground and excited states (blue solid and red dashed lines, respectively) for the field configuration parameters $U_0 = 0.2$, $\delta_0 = -3$, $\delta_2 = 1$.

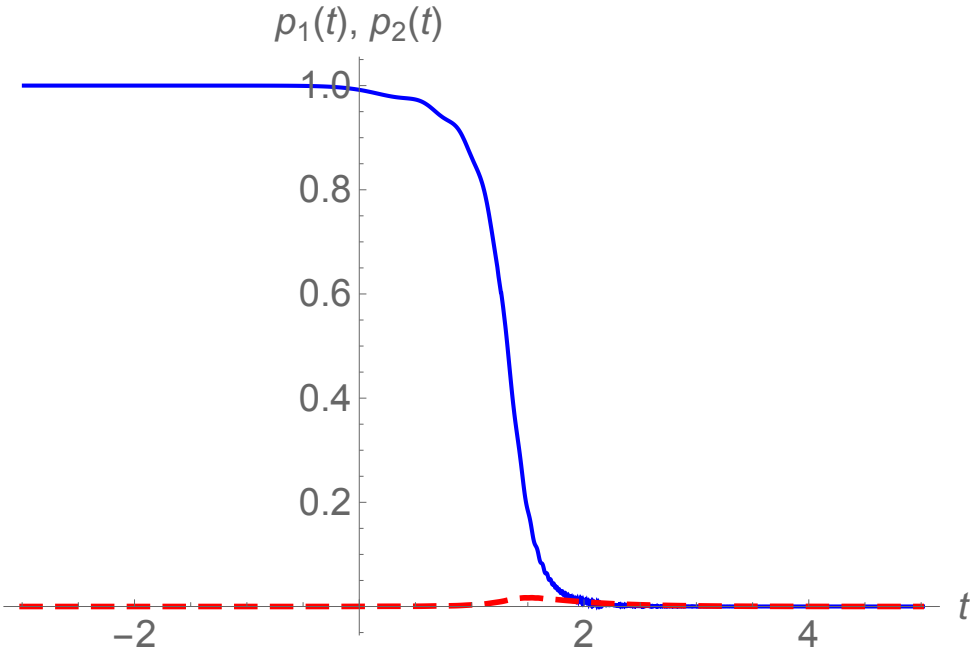

Figure 4.5: Occupation probabilities for the first and second levels (blue solid and red dashed lines, respectively) for the weak but long interaction: $U_0 = 0.2$, $\delta_0 = -3$, $\delta_2 = 0.2$.

4.7 Discussion

Thus, we have presented an analytic model of a dissipative semiclassical quantum two-state problem associated with an external optical field of a level-crossing configuration. The

physical processes responsible for the dissipation may include photoinduced decomposition of particles, spontaneous emission of photons, collision relaxation, and etc. In the model we treat, the excited state is supposed to decay irreversibly out of the system, while the decay transition from the excited to the ground state is neglected.

We have reviewed the specific field configurations for which the time-dependent two-state problem is reduced to the bi-confluent Heun equation which is a second-order ordinary linear differential equation having a regular singularity and an irregular singularity of rank 2. In order to treat the derived solution, we have applied an expansion of the involved bi-confluent Heun function in terms of the non-integer order Hermite functions of a scaled and shifted argument. The expansion is governed by a three-term recurrence relation between the successive coefficients of the expansion. We have discussed the conditions for the derived series to terminate thus resulting in finite-sum solutions.

As an application of such a termination to the two-state problem under consideration, we have identified a conditionally integrable resonance-crossing field configuration for which the termination results in a general solution written through fundamental solutions each of which involves an irreducible linear combination of two Hermite functions. This is a configuration given by an exponentially diverging Rabi frequency and a level-crossing detuning that starts from the exact resonance and exponentially diverges at the infinity. Using the two-term Hermite function explicit solution, we have studied the population dynamics in different interaction regimes.

Conclusion

The main conclusions that come out from this work are as follows:

It is possible an efficient adiabatic passage in a basic quadratic-nonlinear quantum two-state system describing the weakly bound molecule formation in atomic Bose-Einstein condensates through photoassociation by laser fields. This passage may also be robust. We have developed an example of such a transfer.

An efficient adiabatic transfer is also possible if the third-order nonlinearities describing the atom-atom, atom-molecule, and molecule-molecule elastic scattering are taken into account. The transfer is achieved by choosing a proper detuning derived by solving the inverse problem. One of the two branches of the derived tracking detuning provides an efficient transfer if the Rabi frequency is larger than the Kerr scattering length. Whereas, in the second case we always have an efficient transfer.

It is possible a stimulated Raman exact tracking in a quadratic-nonlinear quantum three-state system. In contrast to the ordinary linear case, in the nonlinear case for an efficient transfer one needs to take the pump pulse considerably stronger than the Stokes one. This transfer may also be robust. The most robust regime is achieved in the vicinity of the one- and two-photon resonances.

It is possible to avoid the irreversible losses from the intermediate weakly bound molecular state in a passage of free atoms to the stable molecular state by a two-colour three-state scheme in the case of one- and two-photon resonances for the associating laser fields. This is achieved by the same above-mentioned exact tracking technique developed for a given evolution scenario.

The linear time-dependent two-state bi-confluent Heun models allow solutions in terms of linear combinations of a finite number of the Hermite functions of non-integer order. We have presented a model the solution for which involves just two Hermite functions. This is a resonance-crossing field configuration given by an exponentially diverging Rabi frequency and a detuning that starts from the exact resonance and exponentially diverges at the infinity. It is worth mentioning that the model takes into account the irreversible losses from the second state.

Bi-confluent Heun functions allow an expansion in terms of the incomplete Beta functions. Such a series is governed by a three-term recurrence relation between the successive coefficients of the expansion. This recurrence relation allows termination of the series.

Appendix. Comparison of the linear Demkov-Kunike model with the nonlinear model

In this section we consider more physical model: Demkov-Kunike level crossing model, for which the Rabi frequency and detuning are given by

$$U(t) = U_0 \sec h(t), \qquad \delta_t(t) = \Delta_0 \tanh(t). \tag{4.77}$$

For comparison are presented numerical calculations of linear and nonlinear Demkov-Kunike

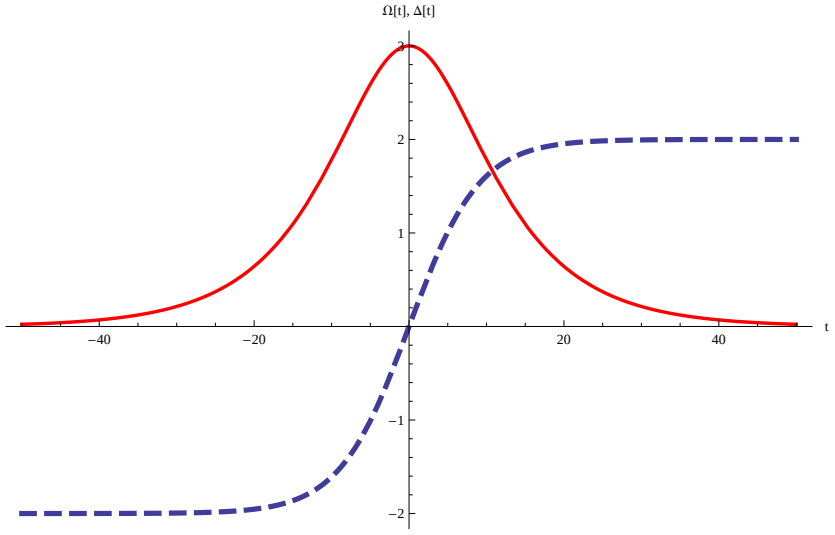

Figure 4.6: The Demkov-Kunike model. Red solid line is the Rabi frequency, and the blue dashed line is the detuning.

models, in the case of different values of parameters. We will start with linear set of equations

$$i\dot{a}_{1L} = \Omega(t)e^{-i\Delta(t)}a_{2L}, \tag{4.78}$$

$$i\dot{a}_{2L} = \Omega(t)e^{i\Delta(t)}a_{1L}. \tag{4.79}$$

This linear system describes the interaction of an isolated atom with an optical laser radiation [126]. Demkov-Kunike model gives any value of transition probability. However, in this case there exist big oscillations of populations in the system, which is not a desired result. There is a crossing of resonance leading to strong oscillations, which is not acceptable.

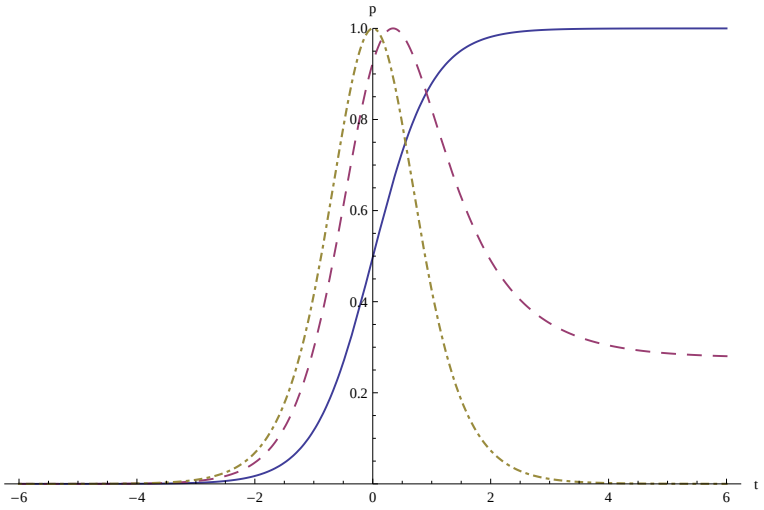

Figure 4.7: Transition probability $P(t)$ for the Demkov-Kunike model, linear case. The solid, dashed and dashed-point lines correspond to $\Delta_0 = 0$, $\Omega_0 = 0.5, 0.825, 1$, respectively.

For the nonlinear Demkov-Kunike model the set of equations are

$$i\dot{a}_{1L} = \Omega(t)e^{-i\Delta(t)}a_{2L}\bar{a_{1L}}, \tag{4.80}$$

$$i\dot{a}_{2L} = \Omega(t)e^{i\Delta(t)}a_{1L}a_{1L}. \tag{4.81}$$

Note that

$$|a_1|^2 + |a_2|^2 = J_L = 1$$

$|a_1|^2$ and $|a_{2L}|^2$ are interpreted as probabilities of the first and second states, respectively. It

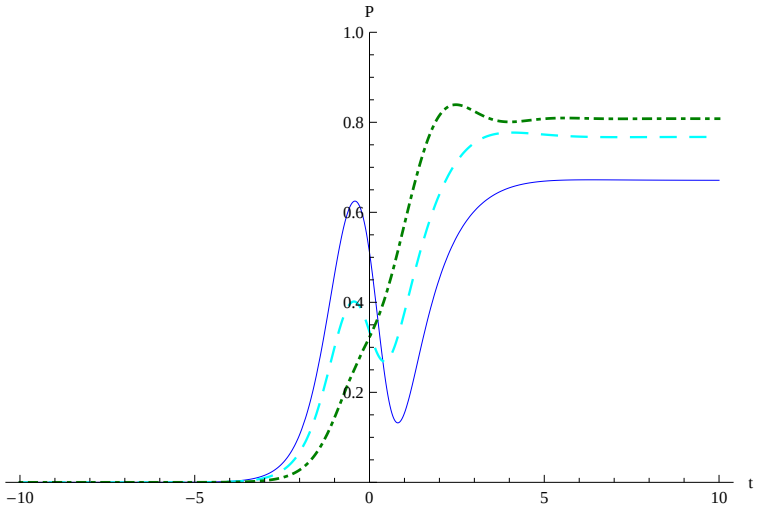

Figure 4.8: Transition probability $P(t)$ for the Demkov-Kunike model, nonlinear case. The solid, dashed and dashed-point lines correspond to $\Omega_0 = 1$, $\Delta_0 = 0.5, 1, 2$, respectively.

is followed by listing the model, which will be discussed in the present section. Also, will be described their main characteristics.

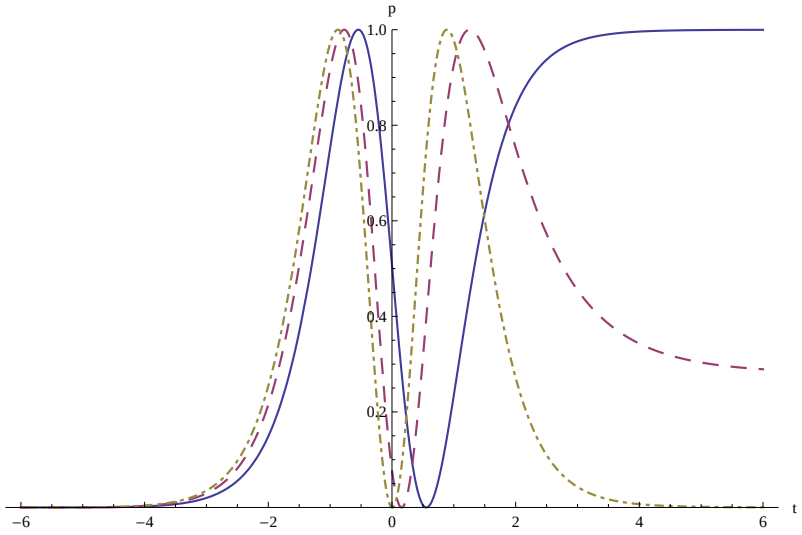

Figure 4.9: Transition probability $P(t)$ for the Demkov-Kunike model, linear case. The solid, dashed and dashed-point lines correspond to $\Omega_0 = 1.5, 1.825, 2$, $\Delta_0 = 0$, respectively.

Thus, we describe the linear two-state level-crossing and avoided-crossing model. Such a model is the Demkov-Kunike level-crossing model, which has a bell-shaped coupling [106], Fig. 4.6, for which the amplitude and detuning are defined as

$$\Omega = \Omega_0 \mathrm{sech}(t/\tau), \qquad \Delta_t = 2\Delta_0 \tanh(t/\tau), (\tau > 0). \tag{4.82}$$

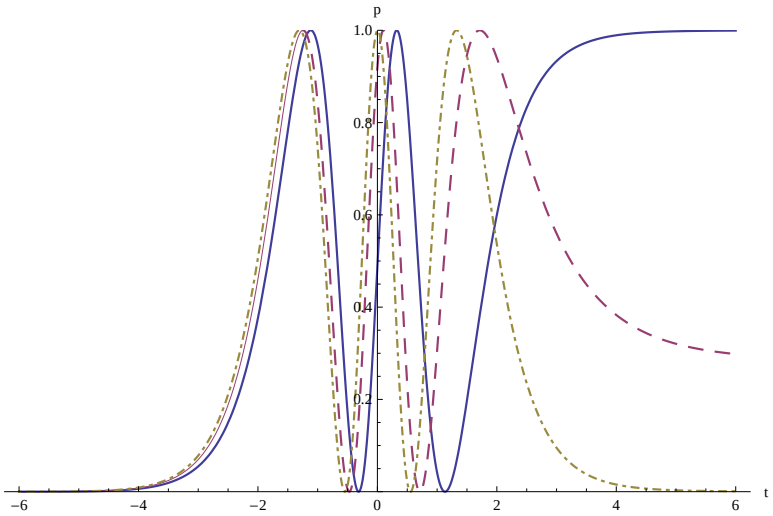

Figure 4.10: Transition probability $P(t)$ for the Demkov-Kunike model, linear case. The solid, dashed and dashed-point lines correspond to $\Omega_0 = 2.5, 2.825, 3$, $\Delta_0 = 0$, respectively.

For the Demkov-Kunike model the exact solution of the linear set of equations (4.78) and (4.79) is given in terms of the Gauss hypergeometric functions ${}_2F_1$ [127].

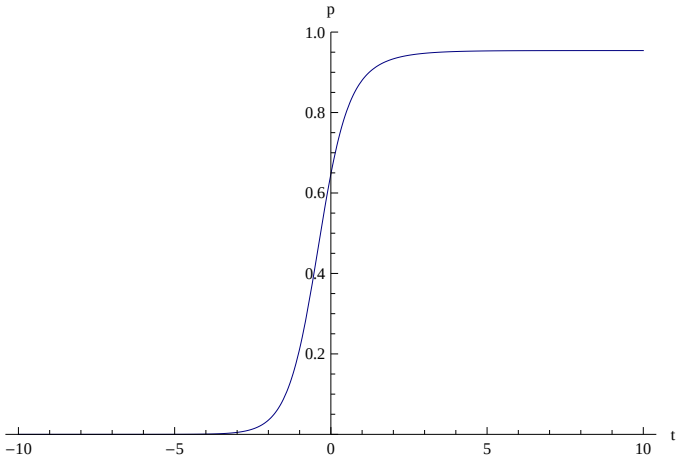

Figure 4.11: The nonlinear Demkov-Kunike model, with parameters $\Omega_0 = 1$, $\Delta_0 = 0$.

In the nonlinear case there exists transfer without oscillation, but for a narrow range of parameters. According to the Fig. 4.8 (concerning nonlinear Demkov-Kunike model), the model gives nonoscillatory regime. In the Fig. 4.11 we have a model, which will give as nonoscillatory part, it is a resonance case, but the model is not robust.

These behaviours, which are obtained from different models are not acceptable. We need to find a model, which will not have an oscillation. Thus, we need to find a model, which will give as nonoscillatory regimes, a model will be robust.

Bibliography

Papers included in the thesis

[1] S. Guérin, M. Gevorgyan, C. Leroy, H. Jauslin and A. Ishkhanyan, "Efficient adiabatic tracking of driven quantum nonlinear systems", Phys. Rev. A. **88**, 063622 (2013).

[2] M. Gevorgyan, S. Guérin, C. Leroy, A. Ishkhanyan, and H. R. Jauslin, "Adiabatic tracking for photo- and magneto-association of Bose-Einstein condensates with Kerr nonlinearities", Eur. Phys. J. D **70**, 253 (2016).

[3] T.A. Ishkhanyan, Y. Pashayan-Leroy, M.R. Gevorgyan, C. Leroy, and A.M. Ishkhanyan, "Expansions of the solutions of the bi-confluent Heun equation in terms of incomplete Beta and Gamma functions", J. Contemp. Phys. (Armenian Ac. Sci.) **51**, 229-236 (2016).

[4] M. Gevorgyan, "A dissipative conditionally integrable two-state level-crossing model exactly solvable in terms of the bi-confluent Heun functions", Armenian J. Physics **9**, 192-200 (2016).

Conference thesis and abstracts

[5] M. Gevorgyan and A. Ishkhanyan, "A time-dependent level-crossing model solvable in terms of the Hermite functions", 4^{th} International Symposium on Optics and its Applications (OPTICS-2016), 25-28 July, Yerevan-Ashtarak, Armenia (2016). Book of Abstracts, P-71.

[6] M. Gevorgyan, S. Guérin, C. Leroy, A. Ishkhanyan, and H. R. Jauslin, "Efficient adiabatic tracking for molecular Bose-Einstein condensate production with Kerr nonlinearities", International Conference Laser Physics 2015, 6-9 October, Ashtarak, Armenia (2015). Book of Abstracts, P-41-42.

[7] M. Gevorgyan, S. Guérin, C. Leroy, A. Ishkhanyan, and H. R. Jauslin, "Adiabatic tracking for photoassociation of ultracold atoms with Kerr-type elastic scatterings", 3^{rd} International Symposium on Optics and its Applications (OPTICS-2015), 1-5 October,Yerevan-Ashtarak, Armenia (2015). Book of Abstracts, P-89.

[8] M. Gevorgyan, C. Leroy, H. R. Jauslin, S. Guérin, A. Ishkhanyan, "Nonlinear stimulated Raman exact tracking", QuantArm 2014, 22-26 September, Yerevan-Tsaghkadzor, Armenia (2014). Book of Abstracts, P-51-53.

[9] M. Gevorgyan, S. Guérin, C. Leroy, H. R. Jauslin, and A. Ishkhanyan, "Adiabatic tracking of molecule production in Bose-Einstein condensates with Kerr terms", 2^{nd} International Symposium on Optics and its Applications (OPTICS-2014), 1-5 September, Yerevan-Ashtarak, Armenia (2014). Book of Abstracts, P-91-92.

[10] M. Gevorgyan, S. Guérin, C. Leroy, H. R. Jauslin, A. Ishkhanyan, "Adiabatic tracking for molecule production in Bose-Einstein condensates", International Conference Laser Physics 2013, 6-9 October, Ashtarak, Armenia (2013). Book of Abstracts, P-40.

[11] A. Grigoryan, M. Gevorgyan, H. Azizbekyan, A. Ishkhanyan, "Analytic solutions of quantum two-state problem in terms of confluent Heun functions", IONS conference in Optics and Photonics, 11-14 September, Yerevan-Ashtarak, Armenia (2013). Book of Abstracts P-55.

[12] S. Guérin, M. Gevorgyan, A. Grigoryan, C. Leroy, H. R. Jauslin, A. Ishkhanyan, "Efficient adiabatic passage for driven quantum nonlinear systems", IONS conference in Optics and Photonics, 11-14 September, Yerevan-Ashtarak, Armenia (2013). Book of Abstracts, P-50.

Cited literature

[13] S. Bose, Z. Phys. **26,** 178-181 (1924).

[14] A. Einstein, Sitzungsber. Kgl. Preuss. Akad. Wiss. 3-14 (1925).

[15] W. Ketterle, "Nobel lecture: When atoms behave as waves: Bose-Einstein condensation and the atom laser", Rev. Mod. Phys. **74,** 1131-1151 (2002).

[16] M.H. Anderson, J.R. Ensher, M.R. Matthews, C.E. Wieman, and E.A. Cornell, "Observation of Bose-Einstein Condensation in a Dilute Atomic Vapor", Science 269, 198-201 (1995).

[17] E. Cornell and C. Wieman, "Nobel Lecture: Bose-Einstein condensation in a dilute gas, the first 70 years and some recent experiments", Rev. Mod. Phys. **74,** 875-893 (2002).

[18] C. J. Pethick and H. Smith, Bose-Einstein condensation in dilute gases (Cambridge University Press, Cambridge, 2002).

[19] W. D. Phillips, Rev. Mod. Phys. **70,** 721-741 (1998).

[20] Gorlitz, Axel. "Interference of Condensates (BEC@MIT)". Cua.mit.edu. Retrieved 13 October (2009).

[21] Dutton, Zachary; Ginsberg, Naomi S.; Slowe, Christopher and Hau, Lene Vestergaard (2004). "The art of taming light: ultra-slow and stopped light". *Europhysics News* **35** (2).

[22] M. Greiner, C.A. Regal, and D.S. Jin, "Emergence of a molecular Bose-Einstein condensate from a Fermi gas", Nature 426, 537-540 (2003).

[23] M.W. Zwierlein, C.A. Stan, C.H. Schunck, S.M.F. Raupach, S. Gupta, Z. Hadzibabic, and W. Ketterle, "Observation of Bose-Einstein Condensation of Molecules", Phys. Rev. Lett. **91,** 250401, 1-4 (2003).

[24] S. Jochim, M. Bartenstein, A. Altmeyer, G. Hendl, S. Riedl, C. Chin, J. Hecker Denschlag, and R. Grimm, "Bose-Einstein Condensation of Molecules", Science 302, 2101-2103 (2003).

[25] N.R. Claussen, S.J.J.M.F. Kokkelmans, S.T. Thompson, E.A. Donley, E. Hodby, and C.E. Wieman, "Very-high-precision bound-state spectroscopy near a ^{85}Rb Feshbach resonance", Phys. Rev. A **67,** 060701(R), 1-4 (2003).

[26] S. Kotochigova, T. Zelevinsky, and J. Ye, "Prospects for application of ultracold Sr2 molecules in precision measurements", Phys. Rev. A **79,** 012504, 1-7 (2009).

[27] E.R. Meyer and J.L. Bohn, "Prospects for an electron electric-dipole moment search in metastable ThO and ThF+", Phys. Rev. A **78,** 010502(R), 1-4 (2008).

[28] B.C. Regan, E.D. Commins, C.J. Schmidt, and D. DeMille, "New Limit on the Electron Electric Dipole Moment", Phys. Rev. Lett. **88,** 071805, 1-4 (2002).

[29] D.J. Heinzen, R. Wynar, P.D. Drummond, and K.V. Kheruntsyan, "Superchemistry: Dynamics of Coupled Atomic and Molecular Bose-Einstein Condensates", Phys. Rev. Lett. **84,** 5029-5033 (2000).

[30] D. DeMille, "Quantum Computation with Trapped Polar Molecules", Phys. Rev. Lett. **88,** 067901, 1-4 (2002).

[31] C. A. Regal, C. Ticknor, J. L. Bohn, and D. S. Jin, Nature (London) **424**, 47 (2003).

[32] K-A. Brickman Soderberg, N. Gemelke, and Ch. Chin, "Ultracold molecules: vehicles to scalable quantum information processing", New J. Phys. **11,** 055022, 1-14 (2009).

[33] C.N. Cohen-Tannoudji, Rev. Mod. Phys. **70,** 707-719 (1998).

[34] S. Chu, Rev. Mod. Phys. **70,** 685-706 (1998).

[35] K.B. Davis, M.-O. Mewes, M.R. Andrews, N.J. van Druten, D.S. Durfee, D.M. Kurn, and W. Ketterle, "Bose-Einstein Condensation in a Gas of Sodium Atoms", Phys. Rev. Lett. **75,** 3969-3973 (1995).

[36] J. D.Weinstein, R. DeCarvalho, T. Guillet, B. Friedrich, and J.M. Doyle, Nature (London) **395**, 148 (1998); T. Takekoshi, B.M. Patterson, and R. J. Knize, Phys. Rev. Lett. **81**, 5105 (1998); R. Wynar, R. S. Freeland, D. J. Han, C. Ryu, and D. J. Heinzen, Science **287**, 1016 (2000); H. L. Bethlem, G. Berden, F.M. H. Crompvoets, R.T. Jongma, A. J. A. van Roij, and G. Meijer, Nature (London) **406**, 491 (2000); C. Chin, A. J. Kerman, V. Vuletic, and S. Chu, Phys. Rev. Lett. **90**, 033201 (2003).

[37] E.A. Donley, N.R. Claussen, S.T. Thompson, C.E. Wieman, "Atom-molecule coherence in a Bose-Einstein condensate", Nature **417,** 529-533 (2002).

[38] S. Jochim, M. Bartenstein, A. Altmeyer, G. Hendl, S. Riedl, C. Chin, J. Hecker Denschlag, and R. Grimm, "Bose-Einstein Condensation of Molecules", Science **302**, 2101 (2003).

[39] J. Herbig, T. Kraemer, M. Mark, T. Weber, C. Chin, H.-C. Nagerl, and R. Grimm, Science **301**, 1510 (2003).

[40] M. Greiner, C.A. Regal, and D.S. Jin, "Emergence of a molecular BoseEinstein condensate from a Fermi gas", Nature **426**, 537 (2003).

[41] "Fermionic condensate makes its debut". Physicsweb.org. 28 January 2004.

[42] T. Zelevinsky, S. Blatt, M.M. Boyd, G.K. Campbell, A.D. Ludlow, and J. Ye, "Highly Coherent Spectroscopy of Ultracold Atoms and Molecules in Optical Lattices", ChemPhysChem **9,** 375-382 (2008).

[43] W.C. Stwalley, "Stability of Spin-Aligned Hydrogen at Low Temperatures and High Magnetic Fields: New Field-Dependent Scattering Resonances and Predissociations", Phys. Rev. Lett. **37,** 1628-1631 (1976); E. Tiesinga, B.J. Verhaar, and H.T.C. Stoof, "Threshold and resonance phenomena in ultracold ground-state collisions", Phys. Rev. A **47,** 4114 (1993).

[44] E. Tiesinga, A.J. Moerdijk, B.J. Verhaar, and H.T.C. Stoof, "Conditions for Bose-Einstein condensation in magnetically trapped atomic cesium", Phys. Rev. **46,** R1167-R1170 (1992).

[45] A.J. Moerdijk, B.J. Verhaar, and A. Axelsson, "Resonances in ultracold collisions of 6Li, 7Li, and 23Na," Phys. Rev. A **51,** 4852-4861 (1995).

[46] K.E. Strecker, G.B. Partridge, and R.G. Hulet, "Conversion of an Atomic Fermi Gas to a Long-Lived Molecular Bose Gas", Phys. Rev. Lett. **91,** 080406, 1-4 (2003).

[47] S. Jochim, M. Bartenstein, A. Altmeyer, G. Hendl, C. Chin, J. Hecker Denschlag, and R. Grimm, "Pure Gas of Optically Trapped Molecules Created from Fermionic Atoms", Phys. Rev. Lett. **91,**, 240402, 1-4 (2003).

[48] S. Inouye, M.R. Andrews, J. Stenger, H.-J. Miesner, D.M. Stamper-Kurn, and W. Ketterle, "Feshbach resonances", Nature (London) **392,** 151-154 (1998).

[49] P. Courteille, R.S. Freeland, D.J. Heinzen, F.A. van Abeelen, and B.J. Verhaar, "Observation of a Feshbach Resonance in Cold Atom Scattering", Phys. Rev. Lett. **81,** 69-72 (1998).

[50] A. Fioretti, D. Comparat, A. Crubellier, O. Dulieu, F. Masnou-Seeuws, and P. Pillet, "Formation of Cold Cs^2 Molecules through Photoassociation", Phys. Rev. Lett. **80,** 4402-4405 (1998).

[51] A.N. Nikolov, E.E. Eyler, X.T. Wang, J. Li, H. Wang, W.C. Stwalley, and P.L. Gould, "Observation of Ultracold Ground-State Potassium Molecules", Phys. Rev. Lett. **82,** 703-706 (1999).

[52] J. Weiner, V.S. Bagnato, S. Zilio, and P.S. Julienne, "Experiments and theory in cold and ultracold collisions", Rev. Mod. Phys. **71,** 1-85 (1999); F. Masnou-Seeuws and P. Pillet, "Formation of ultracold molecules $T \leq 200\mu K$ via photoassociation in a gas of lasercooled atoms", Adv. At., Mol., Opt. Phys. **47,** 53-127 (2001).

[53] K.M. Jones, E. Tiesinga, P.D. Lett, and P.S. Julienne, "Ultracold photoassociation spectroscopy: Long-range molecules and atomic scattering", Rev. Mod. Phys. **78,** 483-535 (2006).

[54] K.E. Strecker, G.B. Partridge, and R.G. Hulet, "Conversion of an Atomic Fermi Gas to a Long-Lived Molecular Bose Gas", Phys. Rev. Lett. **91**, 080406, 1-4 (2003).

[55] S. Jochim, M. Bartenstein, A. Altmeyer, G. Hendl, C. Chin, J. Hecker Denschlag, and R. Grimm, "Pure Gas of Optically Trapped Molecules Created from Fermionic Atoms", Phys. Rev. Lett. **91**, 240402, 1-4 (2003).

[56] T. Koehler, K. Goral, and P. Julienne, "Production of cold molecules via magnetically tunable Feshbach resonances", Rev. Mod. Phys. **78**, 1311-1361 (2006).

[57] C. Chin, R. Grimm, P. Julienne, and E. Tiesinga, "Feshbach Resonances in Ultracold Gases", Rev. Mod. Phys. **82,** 1225-1286 (2010).

[58] R. Wynar, R.S. Freeland, D.J. Han, C. Ryu, and D.J. Heinzen, "Molecules in a Bose-Einstein condensate", Science **287,** 1016-1019 (2000).

[59] C. McKenzie, J. Hecker Denschlag, H. Haffner, A. Browaeys, Luis E.E. de Araujo, F.K. Fatemi, K.M. Jones, J.E. Simsarian, D. Cho, A. Simoni, E. Tiesinga, P.S. Julienne, K. Helmerson, P.D. Lett, S.L. Rolston, and W.D. Phillips, "Photoassociation of sodium in a Bose-Einstein condensate", Phys. Rev. Lett. **88,** 120403, 1-4 (2002).

[60] J. Javanainen and M. Mackie, "Coherent photoassociation of a Bose-Einstein condensate", Phys. Rev. A **59,** R3186-R3189 (1999).

[61] M. Kostrun, M. Mackie, R. Cote, and J. Javanainen, "Theory of coherent photoassociation of a Bose-Einstein condensate", Phys. Rev. A **62,** 063616, 1-23 (2000).

[62] M. Mackie and J. Javanainen, "Quasicontinuum modeling of photoassociation", Phys. Rev. A **60,** 3174-3187 (1999).

[63] A. Carmichael and J. Javanainen, "Mean-field stationary state of a Bose gas at a Feshbach resonance", Phys. Rev. A **77,** 043616, 1-15 (2008).

[64] P.D. Drummond, K.V. Kheruntsyan, and H. He, "Coherent Molecular Solitons in Bose-Einstein Condensates", Phys. Rev. Lett. **81,** 3055-3058 (1998).

[65] E.P. Gross, Nuovo Cimento **20,** 454-477 (1961).

[66] L.D. Landau, Phys. Z. Sowjetunion 2, **46,** (1932); C. Zener, Proc. R. Soc. London, Ser. A **137,** 696-703 (1932).

[67] A. Ishkhanyan, R. Sokhoyan, B. Joulakian, and K.-A. Suominen, "RosenZener model in cold molecule formation", Opt. Commun. **282,** 218-226 (2009).

[68] A. Ishkhanyan, J. Javanainen, and H. Nakamura, "A basic two-state model for bosonic field theories with a cubic nonlinearity", J. Phys. A **38**, 3505-3516 (2005).

[69] L. P. Pitaevskii and S. Stringari, Bose-Einstein Condensation (Oxford University Press, Oxford, U.K., 2003).

[70] J. Javanainen and M. Mackie, Phys. Rev. A **59**, R3186 (1999).

[71] P. D. Drummond, K. V. Kheruntsyan, and H. He, Phys. Rev. Lett. **81**, 3055 (1998).

[72] E. Timmermans, P. Tommasini, M. Hussein, and A. Kerman, Phys. Rep. **315**, 199 (1999).

[73] T. Kohler, K. Goral, and P. S. Julienne, Rev. Mod. Phys. **78**, 1311 (2006).

[74] J. Liu, B. Wu, and Q. Niu, Phys. Rev. Lett. **90**, 170404 (2003).

[75] A. P. Itin and S. Watanabe, Phys. Rev. E **76**, 026218 (2007).

[76] A. P. Itin, A. A. Vasiliev, G. Krishna, and S. Watanabe, Physica D **232**, 108 (2007).

[77] A. P. Itin and P. Torma, Phys. Rev. A **79**, 055602 (2009).

[78] U. Boscain, G. Charlot, J.-P. Gauthier, S. Guérin, and H. R. Jauslin, J. Math. Phys. **43**, 2107 (2002).

[79] T. Kato, "On the Adiabatic Theorem of Quantum Mechanics", J. Phys. Soc. Jpn. **5** (6): 435-439 (1950).

[80] V.I. Arnold, V. V. Kozlov, A. I. Neihstadt, *Mathematical Aspects of Classical and Celestial Mechanics* Dynamical Systems III Encyclopedia of Math. Sciences. 3rd edition; Springer-Verlag, Berlin, Heidelberg, (1988).

[81] J. Henrard, The Adiabatic Invariant Theory and Applications; in *Hamiltonian Dynamics - Theory and Applications*, Lecture Notes in Mathematics, Vol. 1861, G. Benettin, J. Henrard, S.B. Kuksin, A. Giorgilli, (Eds.), Springer-Verlag, Berlin, Heidelberg, (2005).

[82] J.R. Cary, D.F. Escande, J.L. Tennyson; Physical Review A 34, 4256 (1986).

[83] A. Fasano, S. Marmi, *Analytical Mechanics*, Oxford University Press (2006).

[84] K. Efstathiou, *Metamorphoses of Hamiltonian Systems with Symmetries*, Lecture Notes in Mathematics Vol. 1864 (Springer-Verlag, Berlin, Heidelberg, 2005).

[85] O. Zobay and B. M. Garraway, Phys. Rev. A **61**, 033603 (2000).

[86] A. M. Ishkhanyan, G. P. Chernikov, and H. Nakamura, Phys. Rev. A 70, 053611 (2004); A. M. Ishkhanyan, ibid. **81**, 055601 (2010).

[87] I.I. Rabi, Phys. Rev. **51**, 652-654 (1937).

[88] L. Allen and J. H. Eberly, *Optical Resonance and Two-Level Atoms* (Dover, New York, 1987).

[89] B.W. Shore, *The Theory of Coherent Atomic Excitation* (Wiley, NewYork, 1990); *Manipulating Quantum Structure Using Laser Pulses* (Cambridge University Press, New York, 2011).

[90] N.V. Vitanov, M. Fleischhauer, B.W. Shore, and K. Bergmann, Adv. At. Mol. Opt. Phys. **46**, 55 (2001); N.V. Vitanov, T. Halfmann, B.W. Shore and K. Bergmann, Ann. Rev. Phys. Chem **52**, 763 (2001); S. Guérin and H.R. Jauslin, Adv. Chem. Phys **125**, 147 (2003).

[91] Xi Chen, I. Lizuain, A. Ruschhaupt, D. Gurery-Odelin, and J. G. Muga, Phys. Rev. Lett. **105**, 123003 (2010); A. Ruschhaupt, X. Chen, D. Alonso, and J. G. Muga, New J. Phys. **14**, 093040 (2012).

[92] D. Daems, A. Ruschhaupt, D. Sugny, and S. Guérin, Phys. Rev. Lett. **111**, 050404 (2013).

[93] Y. R. Shen, *The Principles of Nonlinear Optics* (Wiley, New York, 2002).

[94] M. Wollenhaupt, V. Engel, and T. Baumert, Annu. Rev. Phys. Chem. **56**, 25 (2005).

[95] S. Guérin, S. Thomas, and H.R. Jauslin, Phys. Rev. A **65**, 023409 (2002); G. Dridi, S. Guérin, V. Hakobyan, H. R. Jauslin, and H. Eleuch, *ibid* **80**, 043408 (2009); S. Guérin, V. Hakobyan, and H.-R. Jauslin, *ibid.* **84**, 013423 (2011).

[96] T. Kohler, K. Goral, and P.S, Julienne, Rev. Mod. Phys. **78**,1311, (2006).

[97] Hong Y. Ling, Peter Maenner, Weiping Zhang, and Han Pu, Phys. Rev. A. **75**, 033615 (2007).

[98] M. Mackie, A. Collin, J. Javanainen, Phys. Rev. A **71**, 017601 (2005).

[99] P.D. Drummond, K.V.Kheruntsyan, D.J. Heinzen, and R.H. Wynar, Phys. Rev. A **65**, 063619 (2002).

[100] J. Liu, B. Wu, and Q. Niu, Phys. Rev. Lett. **90**, 170404 (2003).

[101] A.P. Itin and S. Watanabe, Phys. Rev. E **76**, 026218 (2007).

[102] A.P. Itin, A.A. Vasiliev, G. Krishna and S. Watanabe, Physica D **232**, 108 (2007).

[103] A. P. Itin and P. Törmä, Phys. Rev. A **79**, 055602 (2009).

[104] A. P. Itin, S. Watanabe; Phys. Rev. Lett. **99**, 223903 (2007).

[105] A. P. Itin, S. Watanabe, V. V. Konotop; Phys. Rev. A 043610 (2008).

[106] Yu. N. Demkov and M. Kunike, Vest Leningr. Univ. Fiz. Khim. 16, 39 (1969); K.-A. Suominen and B.M. Garraway, "Population transfer in a level-crossing model with two time scales", Phys. Rev. A. **45**, 374-386 (1992).

[107] Y. R. Shen, The Principles of Nonlinear Optics (Wiley, New York, 2002).

[108] H. Suchowski, G. Porat, and A. Arie, Laser Photonics Rev. **8**, 333 (2014).

[109] Xi Chen, I. Lizuain, A. Ruschhaupt, D. Guery-Odelin, and J. G. Muga, Phys. Rev. Lett. **105**, 123003 (2010).

[110] U. Boscain, G. Charlot, J.-P. Gauthier, S. Guérin, and H. R. Jauslin, J. Math. Phys. **43**, 2107 (2002).

[111] A.M. Ishkhanyan, B. Joulakian and K.-A. Suominen, "Two strong nonlinearity regimes in cold molecule formation", European Physical Journal D **48**, 397 (2008).

[112] A. Ishkhanyan, B. Joulakian, and K.-A. Suominen, "Variational ansatz for the nonlinear Landau-Zener problem for cold atom association", J. Phys. B **42**, 221002, 1-5 (2009).

[113] A.M. Ishkhanyan, "Generalized formula for the Landau-Zener transition in interacting Bose-Einstein condensates", EPL **90**, 30007 (2010).

[114] K. Heun, "Zur Theorie der Riemann'schen Functionen Zweiter Ordnung mit Verzweigungspunkten", Math. Ann. **33**, 161 (1889).

[115] A. Ronveaux (ed.), *Heun's Differential Equations* (Oxford University, London, 1995).

[116] S.Yu. Slavyanov and W. Lay, *Special functions* (Oxford University Press, Oxford, 2000).

[117] A.M. Ishkhanyan, "Exact solution of the Schrödinger equation for the inverse square root potential $V_0/\sqrt{x}$", EPL **112**, 10006 (2015).

[118] J. Karwoswki and H.A. Witek, "Bi-confluent Heun equation in quantum chemistry: Harmonium and related systems", Theor. Chem. Accounts **133**, 1494 (2014).

[119] T.A. Shahverdyan, T.A. Ishkhanyan, A.E. Grigoryan, A.M. Ishkhanyan, "Analytic solutions of the quantum two-state problem in terms of the double, bi- and tri-confluent Heun functions", J. Contemp. Physics (Armenian Ac. Sci.) **50**, 211-226 (2015).

[120] T.A. Ishkhanyan and A.M. Ishkhanyan, "Solutions of the bi-confluent Heun equation in terms of the Hermite functions", arXiv:1608.02245 (2016).

[121] F.W.J. Olver, D.W. Lozier, R.F. Boisvert, and C.W. Clark (eds.), *NIST Handbook of Mathematical Functions* (Cambridge University Press, New York, 2010).

[122] A.M. Ishkhanyan and A.E. Grigoryan, "Fifteen classes of solutions of the quantum two-state problem in terms of the confluent Heun function", J. Phys. A **47**, 465205 (2014).

[123] A.M. Ishkhanyan, T.A. Shahverdyan, T.A. Ishkhanyan, "Thirty five classes of solutions of the quantum time-dependent two-state problem in terms of the general Heun functions", Eur. Phys. J. D **69**, 10 (2015).

[124] E.E. Nikitin, "The probability of nonadiabatic transitions in the case of nondivergent terms", Optika i Spektroskopiya **13** (1962) 761.

[125] V.M. Akulin and W.P. Schleich, "Landau-Zener transition to a decaying level", Phys. Rev. A **46**, 4110 (1992).

[126] B.W. Shore, *Theory of Coherent Atomic Excitation* (Wiley, New York, 1990).

[127] M. Abramowitz and I.A. Stegun, Handbook of Mathematical Functions (Dover, New York, 1965).

Résumé en Français

Pertinence du sujet

Les gaz quantiques dégénérés (condensats de Bose-Einstein et gaz de Fermi) sont un sujet de recherche en physique contemporaine qui peut contribuer substantiellement à la fois à la haute technologie et à la compréhension fondamentale de la nature. Notre recherche fait partie intégrante des efforts dans cette direction.

Les modèles avec croisements de niveaux sont au coeur de l'optique quantique dès le début de la physique quantique. En raison du nombre très limité de modèles exactement résolus, tout nouveau modèle peut mener à de nombreux développements essentiels révélant les principales caractéristiques physiques qualitatives de nombreux processus physiques se produisant dans divers domaines.

But du travail

Le but de ce travail est d'analyser la dynamique de conversion atome-molécule dans les gaz quantiques dégénérés pour créer un condensat de Bose-Einstein moléculaire (BEC). Une tâche particulière est de contrôler la photo-association de condensats atomiques de Bose-Einstein en choisissant la configuration du champ laser.

L'essence de la condensation de Bose-Einstein est une occupation macroscopique d'un seul état quantique. Un BEC est un état de la matière, qui se produit dans un gaz bosonique dilué (atomique ou moléculaire) refroidi à des températures très proches du zéro absolu. Dans de telles conditions, une grande fraction de bosons occupe l'état quantique le plus bas. Pour cette raison, les effets quantiques deviennent visibles sur une échelle macroscopique.

La photo-association est un processus dans lequel deux atomes en collision interagissent avec un champ laser pour former une molécule excitée. Il s'agît donc d'un processus chimique.

Ce travail concerne le contrôle du processus de photo-association. Le contrôle peut être réalisé par différentes approches, par exemple, par changement de la densité ou par l'application d'un champ magnétique. Dans notre cas, le contrôle est effectué en choisissant des configurations de champs appropriées.

Les configurations des champs sont décrites par la fréquence Rabi et le désaccord. La fréquence Rabi est le produit du moment dipolaire de la transition et de l'amplitude du champ. Le désaccord est la différence entre les fréquences de transition et du laser. La donnée de la fréquence Rabi et du désaccord est appelée configuration du champ. Dans ce travail, la fréquence et le désaccord de Rabi sont des fonctions dépendantes du temps.

L'idée générale est de rechercher des configurations de champs qui donneront le résultat souhaité. Le résultat souhaité est formulé comme une évolution temporelle donnée de la population.

Le problème est non linéaire, ce qui signifie que l'ensemble des équations décrivant le processus de photo-association n'est pas linéaire. Par conséquent, on a besoin de nouvelles approches, pour lesquelles des étapes importantes sont prises dans le travail.

Nous commençons par un modèle à deux niveaux. Le processus physique que nous étudions est le suivant : nous considérons un condensat atomique initialement pur et nous souhaitons créer un condensat moléculaire en appliquant un rayonnement laser. Nous considérons le condensat atomique comme un seul état et l'état moléculaire comme le second. Un tel procédé dans l'approximation la plus simple peut être décrit par un modèle non linéaire à deux états. Pour rendre le modèle plus réaliste, nous considérons des non-linéarités du troisième ordre qui décrivent les interactions élastiques atome-atome, atomes-molécule et molécule-molécule.

En outre, pour amener des molécules faiblement couplées à l'état fondamental moléculaire stable, nous utilisons le passage adiabatique Raman stimulé (STIRAP). Une tâche particulière ici est d'éviter autant que possible les pertes de l'état moléculaire excité intermédiaire. De plus, nous analysons la robustesse des processus STIRAP linéaires et non linéaires.

Enfin, pour avancer dans la description analytique approximative de la photo-association par un ansatz à deux termes proposée précédemment, qui implique la solution du problème linéaire associé, nous considérons des solutions exactes du problème linéaire à deux états en termes de fonctions de Heun bi-confluentes. Nous introduisons un nouveau modèle avec croisement de niveaux pour lequel la solution du problème linéaire à deux états s'écrit avec certaines combinaisons linéaires de fonctions d'Hermite.

Les objectifs de la thèse

- Développer une technique de passage adiabatique efficace et robuste basée sur le suivi d'une solution souhaitée pour le transfert d'un état atomique à l'état moléculaire.

- Explorer s'il est possible d'effectuer un transfert efficace en présence de non linéarités de Kerr.

- Discuter de la méthode de suivi exacte Raman stimulée comme une procédure de transfert efficace possible. Si possible, inclure les pertes irréversibles du deuxième niveau.

- Identifier des configurations de champs pour lesquelles le problème quantique à deux états est résoluble avec des fonctions Heun.

- Identifier les modèles avec croisements de niveaux résolubles en termes de combinaisons linéaires de fonctions spéciales plus simples que les fonctions de Heun.

Nouveauté scientifique

Nous proposons une technique de passage adiabatique robuste et efficace d'un état atomique à un état moléculaire, basée sur le suivi d'une évolution temporelle souhaitée des populations.

Nous montrons qu'il est possible de réaliser un bon transfert en présence de non-linéarités de Kerr. Ceci est obtenu par un choix approprié du désaccord qui fournit un suivi adiabatique efficace.

Nous présentons un suivi stimulant par effet Raman stimulé dans un système quantique non-linéaire à trois états. Nous montrons que dans le cas non linéaire, pour un transfert efficace il faut prendre l'impulsion de la pompe plus forte que celle de Stokes, contrairement au cas linéaire ordinaire. Ce transfert peut également être robuste.

Nous montrons qu'en utilisant une technique de suivi exacte par effet Raman stimulé, il est possible d'éviter les pertes irréversibles de l'état moléculaire intermédiaire faiblement lié, dans le cas de résonances à un et deux photons.

Nous construisons des extensions des solutions de l'équation de Heun bi-confluente en termes de fonctions bêta incomplètes ainsi que d'autres fonctions mathématiques plus simples.

Nous développons un modèle de croisement de niveaux dissipatif linéaire résoluble en

termes de fonctions Hermite.

Résumé du mémoire

Dans le **chapitre I**, nous présentons la description du système non linéaire à deux états et discutons les propriétés générales de la transition d'un état atomique à un état moléculaire. Nous proposons une technique de passage adiabatique robuste pour un système quantique non linéaire à deux états, piloté par un champ laser qui fournit un transfert efficace. En suivant la dynamique dérivée d'une formulation hamiltonienne dans la limite adiabatique, nous obtenons les caractéristiques des impulsions. La dynamique est analysée en déterminant les points fixes et les séparatrices.

Nous démontrons que ce système non linéaire n'a aucune solution qui mène exactement à un transfert de population complet dans un temps fini. Pour des impulsions avec aire infinie, le transfert complet ne peut être atteint que de manière asymptotique.

La robustesse de cette technique par rapport aux variations de l'aire de l'impulsion et du désaccord est une propriété cruciale pour les implémentations pratiques. La robustesse d'une implémentation particulière nécessite l'optimisation du suivi précis, comme proposé pour le cas linéaire. La possibilité d'une réalisation d'une fidélité ultra haute avec une efficacité exponentielle optimale est une question ouverte.

Dans le **chapitre II**, la méthode de suivi adiabatique est étendue aux modèles, comprenant des non-linéarités Kerr. Dans le chapitre précédent, cette stratégie de suivi a été analysée pour un modèle simplifié, qui ne comprenait pas les collisions élastiques entre les particules. Dans ce chapitre, le point principal est d'étendre l'analyse en incluant les non linéarités Kerr. Le suivi développé évite le croisement de points fixes et de séparatrices, qui sont une source principale de la diminution de la population de l'état moléculaire.

Nous notons qu'en général, les termes de Kerr ont une forte influence qualitative sur la dynamique, comme l'apparition d'autres points hyperboliques qui peuvent interférer avec le suivi souhaité. Par conséquent, on doit obtenir un désaccord approprié particulier qui produit un suivi efficace. Notre résultat principal est qu'il est possible d'avoir un bon transfert et, en même temps, d'éviter les oscillations, en présence de termes de Kerr.

Comme on l'a déjà mentionné, la création d'un BEC moléculaire doit amener les molécules à l'état fondamental. Dans le modèle de Rabi, les particules restent dans l'état moléculaire faiblement lié plus longtemps que dans l'état atomique. Par conséquent, en raison des pertes de cet état moléculaire, le système se dégrade rapidement. Pour éviter cela, on doit amener la population à l'état moléculaire fondamental aussi vite que possible. Il existe différentes approches pour un tel transfert. Une méthode avantageuse est le passage adiabatique Raman stimulé (STIRAP), qui est un modèle spécifique d'interaction champ-matière à trois états.

Dans le **chapitre III**, nous considérons le STIRAP non linéaire. Le but est de créer un condensat moléculaire de Bose-Einstein en couplant l'état atomique pur initial et l'état fondamental moléculaire final en utilisant un troisième état excité de molécules faiblement liées. Nous dérivons une technique efficace de suivi exact par effet Raman stimulé pour un système quantique non linéaire piloté par des champs externes, ce qui permet un transfert efficace d'un condensat atomique à un condensat Bose-Einstein moléculaire. Les résultats montrent que pour que le transfert soit efficace, on doit utiliser une impulsion pompe plus forte que l'impulsion Stokes, contrairement à la situation dans le passage adiabatique Raman stimulé linéaire.

Puisque nous avons des pertes irréversibles de l'état moléculaire excité intermédiaire, nous présentons une technique de suivi exact Raman stimulée qui prend en compte cette dissipation. Nous montrons également comment éviter les pertes dans le cas de résonances à un ou deux photons. De plus, nous montrons la robustesse des procédures STIRAP linéaires et non linéaires.

Dans le **chapitre IV**, nous notons que la solution approchée du problème non linéaire à deux niveaux pour une configuration de champ arbitraire est construite par un ansatz à deux termes suggéré précédemment pour le cas général. Un terme de cet ansatz contient les principales caractéristiques de la dynamique non linéaire, et le deuxième est une correction obtenue à partir d'un modèle linéaire avec des paramètres modifiés. Comme la solution du premier terme est connue pour tous les modèles, le problème est d'étudier le deuxième terme. Cependant, les solutions exactes du problème linéaire sont très rares. Seuls 5 modèles sont

connus, ce sont les modèles Landau-Zener, Rosen-Zener, Demkov-Kunike, Nikitin et Crothers.

Pour construire des nouveaux modèles linéaires exactement résolubles, nous considérons les cas où le problème linéaire à deux niveaux est réduit à l'équation de Heun bi-confluente. En discutant les solutions de cette équation, nous construisons une expansion des fonctions Heun bi-confluentes en termes de fonctions bêta incomplètes et nous présentons un développement en termes de fonctions d'Hermite d'ordre non entier. Nous notons qu'en général ces dernières fonctions ne sont pas des polynômes.

Nous appliquons ce développement pour identifier les configurations de champs pour lesquelles la solution du problème de deux états linéaire dépendant du temps s'écrit comme une combinaison linéaire d'un nombre fini de fonctions d'Hermite.

En outre, nous identifions les modèles de Heun bi-confluents avec croisements de niveaux pour lesquels la solution implique seulement deux fonctions d'Hermite. Nous notons que certains de ces modèles décrivent des processus avec pertes du niveau supérieur.

Enfin, nous présentons un modèle particulier avec croisement de niveaux résoluble, pour le problème linéaire à deux états qui contient des pertes irréversibles du deuxième niveau. Le modèle est donné par une fréquence de Rabi variant exponentiellement et un désaccord de croisement de niveaux qui commence à partir de la résonance exacte et diverge exponentiellement à l'infini. Nous déterminons la solution exacte du problème et nous discutons la dynamique des populations des niveaux du système sous différents régimes d'interaction.

Title : Control of photoassociation of atomic Bose-Einstein condensates by laser field configuration

Summary : In this work we show that it is to perform an efficient adiabatic passage in a basic quadratic-nonlinear quantum two-state system describing weakly bound molecule formation in atomic Bose-Einstein condensates through photoassociation by laser fields.

An efficient adiabatic transfer is also possible if the third-order nonlinearities describing the atom-atom, atom-molecule, and molecule-molecule elastic scattering are taken into account. The transfer is achieved by choosing a proper detuning derived by solving the inverse problem.

We also show that one can perform a stimulated Raman exact tracking in a quadratic-nonlinear quantum three-state system. The irreversible losses from the intermediate weakly bound molecular state in a passage of free atoms to the stable molecular state can be avoided by a two-colour three-state scheme in the case of one- and two-photon resonances for the associating laser fields. This is achieved by an exact tracking technique.

We also studied the linear time-dependent two-state bi-confluent Heun models with solutions in terms of linear combinations of a finite number of the Hermite functions of non-integer order. We have presented a model the solution for which involves just two Hermite functions. This is a resonance-crossing field configuration given by an exponentially diverging Rabi frequency and a detuning that starts from the exact resonance and exponentially diverges at the infinity. The model takes into account the irreversible losses from the second state.

Keywords : Molecular Bose-Einstein condensates, photo-association, magneto-association, nonlinear adiabatic tracking, exact tracking, bi-confluent Heun functions.

Titre : Contrôle de la photo-association de condensats de Bose-Einstein atomiques par configuration de champs laser

Résumé : Dans ce travail, nous montrons qu'il est possible d'effectuer un passage adiabatique efficace dans un système quantique non-linéaire quadratique à deux états décrivant la formation de molécules faiblement liées dans les condensats atomiques de Bose-Einstein par la photo-association par champs laser.

Un transfert adiabatique efficace est également possible si on prend en compte les non-linéarités de troisième ordre décrivant les collisions élastiques atome-atome, atome-molécule et moléculaire-molécule. Le transfert est obtenu en choisissant un désaccord approprié calculé en résolvant le problème inverse.

Nous montrons également que l'on peut effectuer un suivi Raman stimulé exact dans un système non-linéaire quantique à trois états. Dans le passage d'atomes libres à l'état moléculaire stable, les pertes irréversibles de l'état moléculaire intermédiaire faiblement lié peuvent être évitées par un schéma à trois états en deux couleurs dans le cas avec résonances à un ou deux photons. Ceci est obtenu par une technique de suivi exacte.

Nous avons également étudié des modèles linéaires à deux états bi-confluents de Heun, dépendant du temps, avec des solutions en termes de combinaisons linéaires d'un nombre fini de fonctions Hermite d'ordre non entier. Nous avons présenté un modèle dont la solution implique seulement deux fonctions Hermite. Il s'agit d'une configuration de champ avec croisement par résonance donnée par une fréquence Rabi exponentiellement divergente et un désaccord qui commence à partir de la résonance exacte et diverge exponentiellement à l'infini. Le modèle prend en compte les pertes irréversibles du second état.

Mots clés : Condensats de Bose-Einstein moléculaires, photo-association, magneto-association, suivi adiabatique non-linéaire, suivi exact, fonctions bi-confluentes de Heun.